Laser joining of aluminium to hot-dip galvannealed steel for the use of car bodies

A thesis submitted for the degree of Master of Philosophy

By

Sang Cheon Park

Department of Electronic and Computer Engineering,

Brunel University

September 2018

Abstract

Laser welding-brazing (LWB) process with filler wire was developed to join 6000 series aluminium alloy (AA6451) and hot-dip galvannealed (GA) mild steel. LWB is useful to minimize brittle Fe-Al intermetallic compounds (IMCs) that are generated at the interface of the joint and severely degrade the joint strength. The laser melts only filler wire and part of the aluminium and the molten wire braze onto the solid state surface of the steel. Hot-dip galvanized (GI) mild steel also tested to compare the effects of zinc coating layers of each steels. For the brazing trials, these materials were cleaned and fitted up in one of two joint configurations: overlap or flare bevel groove joint. And four kinds of filler wires, AlSi12, AlMg5, ZnAl15 and flux cored wire (FCW) were tested for each joint configuration.

Having identified the most suitable LWB parameters that best met requirements for braze quality and property characterisations, the selected braze joints have undergone a detailed qualitative and quantitative analysis.

At the high laser moving speed of 3m/min, braze joints of aluminium on GI steel shows better joint strength than those of aluminium on GA steel. The failures of tensile test samples with the GI steel occurred across the heat affected zone (HAZ) of the aluminium, whereas those with the GA steel occurred at the joint interface. This result could be explained by the presence of the pure zinc layer (melting temperature of 419℃) of GI steel which melts before AlSi12 filler wire (melting temperature of 582℃) and help to spread the molten filler wire by forming liquid layer on the steel surface. On the other hands, since Fe-Zn alloy layer of GA steel melts at a high temperature close to 1200℃, thus this layer requires higher heat energy to remove it before wetting. The higher heat energy can be assumed that promotes the growth of IMCs at the interface of the joint which reduce the joint strength.

When the laser moving speed was slower down to 1m/min, the joint strength of aluminium and GA steel was increased and the failure of the tensile samples occurred in a combination of the braze throat and the interface of the joint. This is likely to be due to the larger braze widths with thin IMC layers by granting more time to feed the filler wire and remove the zinc coating of the steel parent material with lower heat energy conditions.

Acknowledgements

I am greatly indebted to Sullivan Smith who suggested NSIRC MPhil programme and made my research at TWI possible. His understanding of the automotive industry and expertise in metallurgy have been the most supportive of achieving the goal of the research. I will never forget his kindness and understanding of my difficulties at TWI.

I sincerely thank Professor Balachandran who taught me the importance of an academic approach to my research work. Without his guidance throughout my research, my thesis could not be properly filled and organized. Also his warm attention to my family is unforgettable.

I would like to show my gratitude to Dr. Chris Allen and Tony Pramanik who taught me the principal and techniques of laser welding and brazing. Their guide and instruction enabled the amazing achievement in a short period of time.

Finally, thank you to my family who gladly came to the UK together and gave me endless support and love.

List of figures

Nomenclature

Abbreviations	Description
LWB	laser welding brazing
IMC	intermetallic compound
GA	hot-dip galvannealed
GI	hot-dip galvanized
IIHS	insurance institute for highway safety
FCW	flux cored wire
DOE	design set of experiments
PW	pulsed wave
CW	continuous wave
MIG	metal inert gas
HAZ	heat affected zone
SEM	scanning electron microscopy
EDX	energy-dispersive X-ray
L+T	leading and trailing
PM	parent metal
WM	weld metal
FB	fusion boundary
WFS	wire feeding speed

Symbol	Description	unit
E_l	Liner energy density	kW·sec/mm
V_w	Volume of filler wire delivered	mm^3/mm

Table of Contents

1. Introduction

1.1 Background

In recent years, the automotive industry has prioritised weight reduction of cars to meet the exhaust gas emission regulations. From 2021, vehicles in Europe are supposed to emit less than 95g CO_2 per kilometre under EU legislation. According to explanation of European Commission, this target means a fuel consumption of around 4.1l/100km of petrol or 3.6l/100 km of diesel and is 40% stricter than that in 2007. In case of cars using internal combustion engines, there are few options to meet the regulation without weight reduction. According to an fka study [1], 10% reduction in mass can result in a 6 to 8% reduction in fuel consumption.

At the same time, higher structural performance of car bodies is strongly demanded for crash safety of vehicles. For example, in 2012, the Insurance Institute for Highway Safety (IIHS) of the United States firstly announced the small overlap frontal test which simulates what happens when the front left or right corner of a vehicle collides with another vehicle or an object like a tree or utility pole. For the test, 25% of the front of the test car hits a rigid barrier at a travelling speed of 64km/h. Compared to the existing frontal crash test with 40% overlap into deformable barrier, this test results in huge damage and deformation in the occupant compartment which can cause severe injury to passengers in the car. At the start of the new test, most of car companies had big troubles to achieve good grades, and needed to apply additional parts or reinforce the frontal area of cars to protect the occupant compartment from the crash. Consequently, the enhanced crash safety requirements resulted in an increase in the weight of car bodies.

In order to meet these two conflicting demands, weight reduction and crash performance improvement of cars, low density materials, such as aluminium, are seen as an alternative to replace steel in automotive bodies. However, the price of aluminium is 2 to 5 times higher than that of steel, depending on its processing conditions, rolled sheet, casting or forging. For this reason, full aluminium car bodies are limited to premium class cars. On the other hand, in mid-priced cars, the use of mixed materials has been widely discussed. In particular, the combination of steel which has advantages of cost and mechanical properties and aluminium which has high specific strength and corrosion resistance along with relatively lower price comparing to other low-density materials is the most preferred option for the car manufacturers.

However, to mix both materials, appropriate joining methods should be selected and optimized for each particular joint type. For example, mechanical joining such as rivets, screws and clinching are the most well-known methods for joining aluminium and steel. They promise

outstanding joint strength and have been proven their good productivity in serial production lines of many automobile manufacturers. But mechanical joining is characterised by difficulty in avoiding cost and weight increases due to the need for additional joining elements. Moreover, mechanical joining can only be applicable in components with large overlapping flanges to which these elements can be fastened. Large flanges themselves increase component weight and they are not practical in all car body joints, particularly external (visible) joints.

A relatively new technology, Friction Stir Welding (FSW), which employs solid state joining by mixing materials with a rotating probe tool has also shown good joining strength with small joint areas, lower heat inputs and low residual stresses [2]. However, this joining method has limited use in serial production lines yet, due to high maintenance cost of the probes and low traverse speed to reach sufficient weld temperature, compared to conventional welding.

Meanwhile, the thermal joining techniques, welding or brazing, are well known for high productivity, low processing costs and flexibility on joint configurations. For dissimilar joining such as aluminium and steel, the use of thermal method is still a big challenge because of the large differences of two metals in thermo-physical properties such as; melting points, thermal conductivity and thermal expansion rate between the two metals. These differences result in large stresses. A lack of miscibility between the crystal structure of steel and aluminium means that liquid phase joining results in the formation of brittle Fe-Al intermetallic compounds (IMCs). The brittle nature of the IMCs formed between Fe and Al can induce cracking in the weld and produce joints with low fracture toughness. To tackle these issues, low heat input, fast heating and cooling cycles are required [3]. In these regards, laser processes can be the best choice for thermal joining between aluminium and steel.

Laser technologies particularly have advantage to control the IMC layer between aluminium and steel by inducing the beam with high energy densities and a small focal area. Moreover, modern fibre and disc laser sources can be easy automated with a robot and used to join metal sheets at extremely high speeds, with good joint integrity, giving excellent process economics. Many examples in literatures have suggested various techniques for aluminium and steel joining with laser beam. The first method is heating steel with an induced laser beam and melting aluminium by thermal conduction resulting in molten aluminium wetting the solid steel [4][5][6]. Secondly, a laser welding-brazing (LWB) uses the laser beam to melt aluminium directly with or without filler wire, thus the molten alloy spreads on the solid steel surface and wets to it. Lastly, laser welding which melts both metals produced a sound joint when it performed with advanced energy distribution methods such as dual-spot-laser optics [7].

1.2 Aluminium roof and its joining issues

Car roofs can be the best choice of component for aluminium applications considering weight reduction as well as improving driving performance. It is the second largest component among car body parts, so weight reduction efficiency is also bigger than other ones. Since car roofs are placed at the top of cars, the weight reduction of them can effectively lower the centre of gravity of cars and reduces the rollover possibility during corner driving. Generally, rollover situations have a higher fatality rate than other types of car accidents.

Meanwhile, to apply aluminium to the roof, there are two joining issues to consider.

The first one is joining structure with car body-sides. Typically, two kinds of joint configurations are used for joining the roof and the body-side: overlap joint (Figure 1.1) and flare-bevel-groove joint (Figure 1.2). Overlap joint is more common and spot welding, rivet or adhesive bond can be applied to it. However, there is an inevitably of discontinuous space between the roof and the body-side for joining, and additional plastic mouldings (trims) are needed to hide it. For saving cost by removing the mouldings or design preference, several car companies have started to use flare-bevel groove joint and laser brazing method to join it. To join the aluminium roof to the steel body-side with this joint configuration, appropriate laser joining technology between aluminium and steel should be developed.

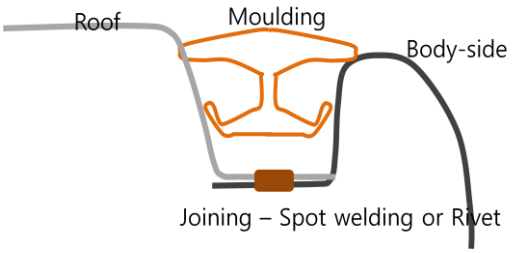

Figure 1.1) Cross section of roof/body-side (Overlap joint) and moulded trim that is typically used to cover the spot-welded seam.

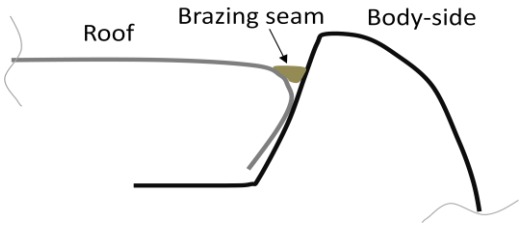

Figure 1.2) Cross section of roof/body-side joint (Flare-bevel groove joint), the overlap has been removed and there is no need for trim.

The second issue for joining of the aluminium roof is a coating of the steel body-side which critically effects on the brazing quality. The body-sides of cars are likely to be in contact with water or pollutants from its surrounding environment. Therefore, coated steel must be used for it, such as hot-dip galvannealed steel (GA) or galvanized (GI) steel. Two types of Zn-coated steels exhibit extremely different results during laser brazing with aluminium because of their different melting points. The coating layer of GI steel is mostly consists of pure zinc with a melting temperature of 419℃. On the other hand, that of GA steel is composed of several different phases of Fe-Zn IMCs; zeta, eta, delta gamma1 and gamma2. And according to the Fe-Zn binary phase diagram, the temperature need to rise around 1200℃ to turn all the Fe-Zn IMCs into a fully liquid state [8][9]. As a result, different laser conditions and filler metals should be selected for each coating type of steels to achieve acceptable joint quality.

1.3 Research aim and specific objective

The main aim of this research is to develop laser brazing technology to join the aluminium roof to the GA steel body-side.

In most literature looking at the brazing of aluminium to steel, GI steel is used for their studies, because the majority of this work has been performed by European institutes, who would select GI steel as it is broadly used in European car manufactures. On the other hand, very little work was found in the available literature regarding laser brazing of aluminium and GA steel which is mainly used in Asian car manufactures. Significant difficulty of joining aluminium to GA steel may have inhibited institutes from producing results worthy of publication.

The reason why Asian car companies prefer GA steel can be explained by the advantages of GA steel in car body manufacturing processes such as resistance spot welding or press forming for body panels. The higher melting temperature and surface hardness of the GA coating layer help to reduce the amount of melting or powdering of the layer during the processes. As a result, it reduces the contamination of tools in contact with the GA steel in both processes. The metallurgical differences between GA and GI steel will be mentioned in Section 3.1.

Specific Objectives:

- To review the relevant state-of-the-art published literature and patents that have been published to identify limitations of the technology
- To investigate and optimize laser conditions for avoiding interfacial fracture during shear tensile testing for overlap and flare-bevel groove joints. The brazing tests mainly performed at the brazing speed of 3m/min which is supposed to be the least processing speed

for automotive serial production lines. The base materials of the joint are AA6451 aluminium sheets and GA/GI mild steels which are typical materials for car bodies.

- To identify the best filler wires showing good wettability on each GA and GI steels during the limited heat input applied to minimize Al-Fe IMCs
- To perform metallographic assessments of selected LWB joints to determine the wetting length/angle and the IMC thickness and reveal the presence of any internal defects. The kinds of the IMCs are figured out via scanning electron microscopy and nano-hardness of the selected joints.
- To carry out hardness surveying and tensile testing on selected LWB joints to determine the corresponding mechanical properties.

1.4 Summary of Methodology

- The first laser conditions and LWB processing parameters were roughly selected based on the results of laser welding of 6000 aluminium performed prior to this research work at TWI.
- On the basis of the parameters selected, a design set of experiments (DOE) using a single spot beam condition for the overlap joint was conducted. A wide range of parameters were selected to define process space for stable conductions. However, the parameter set used was too coarse, therefore stable brazing conditions were not found within the experimental set.
- After all, using a trial and error method, hundreds of braze joints of aluminium on GA/GI steel were produced in overlap and flare bevel groove joints with each filler wires. Significant difficulty of joining aluminium to GA steel may have increased the number of trials.
- The conditions were selected from the trials for further evaluations on the basis of producing the most visually acceptable braze deposits and indicating acceptable bend test results. The detail down selection criteria is mentioned in Section 3.5.3
- Micro-sections of the down selected samples were examined using an optical microscopy and braze sizes, IMC thicknesses and other defects were examined. Porosity contents were also examined by X-ray. To figure out the kind of the IMC layers, phase analysis via scanning electron microscopy and nano-hardness of the down-selected brazed joints were performed. Lastly, tensile shear testing was performed to determine the joining strength levels of each down selected samples. Appendix A and B give a summary of the

trials that were performed, the reason for each and what was learned in chronological order.

- Lastly, report the detailed analysis of the brazed joint, which best met the requirements, produced for each base steel and wire combination evaluated in overlap and flare bevel groove joints.

1.5 Organization of the thesis

Chapter 1 describe the needs of mixed materials on car bodies and their joining techniques. And introduce an example of mixed material for car bodies: aluminium roofs and steel body-sides, and the research aim to join both materials with LWB process. Lastly, a methodology used to achieve the aim is given.

Literatures about LWB between aluminium and coated or uncoated steel are reviewed in Chapter 2. Firstly, define the obstacles of thermal joining of aluminium to steel from previous literatures, followed LWB techniques to join aluminium and GI steel. Limited literatures performed laser welding-brazing tests with aluminium and GA steel are briefed. Lastly, key considerations to perform LWB with GI and GA each are given.

Chapter 3 lists materials and their joining configurations used in this research, followed laser equipment set-up and filler wires to achieved good appearance and joining strength. Then, describe the scope of work: experimental parameters, joining quality and property characterisations and qualitative and quantitative methods undertaken.

Chapter 4 illustrate the optimized process parameters for the overlap joint and the flare bevel groove joint, with GI and GA steel each and their test results: internal qualities, critical dimensions, IMC thickness, electron microscopy, nano-hardness, and tensile shear testing of the down-selected braze joints. To achieve the goal which avoid interfacial failure between braze metal and the base metal of GA steel while tensile shear tests, additional tests with slower laser moving speed of 1m/min than the targeted laser moving speed of 3m/min were performed and the results are given. Lastly, discussion of parameters employed, influence of the GA and GI coating, the requirements for good joint quality are described.

In chapter 5, conclusions of this project are summarized including key findings for LWB with the overlap joint and flare bevel groove joint. To achieve acceptable joining strength and avoid interfacial failure between the braze metal and the base metal of GA steel, further work is recommended.

2. Literature review

2.1 Obstacles of thermal joining of aluminium to steel

The first issue is the generation and growth of brittle Fe-Al intermetallic compounds (IMCs) at the interface of the joint. According to Fe–Al binary phase(Figure 2.1), the solid solubility of Fe in aluminium solid solution is almost zero (< 0.04wt%), thus the formation of Fe-Al IMCs is inevitable during the thermal joining of aluminium and steel [4]. Among the primarily five types of Fe–Al IMCs (Fe_3Al, FeAl, $FeAl_2$,Fe_2Al_5 and $FeAl_3$ phases), Fe_2Al_5 and $FeAl_3$ have a high micro-hardness, 1100HV and 700HV each, and initially formed (in the order written) at the brazing interface of aluminium and steel(Figure2.2). [10] Both IMCs are known to cause the critical degradation of the joint strength due to brittleness, thus Kreimeyer et al. [11] suggested that they should be controlled less than about 10 ㎛ thick to prevent the crack initiation at the IMC layer during the tensile testing to achieve sound joints.

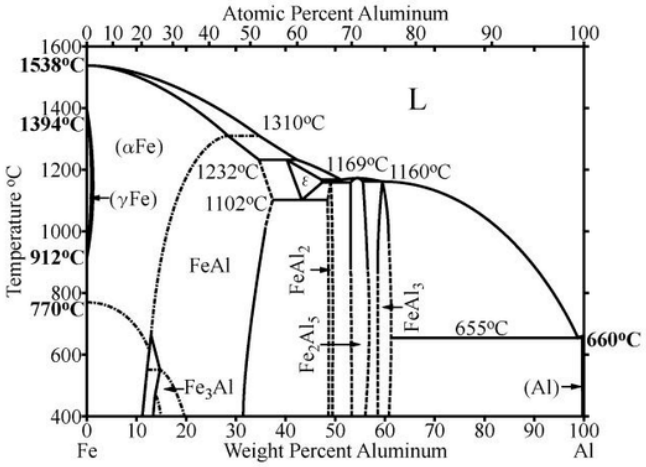

Figure 2.1) Binary phase diagram of Fe-Al [4]

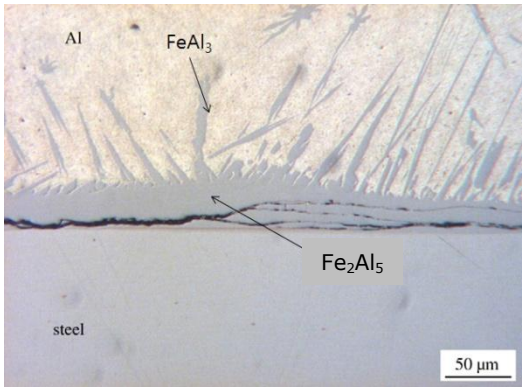

Figure 2.2) Fe-Al IMC layer between steel and aluminium [10]

Secondly, the highly tenacious oxide layer on the aluminium surface is another issue to consider. Because the melting point of aluminium oxide(2050 °C) is higher than that of aluminium base materials and filler wires, many researches applied chemical flux [4][6][12][13][14] or abrasive [5][15][16] on the surface of base materials to remove the oxide layer. However, fluxing or abrading processes are not suitable for car body manufactures because they are difficult to automate in serial production lines without significantly increasing the manufacturing costs.
Thirdly, the vaporization of zinc from GI steels is almost inevitable during brazing because zinc layers of GI steels consist of nearly pure zinc, and the boiling point of zinc (906°C) is considerably lower than that of Al (2520°C) and Fe (2862°C). The zinc vapour can become trapped inside the bead during brazing and lead to the production of pores and defects. Especially, in case of overlap joints, zinc vaporizes creating a high pressure between the materials and is likely to form large and critical pores inside the braze beads which lead to a serious decrease of joint strength [17].
The last obstacle is the high melting temperature of GA coating mentioned in Chapter 1.1.

2.2 LWB process for aluminium and GI steel

Peyre et al. [13] and G. Sierraet al. [14] studied the effects of flux and zinc coating of GI steel by lap joint tests between mild steel with or without zinc coating and 6016 aluminium alloy which are typical materials for car bodies. Like other conventional LWB research, aluminium was positioned on top of the steel plate and a single continuous laser beam in defocused condition with argon shielding gas was applied. For the uncoated steel, a joint strength could be reached of 110MPa using flux, whereas without flux the IMC layer was very thick and the wetting was close to zero. For the coated steel, a joint strength was up to 150MPa even without flux. This result could be explained by the presence of the zinc layer which improves the spreading and wettability of the molten aluminium by forming liquid layer on the steel surface[14]. Moreover, Zn prohibits the formation of Al-Fe IMC by forming Fe-Zn IMC which is not as brittle as the Al-Fe IMC, because the compatibility of Fe-Zn is much higher than that of Al-Fe. Also, Zn penetrates through the aluminium oxide layer, forming a low melting point liquid which can decrease the heat energy required to melt aluminium [3]. However, after brazing, as mentioned previously, high density of pores by vaporized zinc were formed in the bead closed to the heat affected zone (HAZ) of aluminium which were potential locations for crack initiation. When employing flux, these pores could be reduced along with decreasing the IMC thickness by forming a “thermal barrier” which allowed a joint to be made with less heat input into the steel parent material[14]. This “thermal barrier” of flux prohibited zinc vaporization and slowed down the IMC growth. For this reason, the joint

strength of coated steel with flux increased the maximum shear strength to 250MPa which is close to 96% of the tensile strength of the aluminium base material. For these tests, laser scanning speeds from 0.6 to 1.4m/min were used and as the speed was increased, a higher wetting angle and thinner IMC layer were achieved.

Junhao Sun et al. [15][18] showed successful control of the IMC thickness to less than 10 ㎛ without flux for the butt joint configuration between aluminium and uncoated mild steel. They achieved a joint strength of 150MPa, but the oxide layer on the aluminium surface needed to be removed by brushing its surface before brazing. For this test, 4043 Al-Si filler wire (AlSi5) was introduced with laser travelling speed of 1.8m/min. Al-Si filler wire is known for improving the wettability onto steel. Silicon in the filler wire inhibits the formation of IMC phases by reducing the diffusion of iron in the aluminium as Zn does [19].

A Zn based filler wire can improve the joint strength of aluminium and steel comparing to Al based filler wire because the melting point of Zn is lower than that of Al, consequently achieving better spreading and wetting of molten wire on the steel surface. C. Dharmendra et al. [20] improved the joint strength up to 208MPa between aluminium and galvanized DP600 steel without using a fluxing or abrading process, only using Zn-15%Al filler wire. The thickness of IMC was between 8-12μm, but the laser scanning speed was limited to 0.5~0.8m/min.

2.3 Advanced LWB process without flux for aluminium and GI steel

For the use of LWB in the car industry, higher laser travelling speeds and joint strength are required along with minimizing the need for additional processing such as fluxing or abrading the base material. To meet these goals, efficient heat energy distribution is required to; melt the filler wire, melt the aluminium and heat the steel to promote wettability of molten bead. However, under these conditions controlled, proper melting of the zinc coating on the steel surface to prevent the vaporized Zn gas from forming pores in the weld bead can be a key issue.

And literatures in this chapter suggest specific joining strengths of their brazed joints, however it is hard to find a strength criterion required for each joining condition. But commonly the desirable joining strengths were acquired when the fracture of the tensile specimens during tensile testing was occurred across aluminium parent materials not at the interface of the joints.

Mathieu et al. [17] showed that the use of a hot wire feed system is a good solution for increasing the joint strength. An flare bevel groove

joint (Figure 2.3) was tested with the Al-12Si filler wire which was heated by the Joule effect (electrical resistance heating) with a current range between 160A and 200A before being fed with a speed of 2.0~3.0m/min, thus it was melted more easily by the laser beam and produced a better joint than cold wire. This resulted in a joint strength of 200N/m even with the laser moving at a speed of 2m/min.

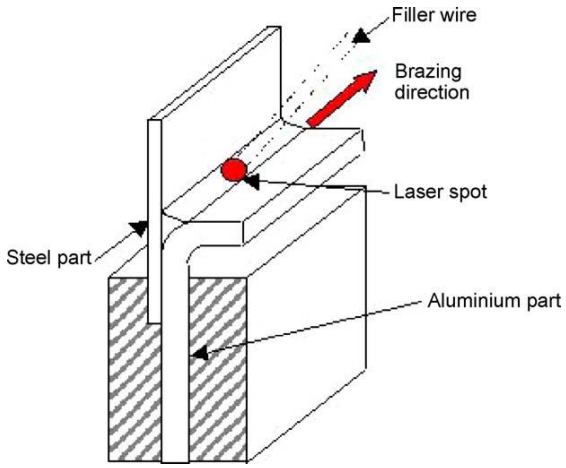

Figure 2.3) LWB with flare-bevel-groove joint using hot wire [17]

For better shielding against the oxidation of molten bead, a mixture of 70% helium and 30% argon was used for this test. Filliard et al. [21] achieved a higher brazing speed for a similar angular joint configuration, which corresponds to an aluminium roof and steel body side of car using the hot wire method. For the industrial use of LWB on car roofs, 4m/min is mentioned as the minimum brazing speed. Applying the speed of 4m/min and 6m/min, the IMC thickness was controlled less than 5μm and the joint strength was up to 145N/m. For this test, only argon gas was used for shielding the bead.

The use of two heat sources is also beneficial for flexible energy distribution in LWB. Laser beam and MIG arc were used for lap joints between 6013-T4 and GI steel [22]. Figure 2.4 shows the schematic view of laser and MIG arc joining process. The 2.0kW laser spot with 5mm in diameter on the top surface of the aluminium was used 4mm ahead of AlSi5 filler wire and MIG arc. Preheated steel surfaces by laser increased the wettability of molten aluminium and resulted in good weld appearance. The IMC thickness was controlled up to 4μm and the joint strength was maximum 247.3MPa which was 85% of that of the aluminium base metal with the laser travel speed of 1.0m/min.

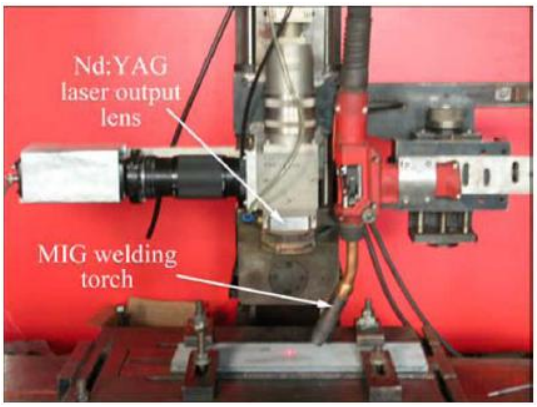

Figure 2.4) Nd:YAG laser + MIG arc hybrid welding head for lap joint LWB [22]

For this test, no pores in the bead were found. It could be explained that the proper preheating of the steel surface by laser beam vaporized some amount of the zinc coating so limiting the zinc gas formation in the bead.

A dual-spot-laser, which was created from a single laser source with two separated beams by a diffractive optic, was used for LWB [23]. One of the beams having less than 60% of energy intensity was spotted on the steel surface slightly ahead of the other main beam (Figure 2.5). The main beam was focused on the joint line along with the fume extraction nozzle which was used to remove vapour coming from the wire and zinc coating. A better weld seam and high joint strength was achieved by prohibiting the beam energy from being defocused by the fume. Using Zn15Al wire, a joint strength of 210MPa, close to that of the tensile strength of aluminium plate was achieved with the zero gap between two base metals. Zinc gas expansion and generation of pores in the bead were avoided.

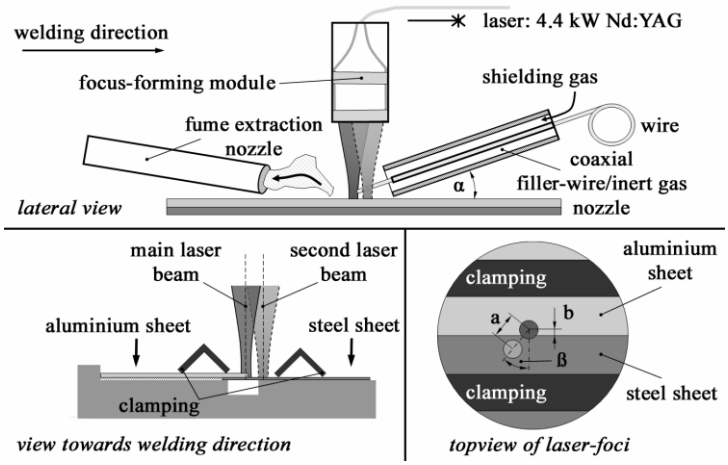

Figure 2.5) Dual-Spot-Laser configuration setup [23]

Superimposed dual-spot-laser, one beam with pulsed wave (pw) and line shaped spot and the other beam with continuous wave (cw) and circular spot was also used for LWB tests for flare v-groove joint (Figure 2.6) and lap joint each [16]. The cw beam provided heat energy for meting wire and aluminium sheet and wetting on the steel surface and pw beam support by removing the oxide layer from aluminium surface. For the flare v-groove joint between GI steel and AlMgSi1, the IMC thickness was less than 4.25 μm and the tensile strength was maximum 231.2MPa using ZnAl2 wire with the laser travelling speed of 0.7m/min. With this test condition, the laser travelling speed could be increased to 3.6m/min without decreasing of the joint strength. When the filler wire was changed to AlSi5, the joint strength slightly decreased to a maximum of 202.9MPa and the bead shape was more concave. It was explained that because of the higher melting point of AlSi5 wire comparing to ZnAl2 wire, more heat energy was introduced to joint area, thus causing more softening of HAZ of aluminium and decreasing the tensile strength. In case of the lap joint, the joint strength with AlSi5 was as much as 189.7MPa whereas it was significantly decreased below 100MPa when using ZnAl2 wire. This was caused by the deformation of the joint by shear loading during the tensile tests and lower ductility of the bead with ZnAl5 wire.

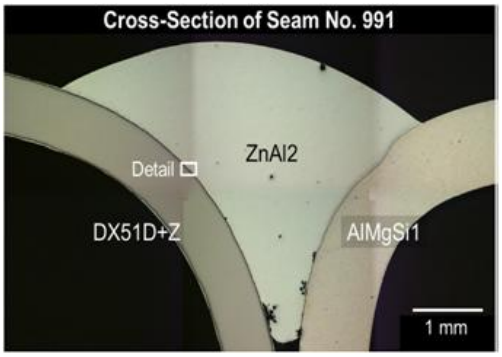

Figure 2.6) Cross-section of flare V-groove joint [16]

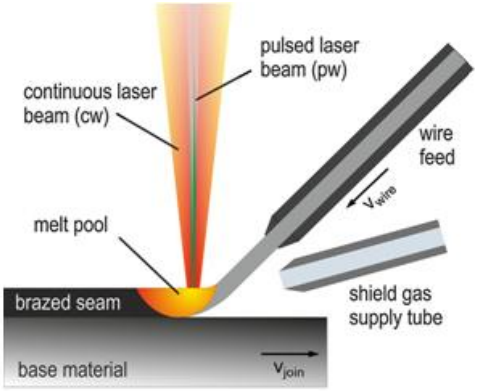

Figure 2.7) Superimposed pw and cw laser process [16]

2.4 LWB process for aluminium and GA steel

Saida et al. [25] used a dual beam laser approach to braze 6000 aluminium to two zinc coated steels, one GI coated and the other GA coated without a flux. A diode laser source was employed with the power distributed to have:

- A lead beam running at 50-100W to preheat the steel
- A higher power trailing beam to create the brazed joint

Overlap joints were made using an AlSi12 filler wire. No information on process speed was provided, but as the maximum laser power used was only 1kW, it is likely the process was slow. It was reported that superior wetting and joint strength was achieved in the GI steel. But in the GA, intermetallic layers of around 3 ㎛ were produced and the maximum joint tensile strength achieved was 150N/mm, which was about 60% of the parent value.

Tsuyoshi [26] performed trials with pre-coating of the parent materials with flux, then employing laser welding with filler wires (trials using MIG were also reported, but are not included here). A Nd:YAG laser source was used in initial experiments on overlapping 1mm thickness 6000 aluminium to 1.2mm thickness GA steel with painted on flux and solid wires of AlSi10, AlSi12 and AlMg5, giving weld strengths of 190N/mm for both AlSi wires and 140N/mm for the AlMg5. Additionally, a newly developed wire was tested giving the same 200N/mm weld shear strength and a superior peel-strength, with intermetallic layer thickness of around 1 ㎛. With the new wire a sheaf was created to perform flux cored wire welding experiments. Several different flux compositions were tested (based on potassium aluminium fluoride and containing either aluminium fluoride and caesium fluoride), and superior laser brazing results were obtained with one flux variant and better MIG results obtained with another flux variant. No information was given regarding the composition of the 'developed wire' or the specific flux that performed the best, but it was found that brazing conditions should be selected to control the intermetallic layer below 3µm to achieve a shear strength of 200N/mm and to below 1 ㎛ to achieve a peel strength of 50N/mm. In follow-on work Tsuyoshi [27] performed laser brazing of the same materials comparing the specially developed flux cored wire with an AlSi12 (AA4047) wire without flux, the flux cored wire recorded weld strengths of 200N/mm and the AlSi12 wire achieved only 110N/mm.

Nishimoto [28, 29, 30] employed a complex approach where scanning optics were used to manipulate a Nd:YAG laser beam, to create a heating profile on the surface of a fillet joint. The GA coating and surface of the aluminium were both melted and alloyed together in solid solution. Pressure was applied into the heated area using wide rollers

(full width of the sheet metals) to compress the materials together, with a pressure of 1 to 3kN. This process was employed to create a full skin joint between aluminium and steel, where the sheets were effectively laminated together. This approach shows the potential for heat pressure joining aluminium to GA steel, but in its present form it is not suitable for narrow flange overlap or flare-bevel-groove joining as employed in a car body. Using this method, pure aluminium was joined to GA steel. Intermetallic layer thicknesses were much greater than those recommended by approaches using lasers with filler wire. Intermetallic layers were measured at 7-20 ㎛, but despite this, in tensile testing failure in the aluminium parent material was achieved. The parent material failure could be attributed to the fact that extremely large overlapping areas were created by this laminating approach. The intermetallic layer produced by this approach contained brittle Fe-Al intermetallic compounds as well as more ductile Zn-Al intermetallic compounds.

A novel new filler wire material was tested by Wakisaka [31] to laser braze aluminium (AA6022) to GA steel without the use of a flux. The filler wire had a ZnSi (ZnSi1) composition. The theory was proposed that the presence of Si inhibited the formation of the intermetallic layer and specifically hard phases such as Fe_2Al_5. The formation of Fe_2Al_5 was inhibited by a layer of $Fe_3Al_2Si_3$ that formed preferentially at the interface between the steel and aluminium materials. This theory is backed up by Achar [32]. Double flange joints were manufactured and tensile strengths of 150N/mm (with failures in the aluminium HAZ) were recorded using the ZnSi filler wire, compared with 110N/mm using a ZnAl6 filler wire, which exhibited failures at the intermetallic layer. The brazed joints made with the ZnSi1 filler wire were examined under SEM and intermetallic compounds<1µm in thickness were observed. These layers appeared to be of ternary $Fe_3Al_2Si_3$, which have superior mechanical properties to the binary Fe-Al phases. The wire used for this application would be classified as a soldering wire rather than brazing wire on account of its low melting point. It is not clear whether this wire is available commercially. However, the application of a wire composition of Zn with 0.25 – 2.5wt% Si for laser joining aluminium and steel components has been patented in the US, Europe and Japan by Honda Motor corporation [33]. Also the very low strength of a pure zinc system at temperatures in excess of 140°C should be taken into account, as joints manufactured with this soldering wire may not survive the E-coat cycle which includes a curing process at 320℃ [34].

2.5 Key considerations for the project

Based on the literature review, the followings are the key considerations which were taken into account to achieve the aforementioned research objectives in Chapter 1.3:

Common:

- Larger brazed interfaces give rise to greater joint strengths. Hence, achieving a large brazed area is critical to achieving higher strength joints.
- The dual laser spot approach can be used to pre-heat the steel substrate and create a larger wetted area, leading to larger brazed areas.
- The strength of joints is dependent on many factors, but filler wire composition is very important. In general, ZnAl15 fillers give the highest strength joints, followed by AlSi12 wires, with AlMg5 giving the lowest joint strengths.

For GI steel:

- To achieve a high joint strength in GI steels, intermetallic layers should be less than 10 ㎛ in thickness.
- GI steels can be laser brazed to aluminium without the use of an additional flux, because the zinc itself acts as a flux under the temperature induced in the laser brazing process.

For GA steel:

- For high joint strength, an intermetallic layer thickness less than 3 ㎛ is required. Some data also indicates that for joints loaded in peel, intermetallic layer thicknesses of 1 ㎛ or less may be required.
- The use of a flux is necessary to achieved high joint strengths.
- Some works have tested a 'developed' flux cored wire that has shown the ability to achieve high strength joints with GA steel. The composition of this wire and the flux are a commercial secret or a patent. The wire was produced as an R&D project and is not commercially available.
- The use of fluxes (either flux cored wires or externally applied flux slurries) results in large deposition of soot on the joint surface after brazing. This soot must be cleaned off in an additional brushing operation after brazing.
- No work reported on laser brazing GA steels has shown high joint strengths with a process speed greater than 1.2m/minute.

For the use of LWB between aluminium and GA steel in the automotive industry, the aim of this research was developing laser conditions and brazing parameters using commercially available filler wires to achieve a high quality joint with a good strength.

2.6 Summary

Various approaches have been suggested in literature for LWB between aluminium and steel. GI steel can be successfully brazed with aluminium without flux, whereas uncoated steel and GA steel still need a flux or oxide removing process to achieve good wettability to aluminium. Some literatures suggested new filler wire materials for GA steel, but there

was no specific material information of the filler wire compositions in the literatures.

In order to achieve a high quality joint, with a good strength it is clear that the Fe-Al intermetallic layer must be controlled:

- By producing a minimum thickness IMC layer (0–10 ㎛ are advised across various research papers).
- And, by inhibiting the formation of hard phases, by the presence of Zn and/or Si to generate ternary IMC and minimise the formation of the brittle $FeAl_3$ and Fe_2Al_5 phase.

A large brazed interface area is required to give strong joints. To generate this large brazed zone, good wetting of the steel substrate is necessary. In the case of GI steel, the liquid zinc generated during brazing acts as a flux providing a highly wettable surface on the steel substrate.

But in the case of uncoated steel or GA steel, no liquid zinc is generated, so low energy wetting onto the steel substrate is not possible. High temperatures are required to remove the GA layer and the resulting high steel temperature generates the formation of thick (>10 ㎛) and brittle intermetallic compounds. The use of fluxes is able to improve the wetting of liquid aluminium onto the steel substrate generating a larger brazed area, but the growth of deleterious intermetallic layers can still occur even when a flux is employed. Additionally, the use of a flux leads to the generation of a significant level of soot on the joint, which must be brushed off in an additional process cleaning step.

The use of special filler wires containing high levels of Zn have been shown to help achieve better joint strengths in GA by inhibiting the formation of brittle Fe-Al phases. Specifically, the ZnSi1 filler wire was shown to produce good joint strength in GA steels without the need for a flux. But it is not clear if this soldering wire is commercially available and its use is restricted by a family of patents submitted by Wakisaka et al [33].

None of the research papers detailed a brazing process for GA steel that was working at speeds above 1.2m/minute, and none of the papers detailed whether the component clamping and fixturing was suitable for application in a real exterior panel joint within a car.

It is also found that all the literature on laser based joining of aluminium to zinc coated steels were research reports, so far, no industrial cases exist where the technology is employed in a car body, for either GI or GA steels.

3. Experimental approach

3.1 Materials and joint configuration

Table 3.1 shows the kind of steel and aluminium used in these experiments. The GI steel is thicker than the GA steel and it might lead less distortion of the GI steel during brazing process.

Base material		Coating type	specimen thickness [mm]
Steel sheet	DC04	hot-dip galvannealed (GA)	0.7
	DC04	hot-dip galvanized (GI)	1.2
Aluminium sheet	AA6451-T4	None	1.2

Table 3.1) List of used coated steel sheets and aluminium sheet

As shown in the Figure 3.1, GI coating mainly consists of 99% zinc solid solution, nearly pure zinc, and its melting point is almost the same with that of pure zinc. On the other hand, GA coating is composed of Zn-Fe intermetallic compounds which have high melting temperatures [35]. The thickness of both coating layers is about 10μm.

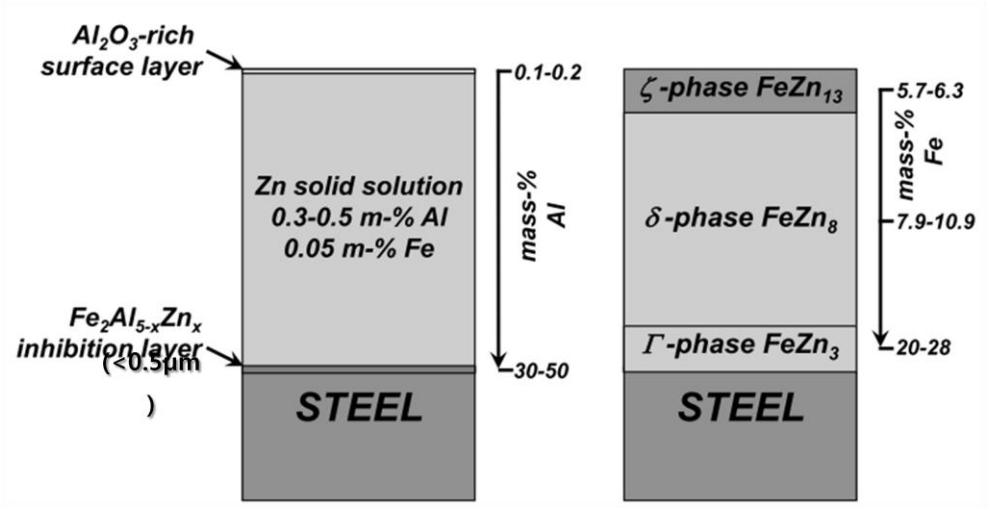

a) GI b) GA

Figure 3.1) Zinc layers on the a) GI and b) GA steel [35]

The two different joint configurations brazed in the trials are shown schematically in Figure 3.2. Figure 3.3 shows the brazing sample with the flare bevel groove joint. It comes from the joint structure of the car roof and body-side.

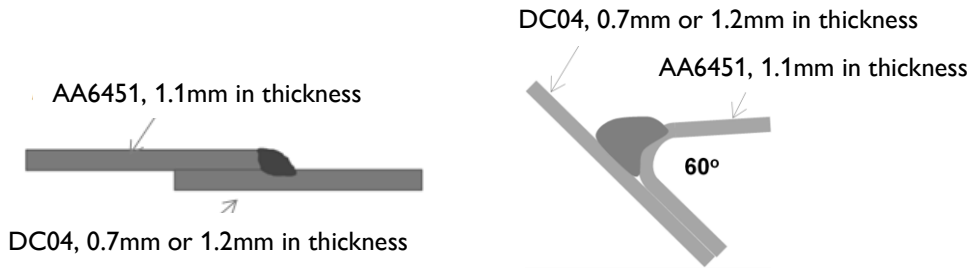

a) Overlap joint b) Flare bevel groove joint

Figure 3.2) Schematic of the joint configurations used in brazing trials

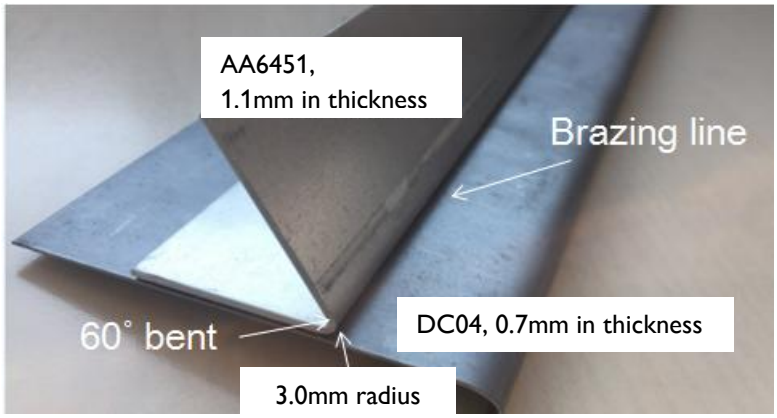

Figure 3.3) Image of the flare bevel groove joint sample for brazing trials

3.2 Filler Wire

Four different filler wires were also investigated in the trials, to compare the visual appearances, porosity contents and joint strengths of the brazed joints achieved:

- AlSi12 (AA4047) solid wire with a diameter of 1.2mm/1.6mm. Its melting temperature is 577 - 582℃. Table 3.2 shows general chemical compositions of the wire.

Si	Fe	Cu	Mn	Mg	Zn	Be	Al
11.0~13.0	0.8	0.30	0.15	0.10	0.20	0.0003	REM.

Table 3.2) Chemical compositions of AlSi12

- AlMg5 (AA5556) solid wire with a diameter of 1.2mm. Its melting temperature is 568 - 635℃. Table 3.3 shows general chemical compositions of the wire.

Si	Fe	Cu	Mn	Mg	Cr	Zn	Ti	Be	Al
0.25	0.40	0.10	0.50~ 1.0	4.7 ~ 5.5	0.05~ 0.20	0.25	0.05~ 0.20	0.000 3	REM.

Table 3.3) Chemical compositions of AlMg5

- ZnAl15 solid wire with a diameter of 1.6mm. Its melting temperature is 382 - 450℃. Table 3.4 shows general chemical compositions of the wire.

Al	Pb	Cd	Sn	Fe	Cu	Zn
14~16	0.005<	0.005<	0.006<	0.05<	0.01<	REM.

Table 3.4) Chemical compositions of AlMg5

- AlSi12 Flux Cored Wire (FCW) with a diameter of 1.6 mm

The FCW was manufactured by Solvay, and the Nocolok flux itself had the chemical name Potassium Aluminium Fluoride. According to the manufacturer, the flux core has the general formula $K_{1-3}AlF_{4-6}$. The melting temperature of the wire is 577°C, the flow temperature is 582°C, and the working temperature is 590-600°C.

3.3 Material cleaning

The materials were manually degreased using an acetone wipe to remove heavy surface contamination which deteriorates the wettability of molten aluminium on steel surface, and then subsequently ultrasonically degreased in acetone to remove finer surface contamination before being fitted together.

3.4 Equipment and set-up

The laser system used was an IPG continuous wave (cw) Yb-fibre laser (YLS 10000), fibre-delivered via a 150μm core diameter optical fibre to Optoskand processing optics. These optics comprised a 160mm focal length collimator, beam bending cube and a 300mm focal length focusing lens. A twin spot optic was also used in a selection of trials. The twin spot optic results in a separation of 0.6mm between the two beams of adjustable power density from 50:50 to 70:30 in the focal plane.

The laser optics were set at an incident beam angle of 10º from vertical in the travel direction. This tilted beam is useful to melt the filler wire by directly contacting wider filler wire. An image of the processing head and work piece clamping arrangements is shown in Figure 3.4.

Figure 3.4) Image of the experimental laser brazing set-up used in brazing trials

The specifications of the laser beam source and optics used are reported in Table 3.5. As Table 3.5 shows, the beam from the cw laser sources has a wavelength of 1070±10nm, and a maximum output power of 10kW depending on which laser was used. The optics used in combination with the 150µm or 200µm core diameter optical fibre resulted in a nominal beam waist of 0.28mm or 0.38mm. Nevertheless, greater spot diameters where the beam impinged on the surface of the work pieces were used in the majority of laser trials. These greater diameters were achieved by positioning the stand-off of the optics such that the beam waist was located above the top surface of the work piece. This is henceforth described as a positive defocus position and can be seen schematically in Figure 3.5.

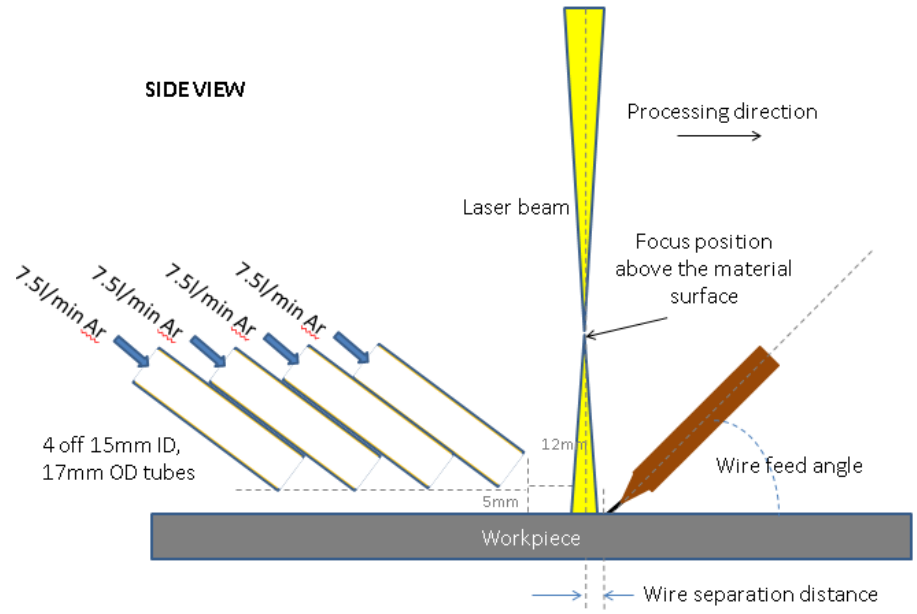

a) Side view

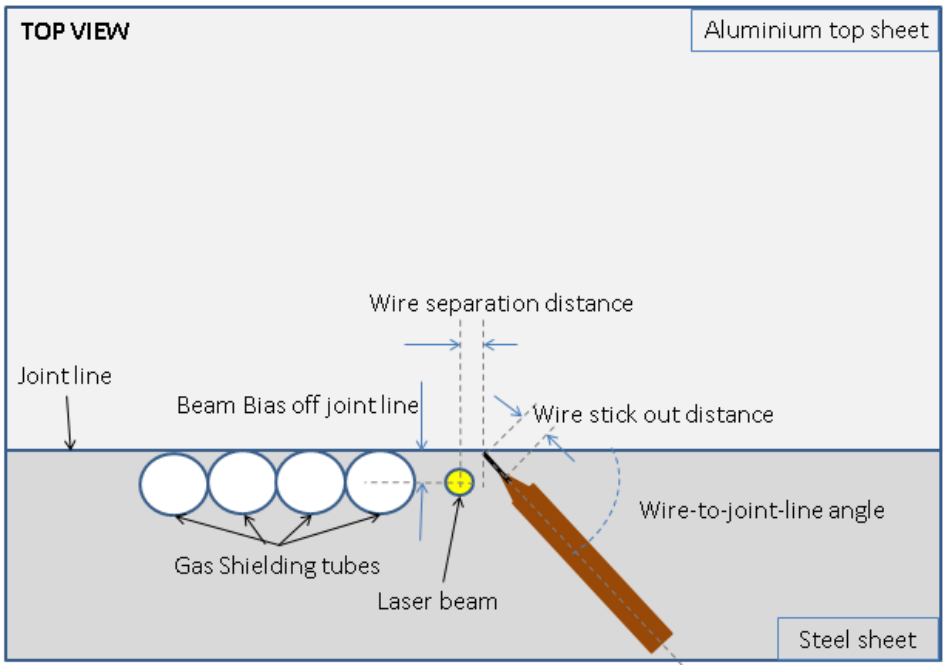

b) Top view

Figure 3.5) Schematic of the experimental laser brazing set-up

Laser parameters	Yb-fibre laser
Wavelength	1070 ±10nm
Operation mode	Continuous wave
Maximum output power, W	10,000
Delivery fibre core diameter, μm	150
Collimating lens focal length, mm	160
Focusing lens focal length, mm	300
Calculated nominal beam waist diameter at focus, mm	0.28

Table 3.5) Specifications of the cw Yb-fibre laser used in the laser trials

An air-knife and infrared transparent cover slide were used to protect the processing head optics from spatter and fume during the trials. A gas shielding arrangement was used to shield the weld cap with argon, through four 15mm internal diameter tubes, as shown schematically in Figure 3.5.

The processing head was manipulated using a six axis Kawasaki welding robot, over stationary work pieces, which were clamped together in a welding fixture.

3.5 Scope of work

3.5.1 Experimental parameters

The effects of a large number of experimental parameters were investigated, in efforts to:

- Balance the heat input into the joints, introducing sufficient heat to achieve stable melting of the braze wire addition, and its wetting and flow.
- Minimise heat input, to limit the extent and sizes of the IMC formed, and achieve braze with acceptable mechanical strength.
- Achieve visually acceptable joints with minimal distortion and acceptable strength values and failure modes.

The laser brazing parameters controlled during this investigation and their effects on the brazing process are described below.

a) Laser beam power: Changes in beam power were investigated to implement corresponding changes in heat input

b) Laser beam defocused position: Changes in beam focus position resulted in changes in energy and thus power densities, and the interaction time of a given point in the material with that of the beam as brazing proceeded.

c) Filler wire type: The use of AlSi12, AlMg5, ZnAl15 and FCW was examined, to alter the inherent properties of the braze wire or its deposit (e.g. strength, melting point, wetting on to the parent materials) and the chemical elements present, to influence the compositions and extent of the IMC present between the braze deposit and the parent steel.

d) Welding speed: Changes in welding speed also resulted in changes in heat input, and the time available at a given point in that material for that heat input to have an influence, e.g. in diffusion-driven reactions.

e) Beam biasing either side of the joint line: Changes in beam positioning with respect to the joint could be used to change the amount of heat input into the aluminium, and that into the steel. Beam biasing either side of the joint line: 0 to 1mm either side

f) Use of either a single spot or twin spot focusing optic: Using a twin spot optic and changes in the configuration of, and energy balance between, those two spots was an additional means of influencing energy and power densities, and interaction times of different points across the joint with the beam. In particular, using a twin spot optic added complication, but greater potential flexibility, in these respects, e.g. allowing for possible preheating of the steel prior to it being covered with the molten braze material, to encourage wetting.

The twin spot optic resulted in a separation of 0.6mm between the centres of two beams, when measured in the focal plane (albeit these two beams were used out of focus). Although the twin spot optic was designed to provide two spots of equal power distribution (50:50), the two spots can be of varied ratio (up to 30:70) of the overall laser power. Figure 3.6 shows the plot of the energy profiles resulting from these single spot and twin spot focusing optics, respectively, when used at a large positive defocus of +36, +38 and +40mm. When the beam spot was at a positive defocus of +36mm which showed the most preferred brazing results, the spot diameter was 3.7mm and the power density was varied from 0.09kw/mm^2 to 0.65kW/mm^2 while the laser power was applied from 1kW to 7kW. This plot was generated by the commercial software programme Prolas, version142.

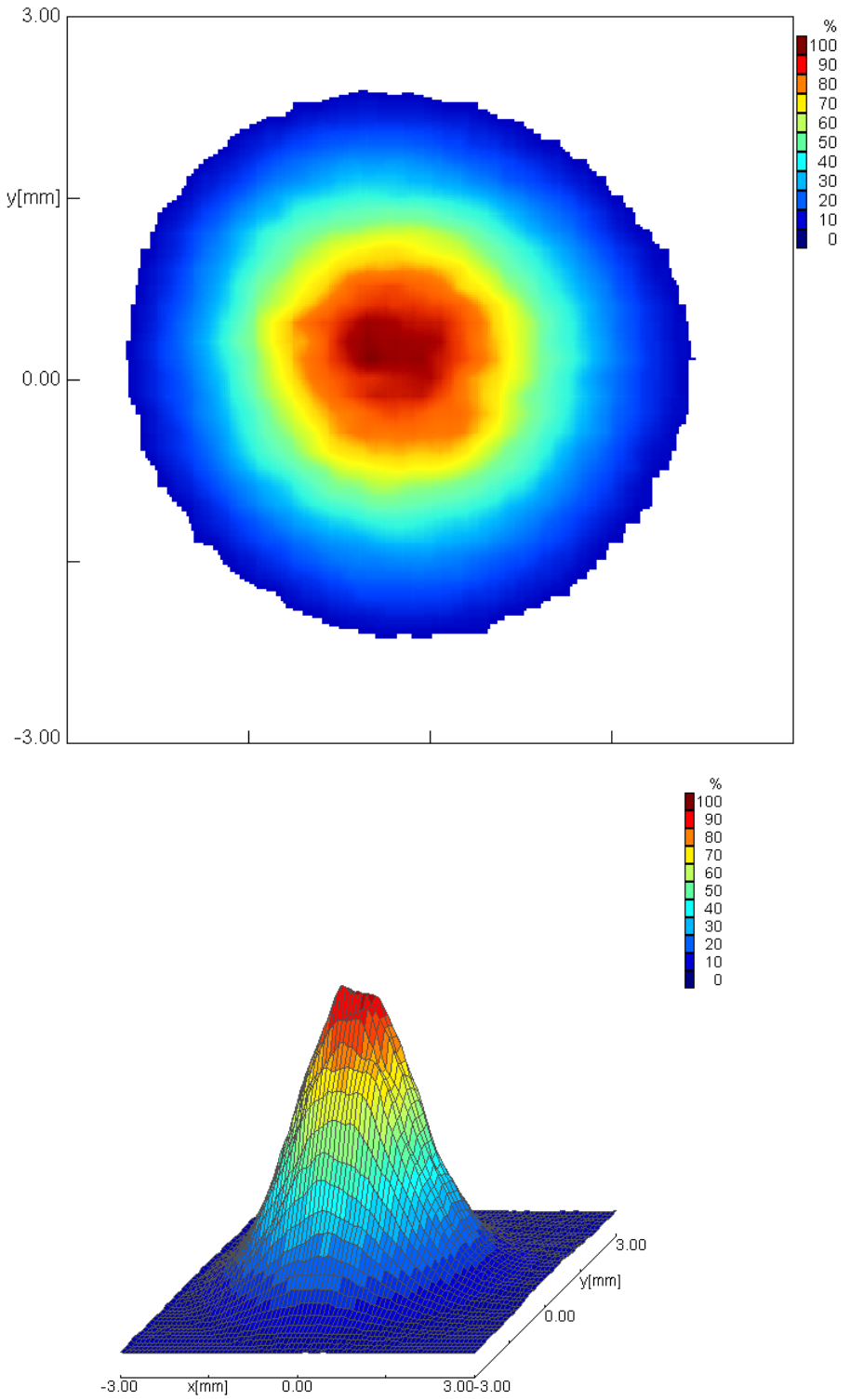

a) Single Spot

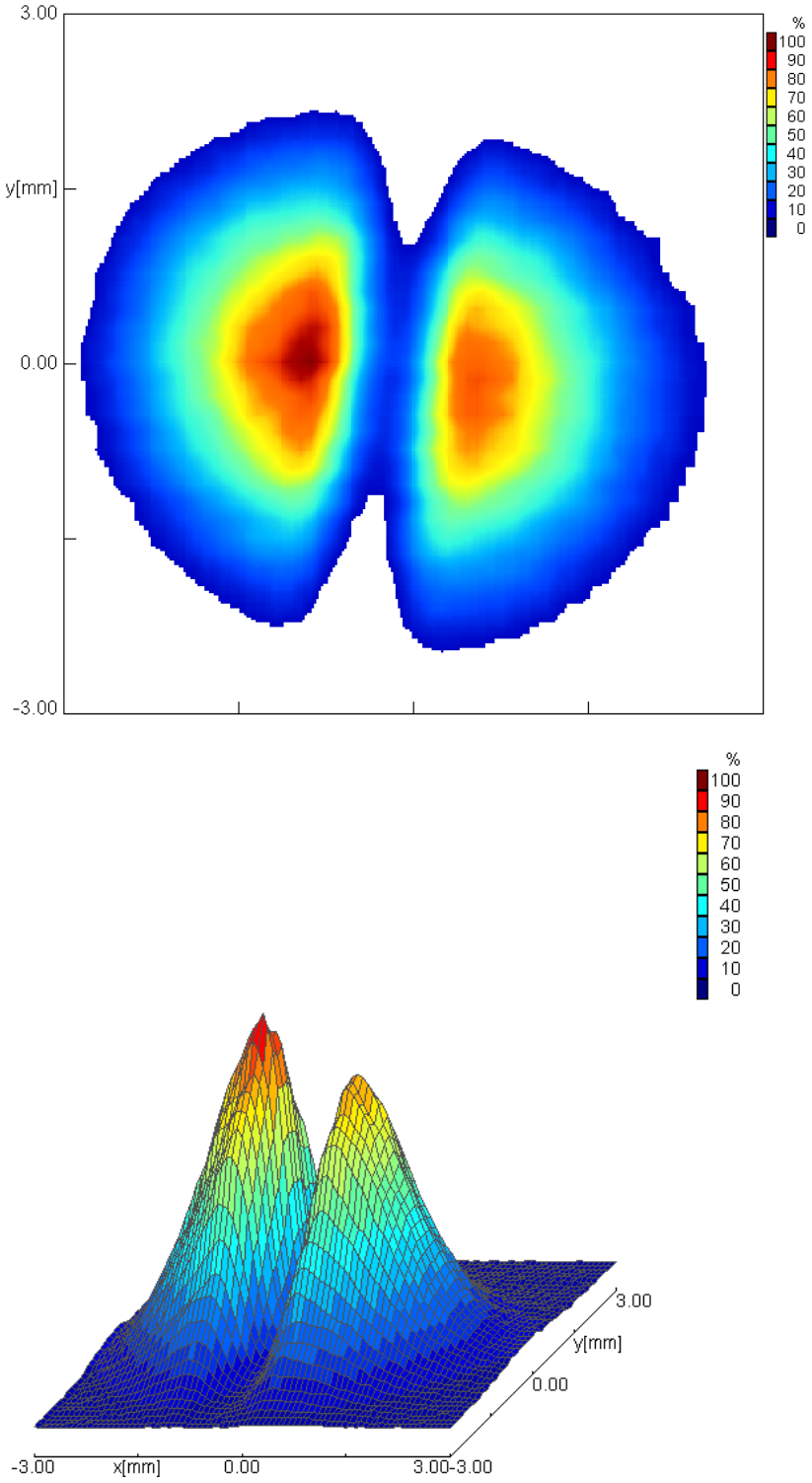

b) Twin Spot

Figure 3.6) Energy profiles resulting from the focussing optic on +36mm defocusing plane

The twin spot optic was used in a leading and trailing configuration, i.e. the two spots were aligned along the joint between the work pieces, see Figure 3.7.

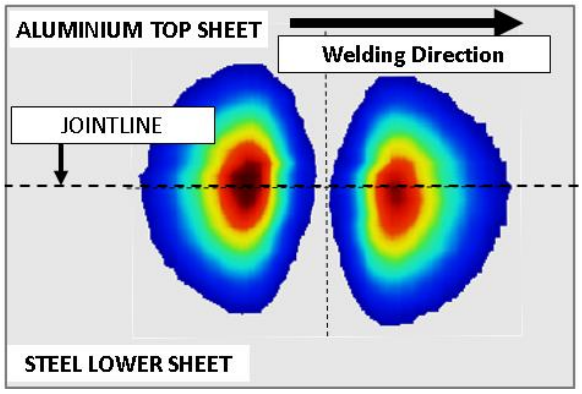

Figure 3.7) The twin spot configuration on the joint line of parent materials

g) Wire feed rate: Changes in wire feed rate resulted in changes in the amount of braze material being added per unit length of joint, and thus the size of the braze deposit which affects the weld width and throat width. Importantly, changes in wire feed rate also affected the amount of heat input available, between wire melting, melting of an amount of the aluminium alloy (with which the braze wire welds) and heating of the parent steel (needed for braze wetting and flow, but to be minimised to control IMC formation at the interface between the braze deposit and the parent steel).

h) Wire feed angle in the travel plane: Changes in the wire feed angle change the volume of wire exposed under the beam, therefore a larger wire feed angle increased the length of wire exposed to the beam and will require greater beam energy to melt, and a lower wire feed angle decreases the length of wire exposed to the beam and requires less beam energy to melt, resulting in greater beam energy interacting with the parent materials.

i) Wire-to-joint-line angle in the work plane: Changes in wire feed angle in the work plane affect the solidified braze bead geometry and also the region of the shadowing effect, resultant of the beam interacting with the wire surface.

j) The wire separation distance: Changes in the wire separation distance affect the amount of the beam's energy that is used to heat and melt the wire, and beam energy used to heat the material surface.

k) Laser beam angle in the travel plane: Changing the laser beam angle in the travel plane mainly ensures that reflected light does not damage the optics, but also changes the beam circularity on the material surface.

l) Laser beam angle in the work plane: Changes in the laser beam angle in the work plane can affect the region of the joint that is to be heated by the beam, such as the steel surface beneath the edge of the aluminium top sheet.

m) Shielding gas flow rate: Insufficient gas flow rate can result in poorly shielded brazed joints, which could result in excess porosity due to oxidation. High gas flow rate can potentially result in turbulence of the solidifying melt pool, affecting visual appearance, weld width and weld throat to name a few. Shielding gas flow rate also influences the cooling rate of the braze joint, which can affect the influence of porosity prior to melt pool solidification.

The range of parameters evaluated is shown below.

a) Laser beam power: 1.0 to 7.0kW.

b) Laser beam defocus position: +36 to +46mm.

c) Filler wire type: 1.2mm and 1.6mm diameter AlSi12, 1.2mm diameter AlMg5, 1.6mm diameter 85%Zn-15%Al and 1.6mm FCW.

d) Welding speed: 1.0 to 4.0m/min.

e) Beam biasing either side of the joint line: 0 to 1mm either side.

f) Use of either a single spot or twin spot focusing optic: Both Single spot and twin spot optics were trialled.

g) Wire feed rate: 2.0 to 10.0m/min.

h) Wire feed angle in the travel plane: 40° to 50°, off the workpiece surface.

i) Wire-to-joint-line angle in the work plane: Constant at 0°.

j) The wire separation distance: 0mm to 2mm.

k) Laser beam angle in the travel plane: Constant at 10°, in the beam spot leading position.

l) Laser beam angle in the work plane: 22° from the vertical axis.

m) Shielding gas flow rate: 30l/min divided into 4 15mm via pipes.

3.5.2 Joining quality and property characterisations

To implement laser brazing in the production line of car manufacturers, certain mechanical properties of the laser brazed joints would need to be met. These were:

- During tensile testing, failure of the test specimens must occur outside of the joint interface, and into the local heat affected region in the aluminium sheet or in the aluminium parent material to achieve sound joint strength.
- To ensure the greatest possibility of this occurring, the braze width as a minimum must be of greater length than the thickness of the aluminium parent material (1.2mm) being used to make the joint.
- The throat depth of the braze seam should be made as large as possible to encourage failure not to occur through the braze throat region.
- A low braze angle was desired which can reduce the stress concentration at the toe of the braze region, to minimise crack initiation.
- Minimising the porosity content (i.e. through the avoidance of flux where possible), and maximising corrosion performance (i.e. by appropriate selection of filler wire and/or avoiding chlorine-based fluxes) were also discussed.

Processing characteristics would also need to be met:

- A minimum brazing speed of 3m/min is required, due to the associated tact time required to complete the laser brazing process on the vehicle. But, to achieve sound joint between aluminium and GA steel, brazing speed was decreased to 1m/min for GA steel braze.
- The brazing process must consist of a single step, and that multi-stage processing to produce the joints should not be considered.
- If possible, the laser brazing process would be completed in such a way that post-braze cleaning operations would be minimal, which could be achieved by using certain filler wire types that are known for producing the least amount of soot and fumes.
- Furthermore, the laser brazed joints would be visible to the vehicle end user, and hence must have a consistent appearance along the whole length of the joint, free from visible defects, such as large surface pores that would be seen after vehicle painting.

3.5.3 Qualitative methods undertaken to assess braze quality and property characterisations

In order to assess each laser brazed joint to ensure it met the requirements, a visual assessment was initially made. This was to inspect for the following:

- A bright silver appearance; as this is evidence that suitable gas shielding took place, which also has implications on the internal porosity content.
- Surface porosity; which can imply that internal pores are also present.
- Braze width and throat depths and their consistency along the sample length
- Heat marks on the rear of the steel sheets; can provide insight into the consistency of the laser brazed joint.

After a visual assessment was made, a bend test was performed by hand. This would provide an early indication of joint strength, and was used to determine whether further samples with the same brazing conditions would be made for quantitative evaluation.

3.5.4 Quantitative methods undertaken to assess braze quality and property characterisations

Selected laser brazed joints were subjected to the following quantitative test methods:

- X-ray radiography was used to detect any internal imperfections or defects, e.g. pores or cracks.
- A metallographic cross-section to measure key dimensions (e.g. fused width at the joint interface, throat depth etc), and to reveal any imperfections or defects, if present in the plane of the section taken. The cross-section also allowed IMC layer thickness to be quantified by light microscopy.
- Micro hardness surveys were carried out, as a first indication of the relative strength of the braze seam and its HAZs with respect to the surrounding parent materials.
- Scanning Electron Microscopy (SEM), Energy-Dispersive X-Ray (EDX), and nano-hardness testing were carried out to provide semi-quantitative data on the elemental structure and phase of the IMC.
- Tensile shear testing, to understand the mechanical performance of the brazed joint.

3.6 Summary

Overlap and flare bevel groove joints between AA6451 and GA/GI steel were used for LWB tests. The materials were cleaned in an acetone ultrasonic bath before brazing. And four different filler wires, AlSi12, ZnAl15, AlMg5 and FCW were chosen to braze the joints.

IPG cw Yb-fibre laser with single or twin spot beam was used to melt filler wire and aluminium base metal. The effects of experimental parameters were investigated to achieve sound joint strength. One of the main goals was to avoid the interfacial failure of tensile specimens. Before cross section analysis and tensile shear tests on the down selected joints, visual assessments and simple bending tests were performed.

4. Results

4.1 Overview

The overlap joint and the flare bevel groove joint shown in Figure 3.2 were examined in the order written. These joints were made with two different material combinations, aluminium-GA steel sheets and aluminium-GI steel sheets. These joints were brazed using four different brazing wires.

4.2 Laser brazing of overlap joints

4.2.1 Processing parameters

Close to 300 overlap joints were brazed and Appendix A gives a detailed summary of all the trials that were performed in chronological order, the technical reasoning for each trial and the findings from each trial, which was then used to steer future project work.

Table 4.1 summarises the laser brazing trials made in the overlap joint configuration, in terms of the different combinations of wire types and base steels used. The base steels that have been used for the trials were GA and GI steels. Laser brazing trials have focussed on optimising joining parameters using 1.2mm AlSi12 wire, 1.2mm AlMg5 wire, 1.6mm ZnAl15 wire and 1.6mm FCW.

Wire types	Base Steel	
	GA	GI
1.2mm AlSi12	✓	✓
1.2mm AlMg5	✓	
1.6mm ZnAl15 wire	✓	
1.6mm FCW	✓	

Table 4.1) Laser brazing trials made in the overlap joint configuration

Table 4.2 summarises the brazing conditions selected from the trials for further evaluation. As described in Section 3.5.3, these conditions were selected on the basis of producing the most visually acceptable results and indicating good bend test results. The brazing parameters are defined in Figure 3.6.

Sample Number	Base steel	Wire type	Laser moving speed, m/min	Beam Focal Position, mm	Laser power, kW	Wire feed rate, m/min	Wire-to-joint-line angle, degrees	Number of beams	Beam distribution Trailing beam%/ leading Beam %	Beam bias off joint line, mm
A1	GA	1.2mm AlSi12	3	36	4.5	8	45	Twin L+T	70/30	1mm to steel
A2	GA	1.2mm AlSi12	3	46*	4.5	8	45	Twin L+T	70/30	1mm to steel
A3	GA	1.2mm AlMg5	3	36	4.5	8	45	Twin L+T	70/30	1mm to steel
A4	GA	1.6mm ZnAl15	3	46*	6.0	10	0	Twin L+T	70/30	0.5mm to steel
A5	GA	1.6mm FCW	3	46*	6.0	10	0	Twin L+T	70/30	0.5mm to steel
A6	GI	1.2mm AlSi12	3	46*	5.0	10	45	Twin L+T	70/30	1mm to steel

Key: * = Trials conducted with 200um fibre rather than 150um fibre, therefore +46 focus results in the same spot size at the material surface.
Key: L+T = leading and trailing twin spot configuration.

Table 4.2) Laser brazing conditions selected in the overlap joint configuration for further evaluation from visual inspection

4.2.2 Internal qualities of down-selected brazed joints

Table 4.3 summarises the porosity contents of selected brazed joints, as determined from pore counting of the radiographs. Figure 4.1 shows an example of an x-ray image and pores in braze deposit are seen as black dots. The number and size of dots are measured to calculate the porosity area fraction.

Sample Number	0.1 mm Count	0.2mm Count	0.3mm Count	0.4mm Count	0.5mm Count	1 mm Count	Accum. length, mm	Area of total pores, mm^2	Porosity area fraction
A1	4	1	0	0	0	0	0.6	0.28	0.2%
A2	0	3	5	0	0	0	2.1	3.46	2.9%
A3	4	1	0	0	0	0	0.6	0.28	0.2%
A4	2	5	1	0	0	0	1.5	1.77	1.5%
A5	0	2	0	0	2	4	5.4	22.89	19.1%

Table 4.3) Overlap joint configuration - Internal porosity contents of selected brazed joints

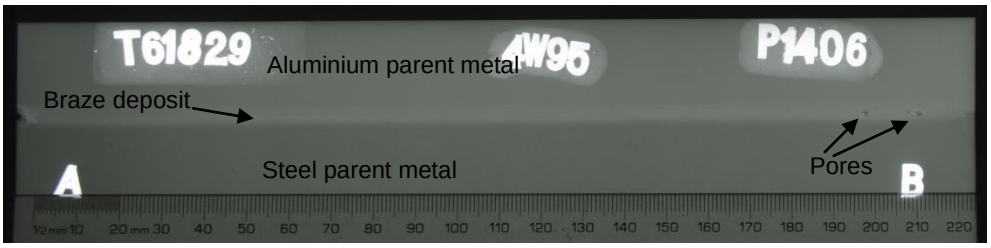

Figure 4.1) X-ray image of a brazed joint shows pores

As Table 4.3 shows, the laser brazing conditions applied to GA base steel and 1.6mm FCW (A5) had the highest area of total pores, which corresponds to a porosity area fraction of 19.1%. This was much greater than the other brazes made with AlSi12 wire and ZnAl15 wire, which had porosity area fractions of 0.2 to 2.9%.

4.2.3 Critical dimensions of down-selected brazed joints

Figures 4.3 to 4.8 show the cross-sections taken from each of the brazed joints selected. The widths of the braze deposits were measured from these sections, as were the throat depths and braze bead contact angle of each. Figure 4.2 is a schematic of the cross section of the overlap joint with the critical dimensions.

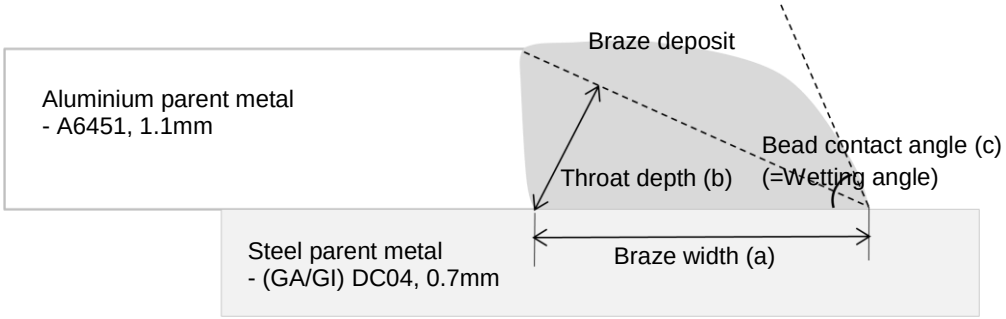

Figure 4.2) Schematic of a cross section of the overlap joint with critical dimensions

These dimensions are summarised in Table 4.4.

Sample number	Braze width mm	Throat depth mm	Wetting angle °
A1	2.9	1.5	41.3
A2	2.8	1.6	47.1
A3	2.2	1.6	62.3
A4	3.3	2.5	62.5
A5	4.3	2.6	37.9
A6	3.3	2.2	39.6

Table 4.4) Critical dimensions of selected braze joints – braze width, throat depth and wetting angle

The brazed width (a) varied between 2.2mm (sample A3, GA base material, 1.2mm AlMg5 filler wire) to 4.3mm (sample A5, GA base material, 1.6mm FCW).

The throat depths (b) varied between 1.6mm (sample A3, GA base material, 1.2mm AlMg5 filler wire) to 2.6mm (sample A4, GA base material, 1.6mm FCW.

The braze bead contact angles (c) ranged from 39.6° (sample A6, GI base material, 1.2mm AA4047wire) to 62.3° (sample A3, GA base material, 1.2mm AA5556wire).

These dimensions could be a result of the laser brazing parameters used, however efforts were made to increase the braze width in the selected joints either by increasing wire feed rate to increase the volume of braze material present, and also to bias the beam and wire feeding location onto the steel as much as possible, whilst still interacting with the aluminium top sheet. It is likely that the viscosity of the different wires and their wettability onto the different base steels is a highly contributing factor to braze width, throat depth and braze bead contact angle.

Figure 4.3 shows the laser brazed joint made using GA base steel, and 1.2mm AlSi12 filler wire, sample A1. This joint was made with a leading and trailing spot configuration with the lower power laser spot leading; this configuration was found to reduce porosity, in comparison with joints made with similar parameters but using a single beam, side by side spots or leading and trailing spots where the higher power spot was leading.

Figure 4.4 shows the laser brazed joint made using GA base steel, and 1.2mm AlSi12 filler wire, sample A2. This joint was made with a leading and trailing spot configuration with the lower power laser spot leading; this configuration was found to reduce porosity, in comparison with joints made with similar parameters but using a single beam, side by side spots or leading and trailing spots where the higher power spot was leading. There is a region where zinc porosity is visible at the interface between the steel and the aluminium, although this was minimised through experimental trials to optimize the beam biasing of the joint line and the energy distribution of the dual beam.

Figure 4.5 shows the laser brazed joint made using GA base steel, and 1.2mm AlMg5 filler wire, sample A3. A sample made with the same parameters performed well during a bend test performed by hand. However, as seen in this cross section, the specimen fractured at the interface during metallographic preparation.

Figure 4.6 shows the laser brazed joint made using GA base material and 1.6mm ZnAl15 filler wire, sample A4. It can be seen that the surface of the steel was exposed to too high a heat input, causing the surface of the steel to melt. In this cross section, no zinc porosity can be seen at the interface region.

Figure 4.7 shows the laser brazed joint made using GA base steel, and 1.6mm FCW, sample A5. The cross-section shows good wettability onto the steel surface, leading to a wide braze width of 4.3mm, and a correspondingly large throat depth of 2.6mm, which are the largest dimensions on all of the samples made in the overlap configuration.

Unfortunately, there is interface porosity which will inevitably reduce the effective braze width and therefore the strength of the joint. There are also large amounts of porosities seen in the matrix of the braze deposit. This will affect the strength of the braze deposit, which is detrimental to the braze strength if failure would occur through the throat region.

Figure 4.8 shows the laser brazed joint made using GI base steel, and 1.2mm AlSi12 filler wire, sample A6. It is apparent that there is a high level of wettability of the braze deposit onto the steel surface, as the braze angle is very low (approx. 40°).

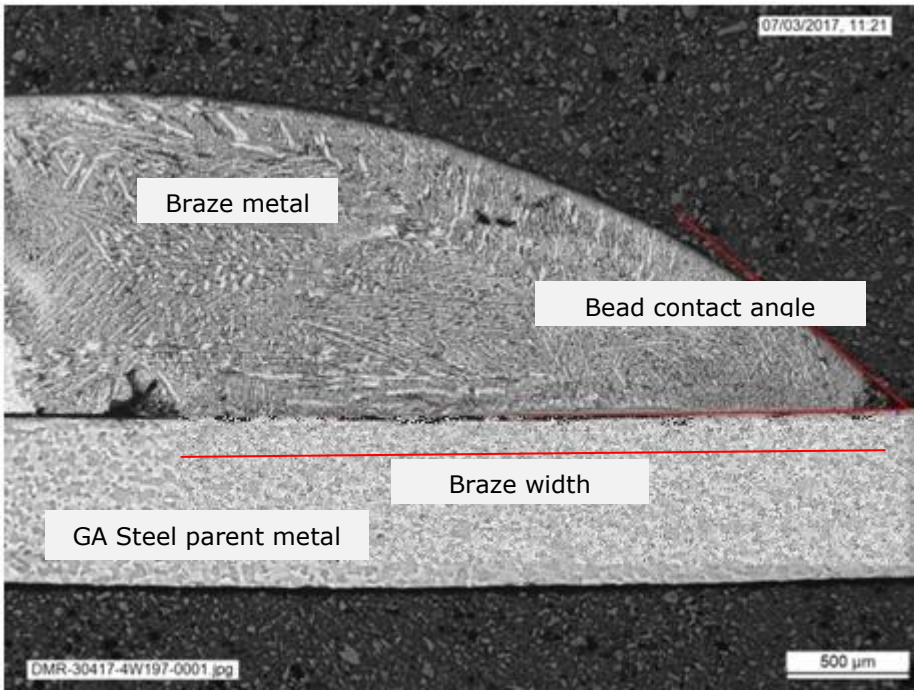

Figure 4.3) Cross-section of A1 (GA, 1.2mm AlSi12 filler wire)

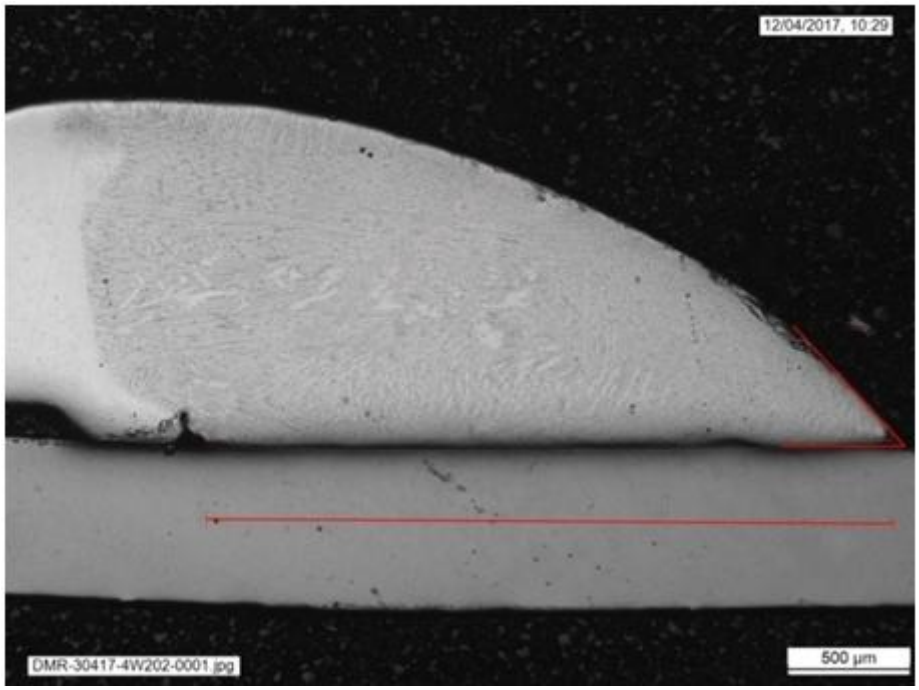

Figure 4.4) Cross-section of A2 (GA, 1.2mm AlSi12 filler wire)

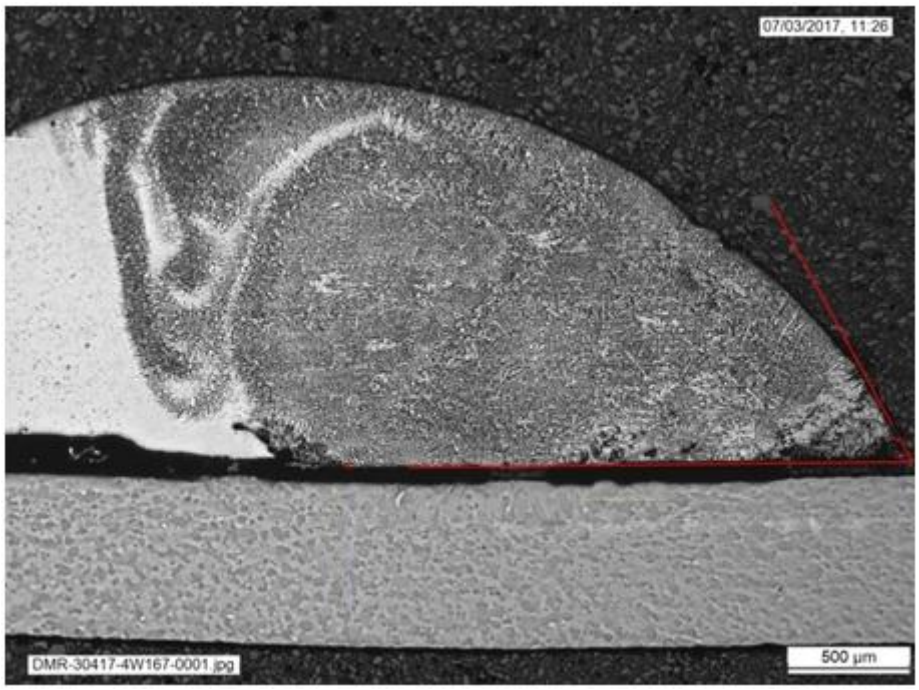

Figure 4.5) Cross-section of A3 (GA, 1.2mm AlMg5 filler wire)

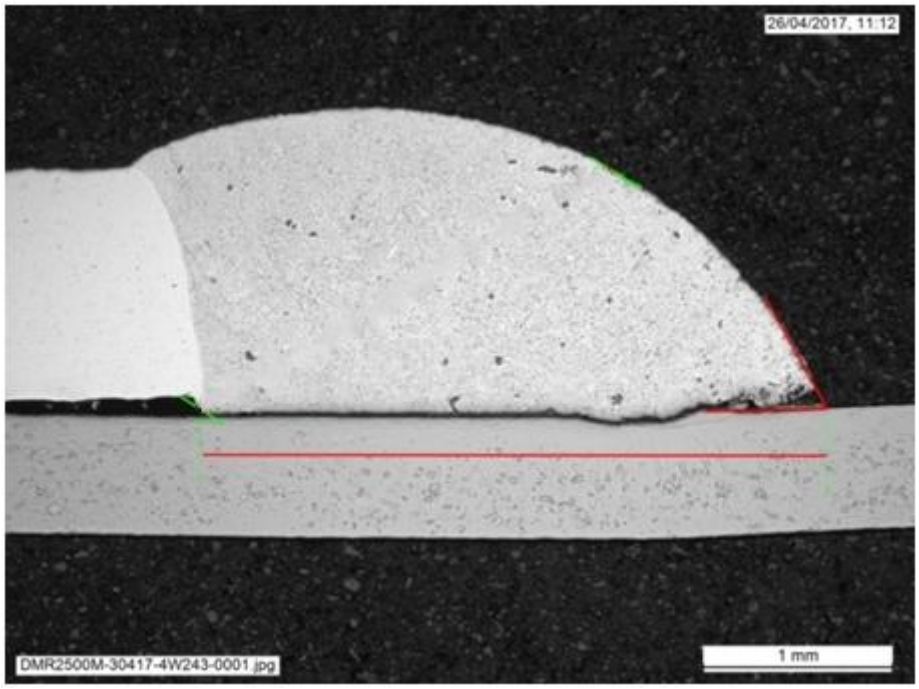

Figure 4.6) Cross-section of A4 (GA, 1.6mm ZnAl15 Filler wire)

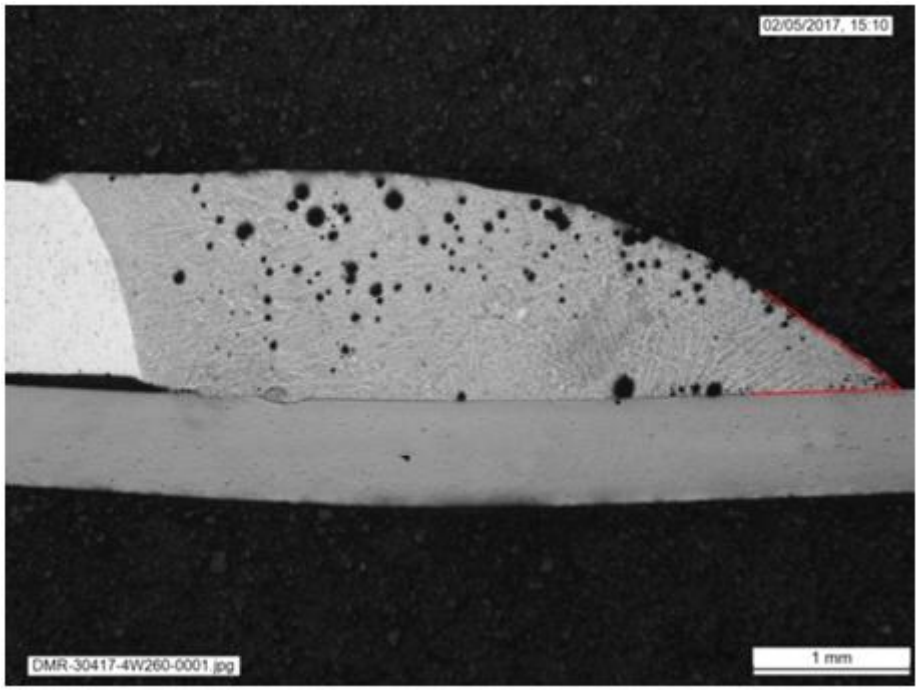

Figure 4.7) Cross-section of A5 (GA, 1.6mm FCW)

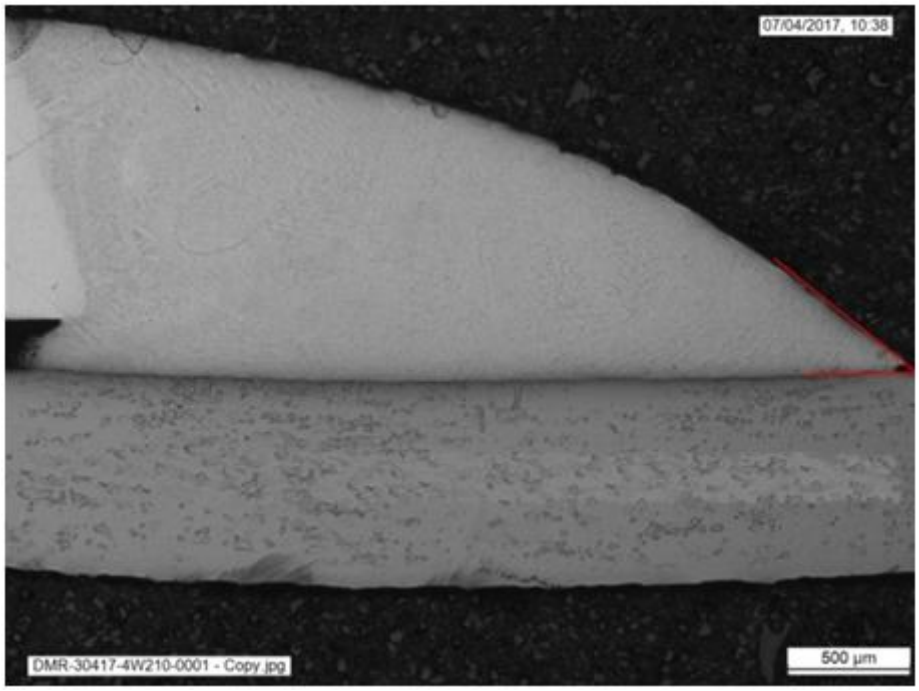

Figure 4.8) Cross-section of A6 (GI, 1.2mm AlSi12 filler wire)

4.2.4 IMC thicknesses in down-selected brazed joints

Figures 4.9 to 4.14 show optical microscopy images of the IMC layers at the interface regions of the selected brazed joints. This section details the thickness of the IMC layers and the number of layers seen.

Figure 4.9 shows the IMC formed in A1 at the interface between the GA base steel and the braze metal. The IMC layer thickness is up to 5µm thick close to the toe of the braze and in regions under the aluminium top sheet. However, the IMC layer thickness increases to up to 45µm at the hottest part of the braze which likely relates to the most intense part of the laser beam that interacted with the braze. There are two types of IMCs present, cracks can be seen between these two compounds, but also in regions between the steel and IMCs.

Figure 4.10 shows the IMCs formed in A2 at the interface between the GA base steel and the braze metal. The IMC layer was typically 5-10µm in thickness, however larger IMCs are present at the region where the laser beam was positioned onto the sample, resulting in a maximum IMC layer thickness of 35µm. No cracks were observed between the base steel and IMC layer, or within the IMC layer.

Figure 4.11 shows the IMCs formed in A3 at the interface between the GA base steel and the braze metal. Typical IMC layer thickness was in the range 9-14µm, relatively evenly distributed through the sample

braze width. Towards the toe of the braze material, the IMC layer has lifted into the matrix of the braze deposit as can be seen in the figure.

Figure 4.12 shows the IMCs formed in A4 at the interface between the GA base steel and the braze metal. The IMC layer was 7-21µm in thickness.

Figure 4.13 shows the IMCs formed in A5 at the interface between the GA base steel and the braze metal. Two types of IMCs were observed, which typically have a total layer thickness of ~9µm. Towards the toe of the braze, the IMC layer thickness of both of these compounds decrease to ~4µm.

Figure 4.14 shows the IMCs formed in A6 at the interface between the GI base steel and the braze metal. There appear to be two types of IMCs visible, a solid layer closest to the surface of the steel that has a thickness of approximately 7µm, and a more irregular layer that breaches into the braze deposit. Some cracks were observed between the two layers of IMCs.

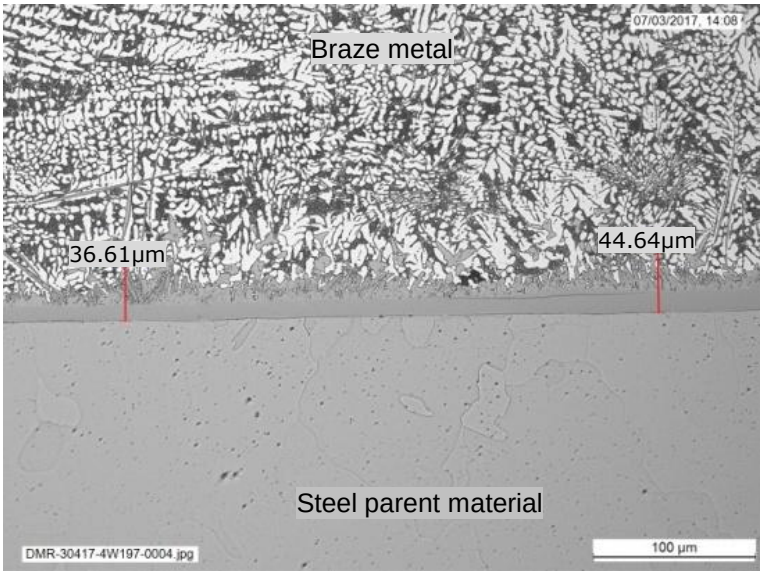

Figure 4.9) Optical microscopy images of the IMC layer from A1

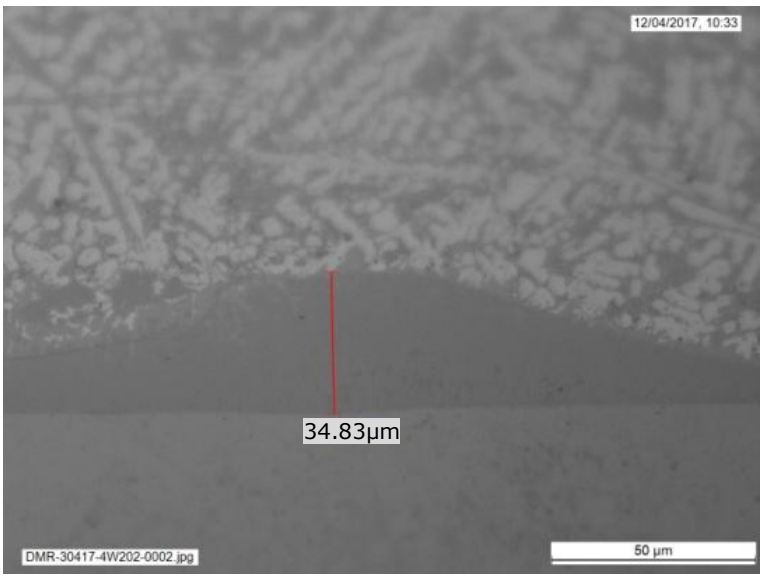

Figure 4.10) Optical microscopy images of the IMC layer from A2

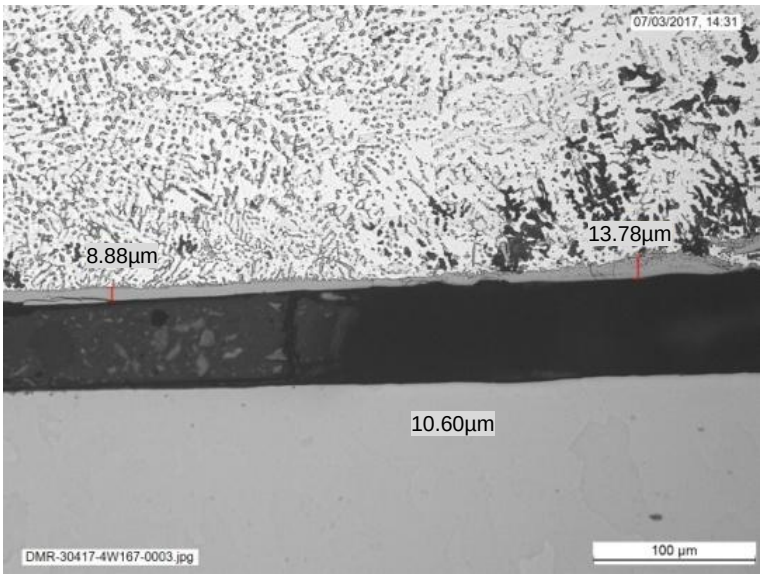

Figure 4.11) Optical microscopy images of the IMC layer from A3

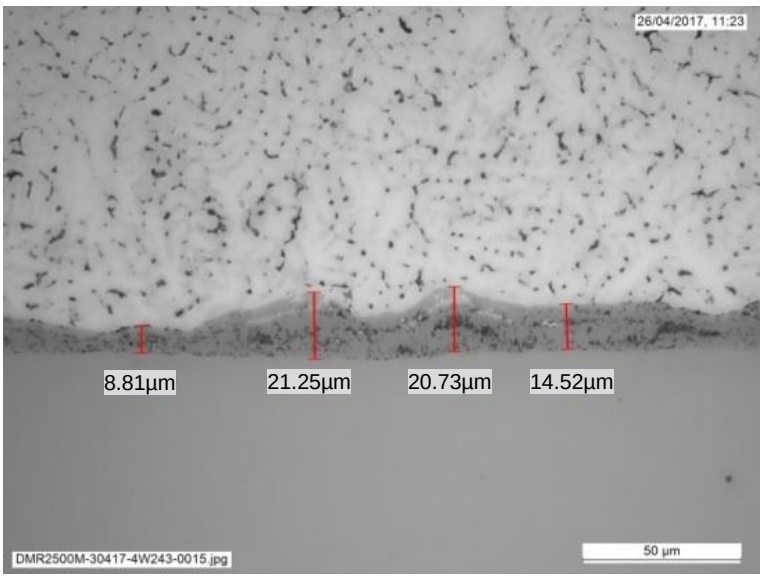

Figure 4.12) Optical microscopy images of the IMC layer from A4

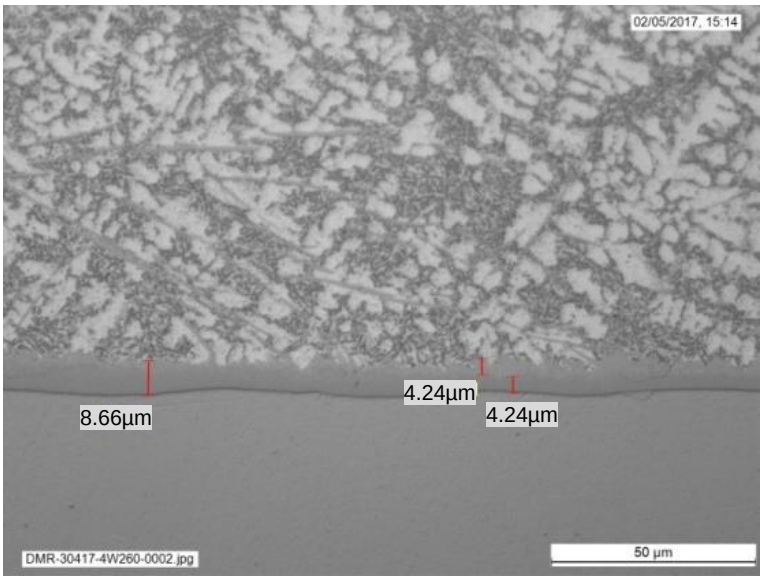

Figure 4.13) Optical microscopy images of the IMC layer from A5

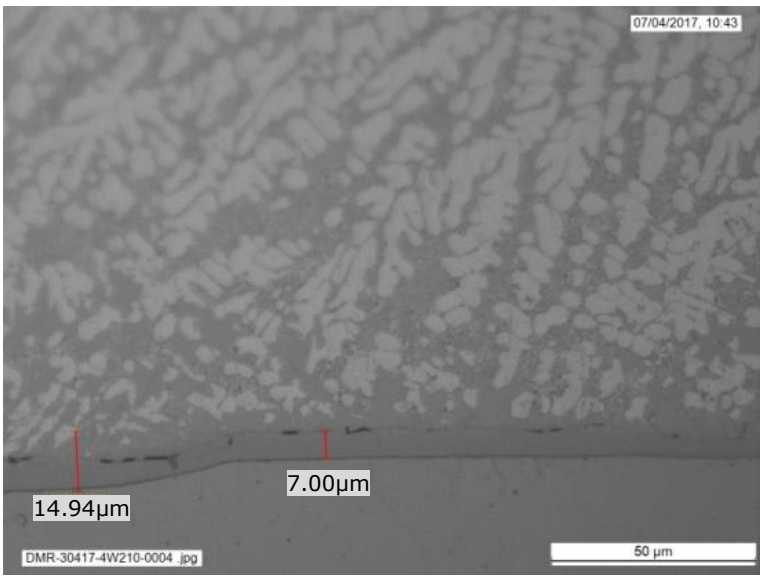

Figure 4.14) Optical microscopy images of the IMC layer from A6

4.2.5 Electron microscopy and nano-hardness of down-selected brazed joints

Sections of brazed joints made phase analysis via scanning with the various filler wire compositions were examined by SEM (scanning electron microscopy) to better view the IMC layer. An analysis of the elements in the IMC layer was performed by employing semi-quantitative EDX (energy dispersive x-ray spectroscopy); using this technique the at. % of elements within the various phases were quantified to help identify the IMC phases present. Specimens were also submitted for nano hardness measurements of the phases present. The nano hardness data was converted to Vickers hardness equivalent in accordance with ISO14577-2, the hardness data was used with the EDX analysis to help identify the IMC phases present. Red arrows in Figures 4.15-4.20 indicate IMCs performed EDX analysis or nano hardness measurement for A1-A6.

Figure 4.15 shows an SEM image of A1 (GA base steel with a 1.2mm AlSi12 filler wire). EDX 1 is taken in the dense continuous region of the IMC layer on the surface of the steel. A value of 27.7at% for Fe in Al, strongly suggests that this phase is Fe_2Al_5, although, significant Si (6.9at%) was also present, indicating there could also be some ternary phase or Si in solution. The nano hardness measurements of Loc 1, Loc 3 and Loc 5 confirm that the phase is likely to be Fe_2Al_5 and that the presence of Si has not reduced the hardness of the phase. EDX 2 was taken in the finger like IMC growth that entered the Al rich braze zone, this phase was 20.5at% Fe and likely to be $FeAl_3$, but with 6.8at% Si, the ternary phase may also have been present, or Si in solution. Nano

hardness of Loc 2 and Loc 4 show a phase softer than expected for $FeAl_3$, this could be because of presence of Si or a ternary phase, or simply because the phase was very small and some partial indentation into the braze material occurred.

Figure 4.16 shows an SEM image of A2 (GA base steel with a 1.2mm AlSi12 filler wire). In this specimen the IMC layer is much thicker than in A1 (Figure 4.15) and more distinct zones were observed. In the hottest part of the joint EDX 1.1 – EDX 1.3 were taken. At the joint edge EDX 2.1 and EDX 2.2 were taken. EDX 1.1 was performed on the Fe rich finger like phase growing into the thicker continuous IMC layer. EDX 1.1 shows 39.3at% Fe and 7.5at% Si suggesting Fe_2Al_5 or even FeAl2 was present, along with some ternary phase of Si, or Si in solution. The rest of the matrix of the thicker continuous IMC layer was measured in EDX 1.2, which at 28.2at% Fe and 7.3 at% Si suggested Fe_2Al_5 and the ternary phase were present, or Si in solution. EDX 1.3 was taken in the finger like IMC phase entering the aluminium braze zone, which had a lower Fe content (1.8at% Fe, 61.at% Si) and was most likely $FeAl_3$. At the joint edge EDX2.1 was located in the dense continuous IMC layer (27.2at% Fe and 7.5at% Si), the composition suggests Fe_2Al_5 with some ternary phase, or Si in solution. EDX 2.2 was taken in the finger like IMC growth into the aluminium braze zone, once again the lower Fe levels (19.7at% Fe and 7.1at% Si) suggest $FeAl_3$ with some ternary phase, or Si in solution.

Figure 4.17 shows an SEM image of A3 (GA base steel with a 1.2mm AlMg5 filler wire). The brazed joint fractured during preparation of the specimen, with the fracture location being in the dense continuous region of the IMC layer. EDX 1 of this layer showed 28.3at% Fe present along with 2.3at% Si along with small quantities of Mg and Zn, this indicates Fe_2Al_5 was the main phase with some possible ternary phase present, or Si in solution. Nano hardness results (Loc 3) were low for Fe_2Al_5 suggesting that ternary phase was present. EDX 2 was taken in the same continuous layer, but closer to the Al braze material, the composition of 26.2at% Fe with around 1% Mg and Zn indicate Fe_2Al_5. Nano hardness of Loc 4 showed a value far too low for Fe_2Al_5 but this can be attributed to the indents being positioned onto very small areas of the Fe-Al phase within the softer braze material.

Figure 4.18 shows an SEM image of A4 (GA base steel with a 1.6mm ZnAl filler wire). EDX 1.1 and 1.2 were taken at the braze edge, where heat input was lower. EDX 1.1 was the aluminium braze zone and consisted of 1.4at% Al, 12.5at% Fe, with the remainder being zinc; this zone mainly consisted of the ZnAl filler material, but also contained a significant amount of Fe in solution. EDX 1.2 was taken from the continuous dense IMC layer at the surface of the steel. At 23.9at%Zn in Al, this is a Zn-Al IMC; no Fe-Al IMC was present here. EDX 2.1 was taken at the braze centre, in this area 23at% Fe and 6.7at% Zn in Al, this was probably $FeAl_3$ and ternary phase, or Zn in solution. The joint

also had a 'hot spot' where thermal deformation of the steel substrate had occurred. EDX 3.1 was taken in a thick area of an IMC penetrating into the steel substrate, this area contained 48at% Al and 1.5at% Zn in Fe and was most likely FeAl. EDX 3.2 was taken in the IMC layer above the FeAl, in contact with the braze material. The composition was 25.2at% Fe and 4.9at% Zn in Al, suggesting Fe_2Al_5 and ternary phase, or Zn in solution.

Figure 4.19 shows an SEM image of A5 (GA base steel with a 1.6mm AlSi12 flux cored wire). Two areas around the centre of the joint were examined. EDX1.1 was performed at the IMC growth into the braze zone, which appears granular in nature, rather than the fingers seen in brazed joints using AlSi12 wire without flux. EDX1.1 consisted of 13.1at% Fe and 9.2at% Si in Al, this composition is much lower in Fe than other IMC phases observed using 4047 wire without flux, and is very likely to be a ternary phase of Al-Fe-Si. EDX1.2 was performed on the continuous layer on the steel surface, which appeared to be Fe_2Al_5 with ternary phase (26.4at%Fe, 1.6at%Zn, 8.7at%Si in Al). EDX 2.1 was taken in an area of a thinner IMC layer, indicating a lower heat input, this area was also very low in Fe, suggesting that a ternary phase of Al-Fe-Si was present (13.6at%Fe, 11.6at%Si in Al).

Figure 4.20 shows an SEM image of A6 (GI base steel with a 1.2mm AlSi12 filler wire). EDX analysis was performed in two areas near to the joint centre. EDX1.1 was taken on the outer part of the IMC layer, which is thought to be ternary phase (12.3at%Fe, 8.7at%Si in Al). EDX1.2 was taken in the dense continuous IMC layer close to the steel substrate, this appeared to be Fe_2Al_5 with ternary phase, or Si in solution (27.7at%Fe, 2.7at%Zn and 7.4at%Si in Al). EDX2.1 was taken in an area of IMC layer that was located as an island within the braze zone, it appeared to be ternary phase (13.5at%Fe, 1.1at%Zn, 8.8at%Si in Al).

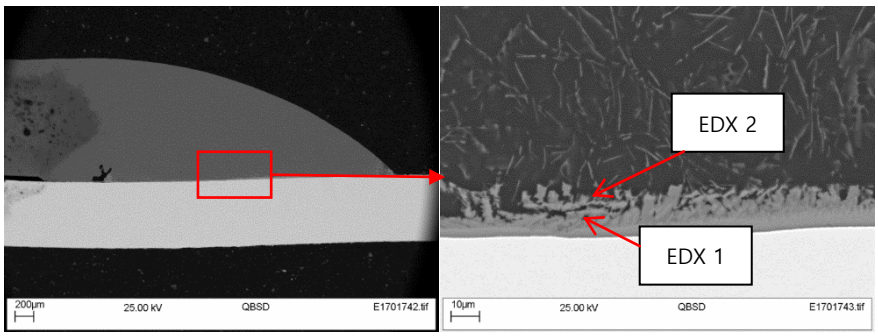

(at. %)

	Mg	Al	Si	Fe	Zn
EDX 1	0.3	Balance	6.9	27.7	0.4
EDX 2	0.4	Balance	6.8	20.5	02

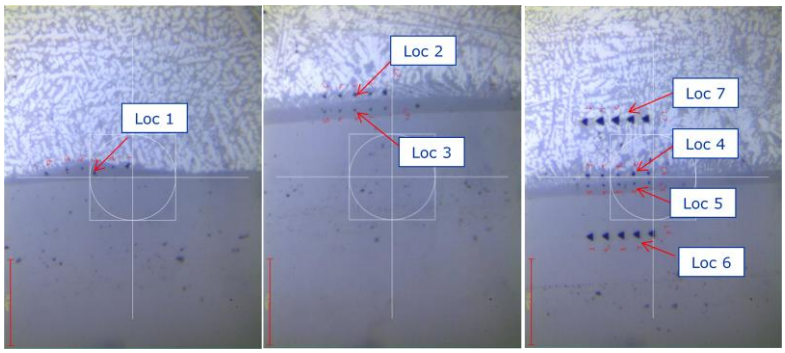

location of Nano-Hardness	Average Vickers Hardness (HV) of indents
Loc 1	1068
Loc 2	516
Loc 3	1085
Loc 4	679
Loc 5	1014
Loc 6	155
Loc 7	125

Figure 4.15) SEM and nano-hardness phase analysis of the IMCs for A1

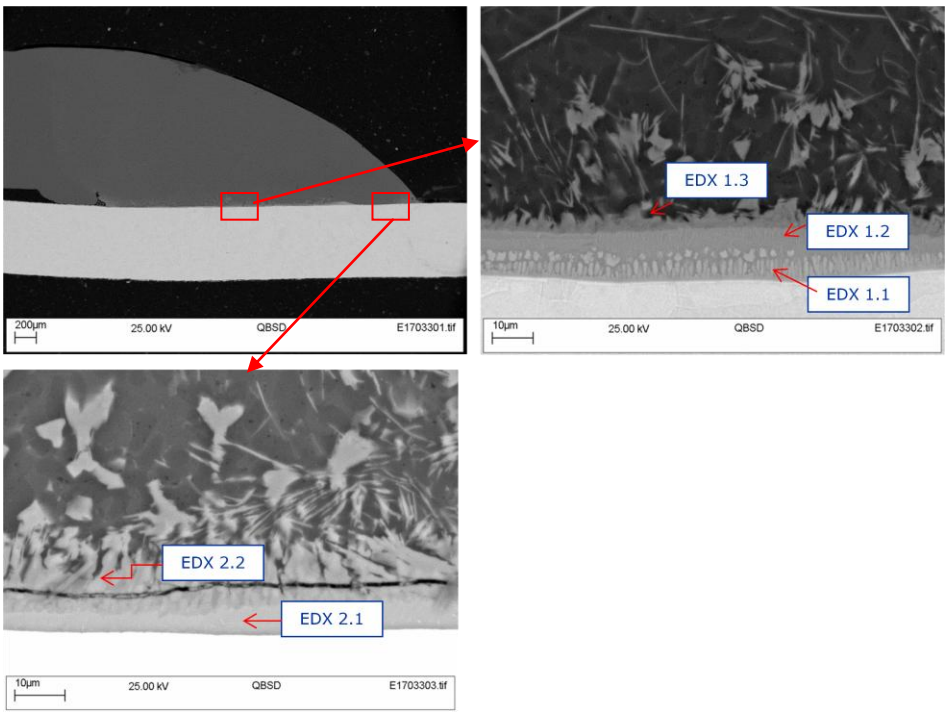

(at. %)

	Al	Fe	Zn	Si
EDX 1.1	Balance	39.3	0.9	7.5
EDX 1.2	Balance	28.2	1.3	7.3
EDX 1.3	Balance	18.4	0.4	6.1
EDX 2.1	Balance	27.2	0.6	7.5
EDX 2.2	Balance	19.7	0.4	7.1

Figure 4.16) SEM phase analysis of the IMCs for A2

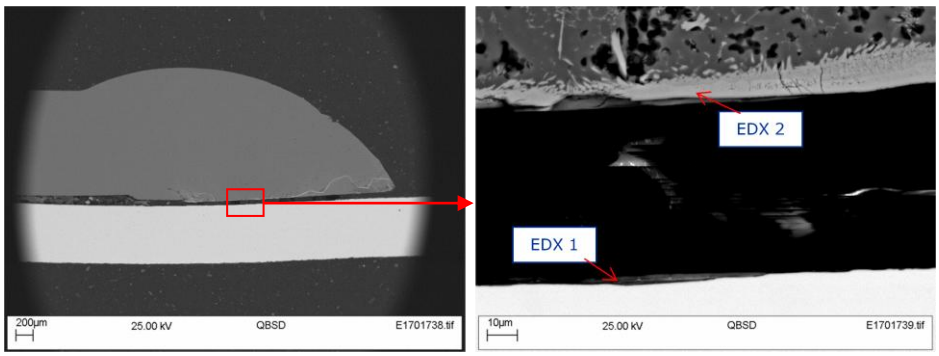

(at. %)

	Mg	Al	Si	Fe	Zn
EDX 1	0.5	Balance	2.3	28.3	0.6
EDX 2	1.0	Balance	0.1	26.2	1.1

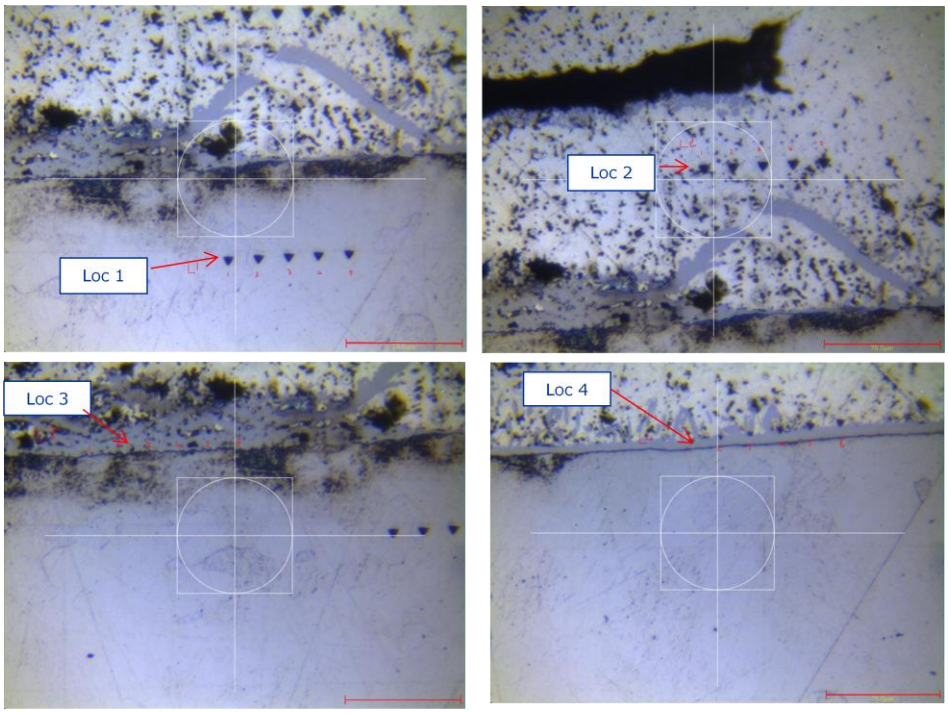

Location	Average Vickers Hardness (HV) of the indents
Loc 1	153
Loc 2	127
Loc 3	621
Loc 4	329

Figure 4.17) SEM phase analysis of the IMCs for A3 and nano-hardness of a sample with same base steel and filler wire

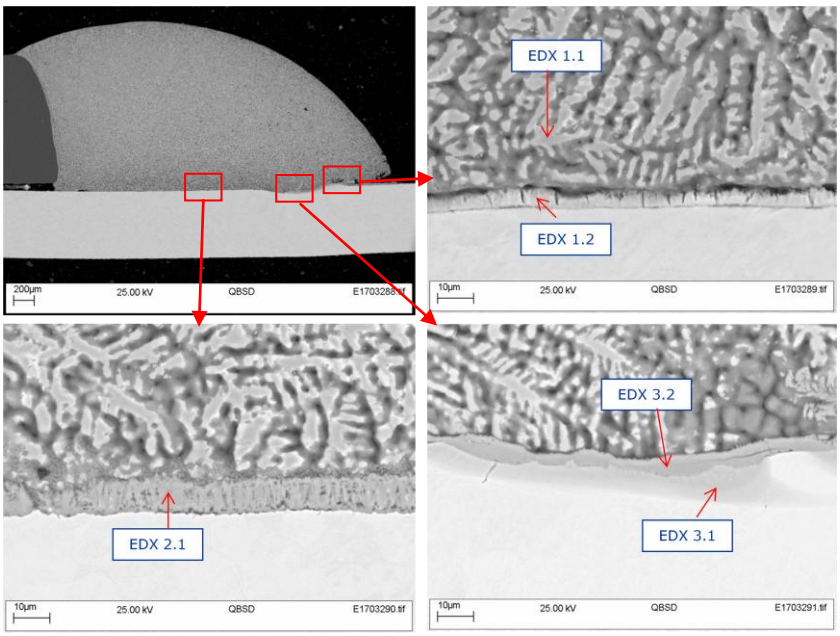

(at. %)

	Al	Fe	Zn	Si
EDX 1.1	14.1	12.5	Balance	
EDX 1.2	Balance	0.4	23.9	
EDX 2.1	Balance	23.0	6.7	
EDX 3.1	48.0	Balance	1.5	0.3
EDX 3.2	Balance	25.2	4.9	

Figure 4.18) SEM phase analysis of the IMCs for A4

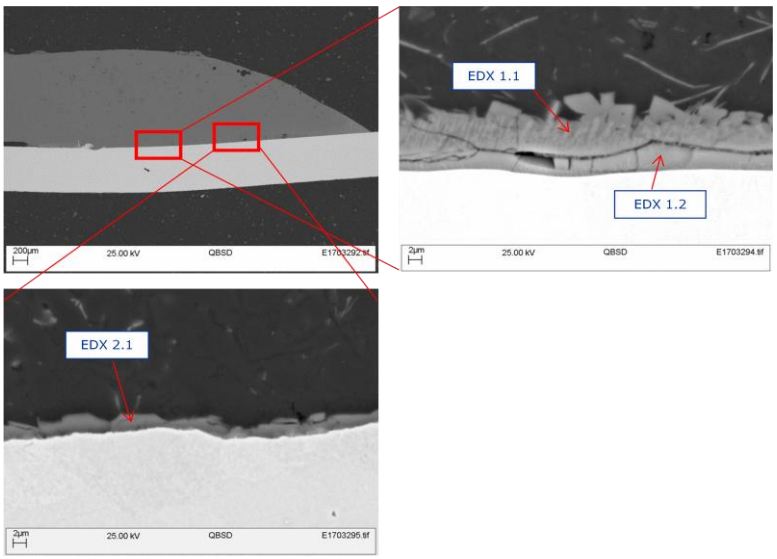

(at. %)

	Al	Fe	Zn	Si
EDX 1.1	Balance	13.1	0.3	9.2
EDX 1.2	Balance	26.4	1.6	8.7
EDX 2.1	Balance	13.6	0.3	11.6

Figure 4.19) SEM phase analysis of the IMCs for A5

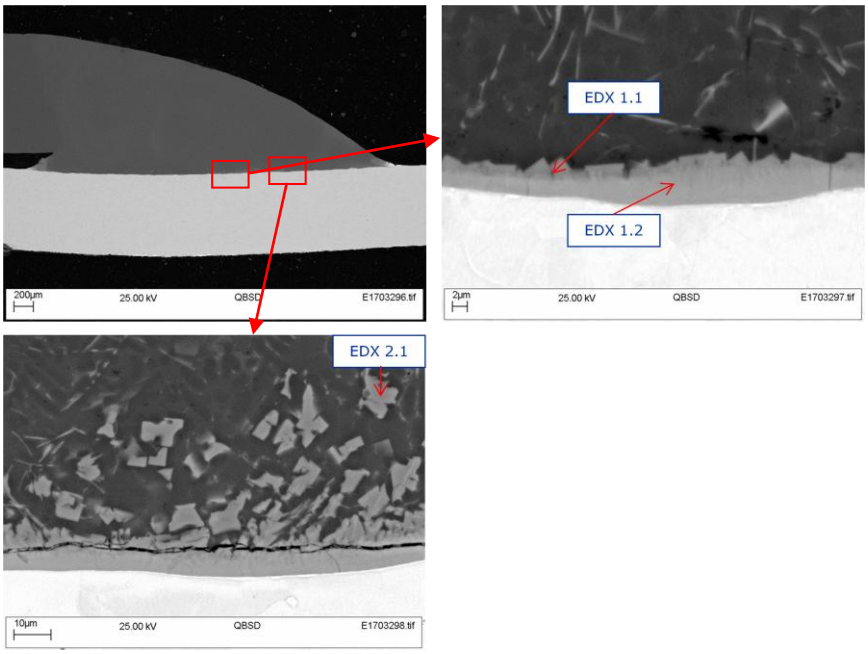

(at. %)

	Al	Fe	Zn	Si
EDX 1.1	Balance	12.3	0.3	8.7
EDX 1.2	Balance	27.7	2.7	7.4
EDX 2.1	Balance	13.5	1.1	8.8

Figure 4.20) SEM phase analysis of the IMCs for A6

4.2.6 Micro hardness surveys of down-selected brazed joints

Micro hardness tests were carried out using a diamond Vickers indenter with a load of 0.1kg, to ISO 6507-1:2005. Figure 4.21 shows example locations of the hardness indents made. The results of these indents are shown in Table 4.5. Diagonal length of indents by the Vickers indenter is in the range of micrometres and the precision of reading the indent size using optical microscopy is ± 0.5μm in length. It might lead to a substantial error in Vickers hardness according to indent size. The reason for wide variation from 88 to 109Hv for steel parents in A1-A6 can be explained by this measuring error.

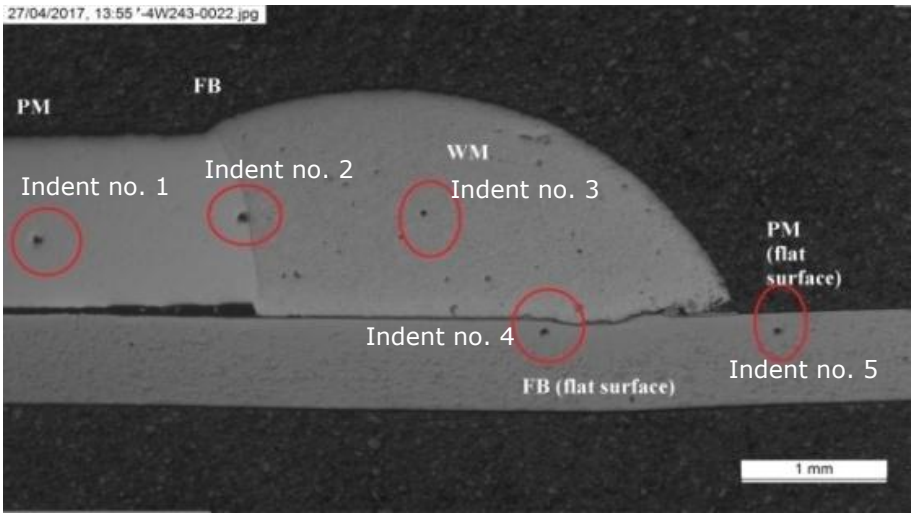

Figure 4.21) Image showing example locations of hardness indents in overlap joints

Sample No.	Indent No.	Indent location (see Figure 4.21)	HV
A1	1	Parent Metal Steel	88
	2	Fusion Boundary - steel to braze deposit	101
	3	Braze Deposit	88
	4	Fusion Boundary – aluminium to braze deposit	63
	5	Parent Metal Aluminium	61
A2	1	Parent Metal Steel	100
	2	Fusion Boundary - steel to braze deposit	103
	3	Braze Deposit	91
	4	Fusion Boundary – aluminium to braze deposit	66
	5	Parent Metal Aluminium	61
A3	1	Parent Metal Steel	92
	2	Fusion Boundary - steel to braze deposit	85
	3	Braze Deposit	79
	4	Fusion Boundary – aluminium to braze deposit	56
	5	Parent Metal Aluminium	59
A4	1	Parent Metal Steel	93
	2	Fusion Boundary - steel to braze deposit	99
	3	Braze Deposit	136
	4	Fusion Boundary – aluminium to braze deposit	56
	5	Parent Metal Aluminium	56
A5	1	Parent Metal Steel	109
	2	Fusion Boundary - steel to braze deposit	96
	3	Braze Deposit	84
	4	Fusion Boundary – aluminium to braze deposit	63
	5	Parent Metal Aluminium	62
A6	1	Parent Metal Steel (flat surface)	105
	2	Fusion Boundary - steel to braze deposit	105
	3	Braze Deposit	85
	4	Fusion Boundary – aluminium to braze deposit	63
	5	Parent Metal Aluminium	66

Table 4.5) Overlap joint configuration – HV0.1 Hardness data from cross sections of selected brazed joints

4.2.7 Tensile shear testing of down-selected brazed joints

Table 4.6 shows the tensile data from selected brazed joints, along with the corresponding equivalent brazed joints which have had their widths and throat depths measured. Up to three specimens were extracted from a single brazed coupon. Figure 4.22 is the schematic of the specimen with its dimensions.

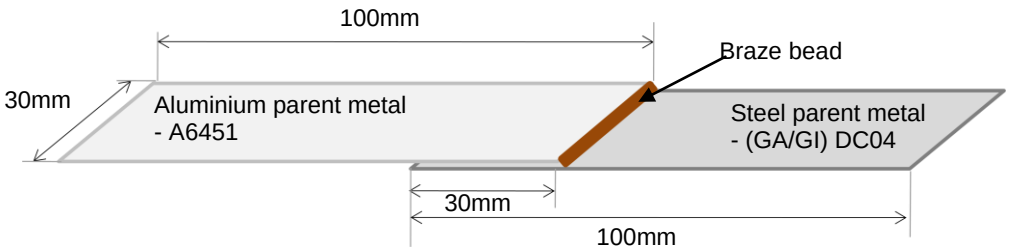

Figure 4.22 Schematic of the specimen for tensile tests

Sample number	Braze width mm	Throat mm	Fracture location	Failure strength kN	Displace-ment mm
A1	2.9	1.5	Interface	3.1	0.50
				2.9	0.45
				3.1	0.61
A2	2.8	1.6	Interface	2.5	0.40
				2.2	0.39
				2.3	0.35
A3	2.2	1.6	Interface	2.7	0.42
				2.3	0.25
				2.2	0.31
A4	3.3	2.5	Interface, partially braze deposit	3.8	1.91
				3.8	1.78
				3.6	1.44
A5	4.3	2.6	Interface	3.6	1.51
				3.5	1.38
				3.5	1.20
A6	3.3	2.2	HAZ	4.1	1.30
				4.7	2.34
				4.9	3.39

Table 4.6) Overlap joint configuration - Failure strengths and displacements to failure from tensile tests of selected brazed joints

The highest failure strength was seen in tensile sample A6 (GI base material, 1.2mm AlSi12 wire), with failure strengths ranging from 4.1 to 4.9kN. These failures occurred across the HAZ of the aluminium parent sheet, and not at the braze interface.

The second highest failure strength was seen in tensile sample A4 (GA base material, 1.6mm ZnAl15 wire), with failure strengths ranging from 3.5 to 3.8kN. These failures initiated at the interface, however the fracture path entered the braze deposit region, as seen in Figure 4.23.

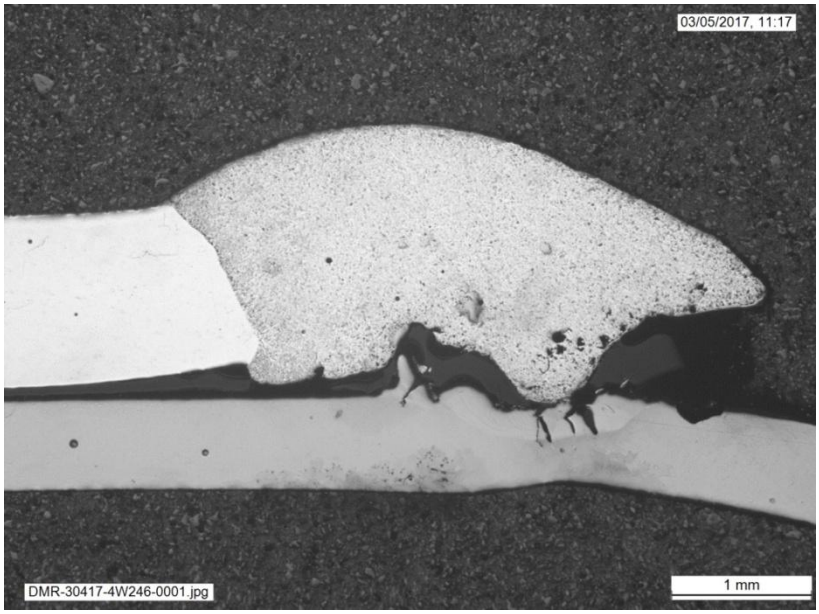

Figure 4.23) Image of tensile shear specimen after testing, GA base material using 1.6mm ZnAl15 filler wire

The specimens with FCW (sample A5) had similar failure strengths to A4, with failure strengths between 3.5 and 3.6kN. These failures however, occurred at the interface between the steel and braze deposit.

The weakest specimen was A2 where made with AA4043 wire, with failure strengths between 2.2 to 2.5kN.

4.2.8 Summary

All failures of the tensile specimens of overlap joints made at the laser moving speed of 3m/min occurred at the interface through the IMC region with exception of brazes of A6 and A4.

A6 made with GI steel and the AlSi12 filler wire had the highest failure strength overall, 4.1 to 4.9kN. And the failures of the tensile specimens of A6 occurred at the HAZ of aluminium parent metals. None of the other samples using GA steel could achieve the failure strength over 4kN.

A4 was made with GA steel and the ZnAl15 filler wire. These brazes failed partially into the braze deposit at strengths of 3.5 to 3.8kN.

The braze dimensions when using ZnAl15 wire (A4) were not as favourable as the dimensions seen using FCW (A5), but resulted in similar failure strengths. A4 had a width and throat dimension of 3.3 and 2.5mm respectively and a braze angle of 62.5° whereas A5 had a width and throat dimension of 4.3 and 2.6mm respectively and a braze angle of 37.9°.

On the other hand, the use of FCW increases the amount of porosity in the braze deposit and soot on the joint surface. And failure of the specimens still occurs at the interface region.

4.3 Laser brazing of flare bevel groove joints

4.3.1 Processing parameters

Appendix B gives a summary of the trials that were performed, the reason for each and what was learned in chronological order.

Table 4.7 summarises the laser brazing trials. As for the overlap joint, the base steels that were used for the trials were GA and GI steels. Laser brazing trials have focussed on optimising joint parameters using 1.2mm AlSi12 wire, 1.6mm AlSi12 wire, 1.6mm ZnAl15 wire, and 1.6mm FCW and also 1.6mm ZnAl15 wire with painted flux solution onto the parent materials.

Wire types	Base steel	
	GA	GI
1.2mm AlSi12	✓	✓
1.6mm AlSi12	✓	
1.6mm ZnAl15	✓	✓
1.6mm FCW	✓	
1.6mm ZnAl15 with painted flux	✓	

Table 4.7) Laser brazing trials

Table 4.8 summarises the brazing conditions selected from the trials for further evaluation. As described in Section 3.5.3, these conditions were selected on the basis of producing the most visually acceptable results and indicating good bend test results.

Sample Number	Base steel	Wire type	Laser moving speed m/min	Beam Focal position (mm)	Laser power (kW)	Wire feed rate (m/min)	Wire stick out distance, mm	Wire feed angle (degrees)	Wire-to-joint-line angle (degrees)	Number of beams	Beam distribution trailing beam% / leading beam %	Beam bias off joint line (mm)
B1	GA	1.2mm AlSi12	4	46*	5.0	10	10	50	0	Twin L+T	30/70	0.5mm to Aluminium
B2	GA	1.6mm AlSi12	3	46*	6.0	6	12	40	0	Twin L+T	30/70	0mm (Joint line)
B3	GA	1.6mm ZnAl15	3	46*	4.0	8	12	50	0	Twin L+T	30/70	0.25 to steel
B4	GA	1.6mm FCW	3	46*	6.0	6	12	50	0	Twin L+T	30/70	0mm (Joint line)
B5	GA	1.6mm ZnAl15 painted flux	3	46*	6.0	6	12	50	0	Twin L+T	30/70	0mm (Joint line)
B6	GI	1.2mm AlSi12	3	36	5.0	9	12	50	0	Twin L+T	30/70	0.5mm to Aluminium

Key: * = Trials conducted with 200um fibre rather than 150um fibre, therefore +46 focus results in the same spot size at the material surface.
Key: L+T = leading and trailing twin spot configuration.

Table 4.8) Laser brazing conditions for further evaluation from visual inspection

4.3.2 Internal qualities of down-selected joints

Table 4.9 summarises the porosity contents of these brazed joints, as determined from pore counting of the radiographs. Sample B5 (GA base material and 1.6mm ZnAl15 filler wire with painted flux) had the highest area of total pores, which corresponds to a porosity area fraction of 30.2%. Sample B4 had the second highest area of total pores, corresponding to a porosity area fraction of 24.3%. The lowest porosity was seen in sample B3, (GA base steel with 1.6mm ZnAl15 filler wire) which had a porosity area fraction of 3.2%.

Sample Number	0.1 mm Count	0.2mm Count	0.3mm Count	0.4mm Count	0.5mm Count	1 mm Count	Accum. length, mm	Area of total pores	Porosity area fraction
B1	0	2	2	0	0	4	5.0	19.6	16.4%
B2	0	5	10	2	0	0	4.8	18.1	15.1%
B3	0	2	6	0	0	0	2.2	3.8	3.2%
B4	30	0	2	0	5	0	6.1	29.2	24.3%
B5	35	2	3	0	4	0	6.8	36.3	30.2%

Table 4.9) Internal porosity contents of selected brazed joints

4.3.3 Critical dimensions of down-selected joints

Figure 4.25 to 4.30 show the cross sections taken from each joint selected for further evaluation. The widths of the brazed joints were measured from these sections, as were the throat depths and brazing angle of each specimen. Figure 4.24 is a schematic showing how to measure the critical dimensions from the cross sections of the joints and these dimensions of the joints are summarised in Table 4.10.

Sample Number	Braze width (a) mm	Throat depth (b) mm	Weld width (c) mm	Bead contact angle (d) °
B1	0.7	0.7	0.8	70.4
B2	3.0	1.7	1.0	35.7
B3	2.7	2.5	1.4	73.1
B4	2.9	1.6	1.8	18.0
B5	3.7	2.9	2.4	58.6
B6	3.1	1.6	1.9	20.1

Table 4.10) Critical dimensions of selected braze joints – braze width, throat depth and wetting angle

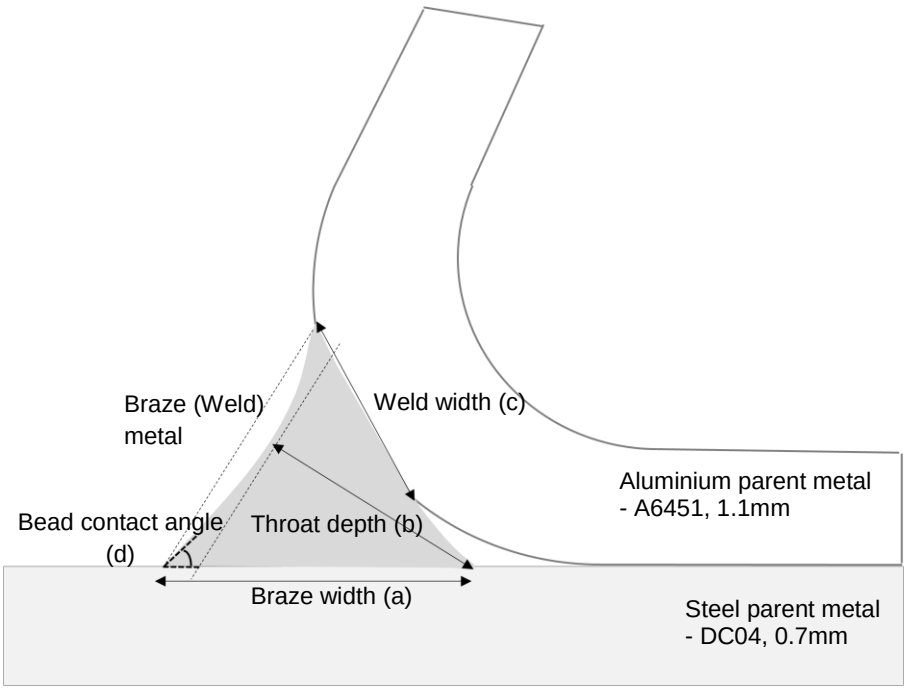

Figure 4.24) Schematic of a cross section of the flare bevel groove joint with the critical dimensions

The measured braze widths (a) of the brazed joints varied between 0.7mm (B1, GA base material, 1.2mm AlSi12 filler wire) and 3.7mm (B5, GA base material, 1.6mm ZnAl15 filler wire with painted flux). The largest width made in a GA material without painted flux was 3.0mm, (B2, GA base material using 1.6mm AlSi12 wire).

The measured throat depths (b) varied between 0.7mm (B1, GA base material, 1.2mm AlSi12 filler wire) and 2.9mm (B5, GA base material, 1.6mm ZnAl15 filler wire with painted flux). The largest throat depth of the braze deposit made in a GA material without painted flux was 2.5mm (B3, GA base material, 1.6mm ZnAl15 filler wire)

The measured braze bead contact angles (d) ranged from 18° (B4, GA base steel, 1.6mm FCW) to 73.1° (B3, GA base steel, 1.6mm ZnAl15 wire). These dimensions were a result of the laser brazing parameters used, such as increasing the wire feed rate whilst maintaining a stable brazing process, and also minimising heat into the steel base material to minimise IMC layer thickness.

The weld widths (c) were varied from 0.8mm to 2.4mm. The two smallest (B1, B2) were shown when the AlSi12 filler wire without flux was applied. However, as mentioned in 4.3.1, the fracture locations of B1 and B2 during shear tensile testing were the interface between the steel parent metal and the bead. Therefore, the weld width is supposed to play little role in joining strength of LWB joints.

Figure 4.25 shows a cross-section of the down-selected laser brazed joint made using GA base steel and 1.2mm AlSi12 filler wire, B1. This

sample has a larger void between the two sheets, and most of the radius of the aluminium has not been wetted by the braze. This braze was made with a wire feed rate of 10m/min, however the brazing speed of 4m/min was possibly too fast for sufficient braze to fill the gap due to the viscosity of the braze medium. In other trials, slower brazing speeds were tested, however they fractured at the interface during specimen preparation. Very low throat depths and braze widths have resulted; these are caused by the laser brazing conditions selected. After visually assessing this cross section sample, it was believed that trialling a thicker AlSi12 wire was necessary so a 1.6mm wire was then purchased and trialled.

Figure 4.26 shows a cross-section of the down-selected laser brazed joint made using GA base steel and the 1.6mm AlSi12 wire, B2, with the expectation that the increase in wire thickness would minimise the size of the void. This was unfortunately not the case, as the braze solidified prior to being able to be drawn into the void region. This braze was made at 3m/min to allow more heat into the brazing process, which is slower than the braze seen in Figure 4.25 at 4m/min.

Figure 4.27 shows a cross-section of the down-selected laser brazed joint made using GA base steel and 1.6mm ZnAl15 filler wire, sample B3. These laser brazing conditions resulted in a very convex braze profile. The braze width and throat depth were 2.7mm and 2.5mm respectively.

Figure 4.28 shows a cross-section of the down-selected laser brazed joint made using GA steel and 1.6mm FCW, sample B4. This braze has the smallest braze angle of 18°, which suggests that the wettability of the FCW onto this steel has been greatly improved. There is a marked increase in fine porosity in the braze deposit, which is likely to be due to the flux. It is assumed at the present time that the flux is hydroscopic, introducing a source of porosity into the deposit.

Figure 4.29 shows a cross-section of the down-selected laser brazed joint made using GA base steel, and 1.6mm ZnAl15 wire with painted flux on both of the parent materials, sample B5. The brazing conditions used on this sample were the same conditions used on sample B4 above. A 40% increase in braze width (from 2.7mm to 3.7mm) and a 16% increase in throat depth (from 2.9m to 2.5mm) has resulted.

Figure 4.30 shows a cross-section of the down-selected laser brazed joint made using GI base steel, and 1.2mm AlSi12 filler wire, sample B6. The wettability of this wire onto the GI surface was found to be good, noted by the low braze angle of 20° and the large braze width of 3.1mm.

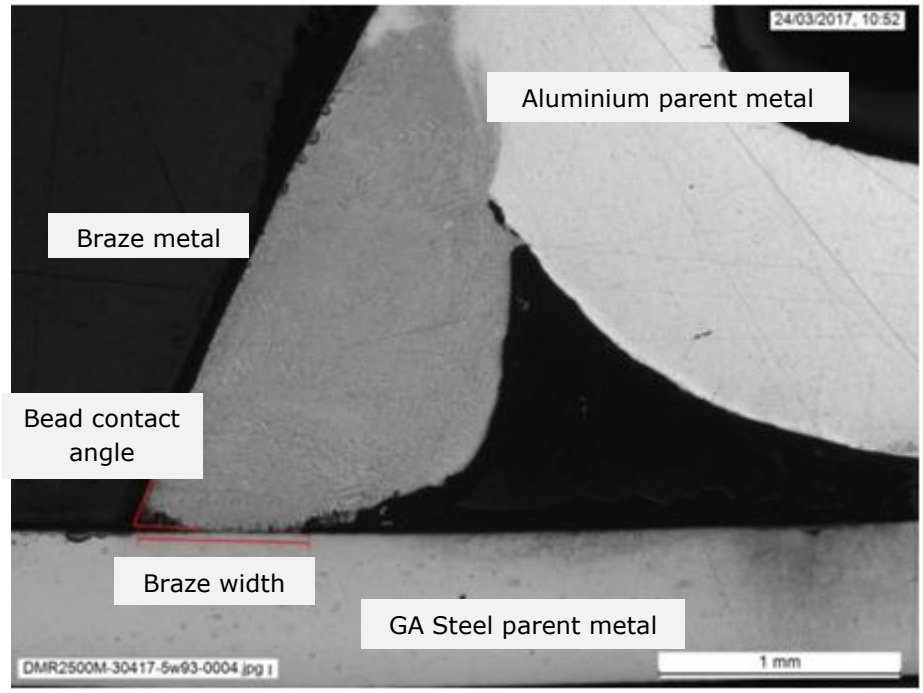

Figure 4.25) Cross-section of B1 (GA, 1.2mm AlSi12 filler wire)

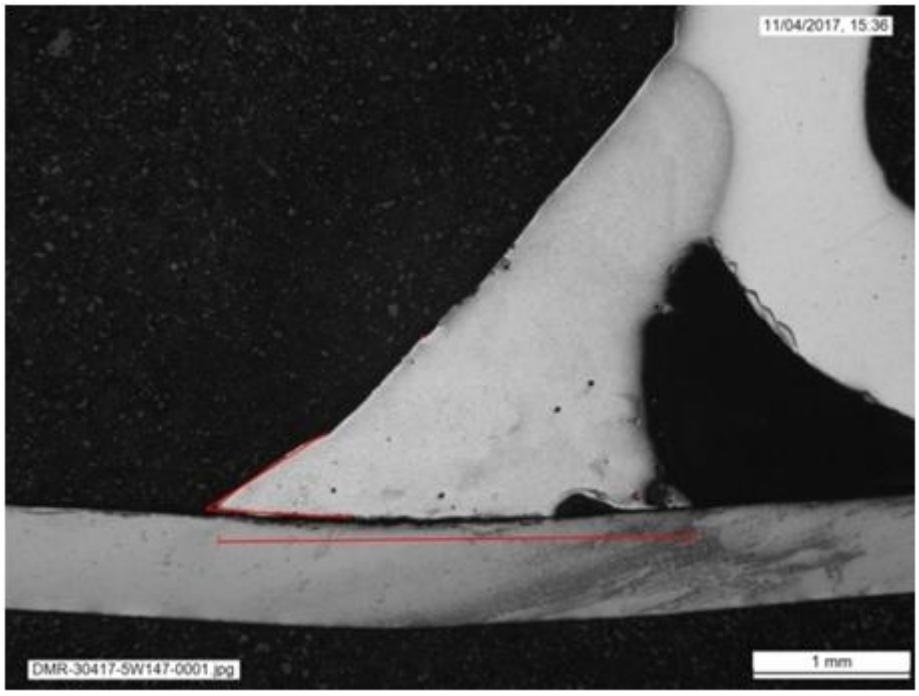

Figure 4.26) Cross-section of B2 (GA, 1.6mm AlSi12 filler wire)

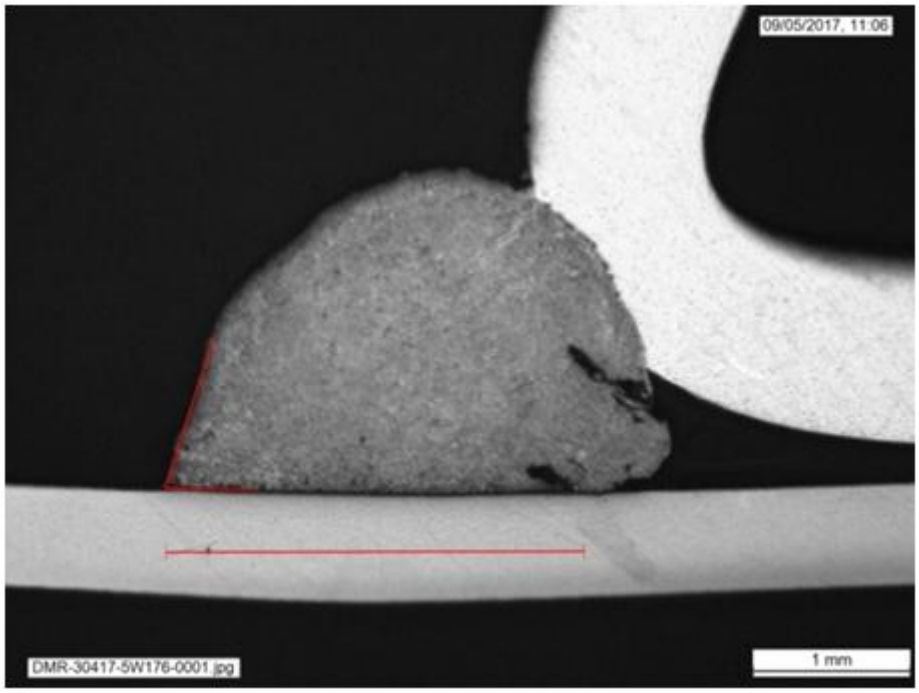

4.27) Cross-section of B3 (GA, 1.6mm ZnAl15 filler wire)

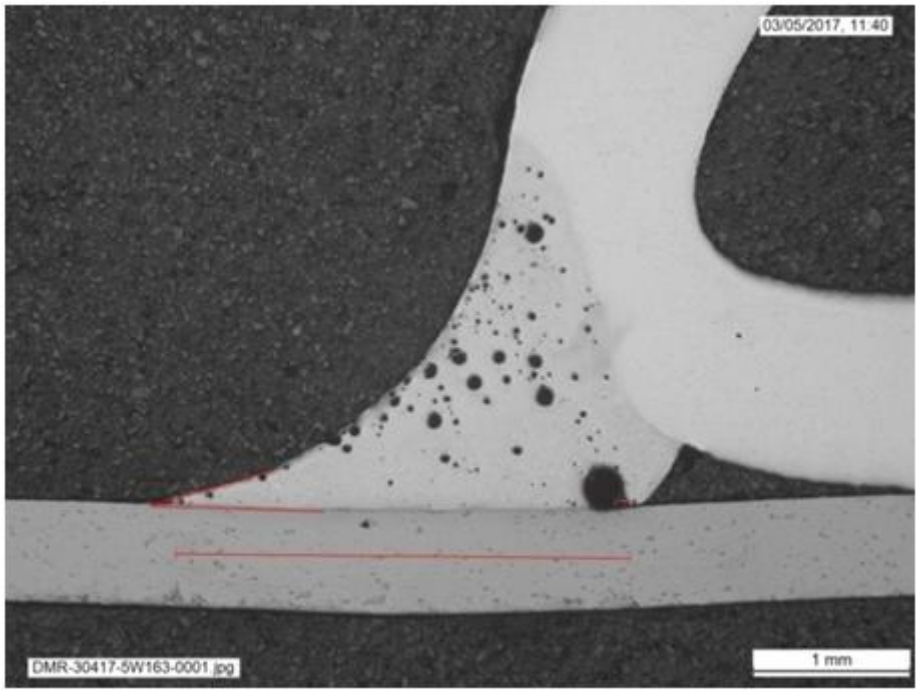

Figure 4.28) Cross-section of B4 (GA, 1.6mm FCW)

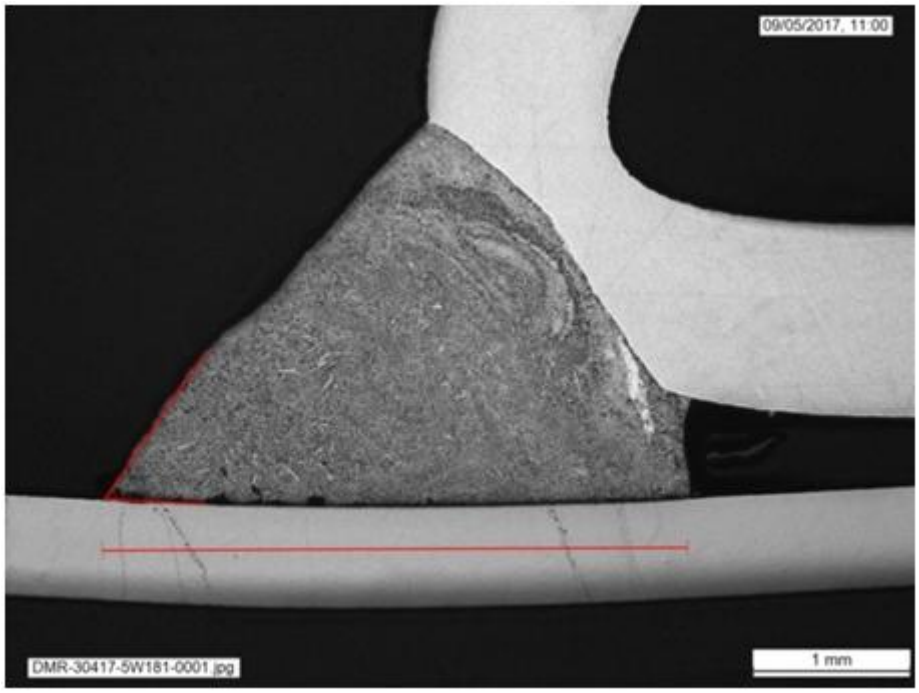

Figure 4.29) Cross-section of B5 (GA, 1.6mm ZnAl15 wire with painted flux on parent materials.)

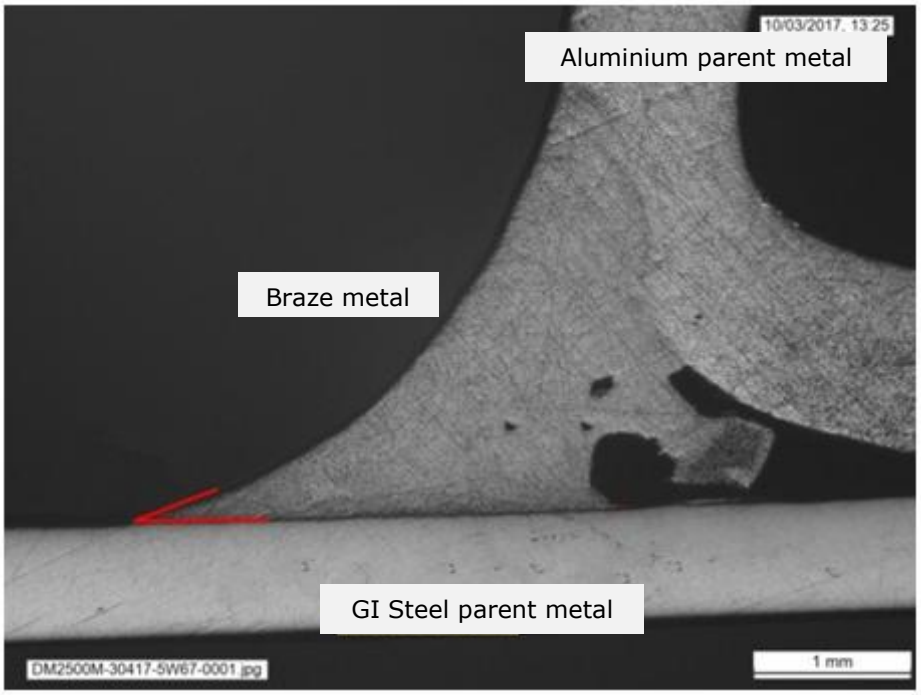

Figure 4.30) Cross-section of B6 (GI, 1.2mm AlSi12 filler wire)

4.3.4 IMC thicknesses of the down-selected joints

Figures 4.31 to 4.36 show optical microscopy images of the IMC layers at the centre of the Al-Fe interface of the down-selected brazed joints. This section reports the overview of the thickness of the IMC layers and the number of layers seen.

Figure 4.31 shows the IMC formed in B1 at the interface between the GA base steel and the braze metal. The IMC layer thickness ranged from 1.6-4μm.

Figure 4.32 shows the IMC formed in B2 at the interface between the GA base steel and the braze metal. As shown, large cracks occurred at the interface in the IMC region. The IMC layer thickness ranged from 6-10μm.

Figure 4.33 shows the IMC formed in B3 at the interface between the GA base steel and the braze metal. No cracks were seen, and the IMC thickness was consistent along the length of the sample. The IMC layer thickness ranged from 16-21μm.

Figure 4.34 shows the IMC formed in B4 at the interface between the GA base steel and the braze metal. Two types of IMC can be seen, one with a more solid structure close to the steel surface and a more irregular layer that breaches into the braze. Small cracks can be seen between these two layers. The IMC layer thickness ranged from 2-16μm.

Figure 4.35 shows the IMC formed in B5 at the interface between the GA base steel and the braze metal. Towards the centre of the braze, the IMC layer was at its thickest, at 20μm. Towards the toe of the braze, the thickness reduced to 7μm.

Figure 4.36 shows the IMC formed in B6 at the interface between the GA base steel and the braze metal. The IMC thickness layer ranged from 1-9μm.

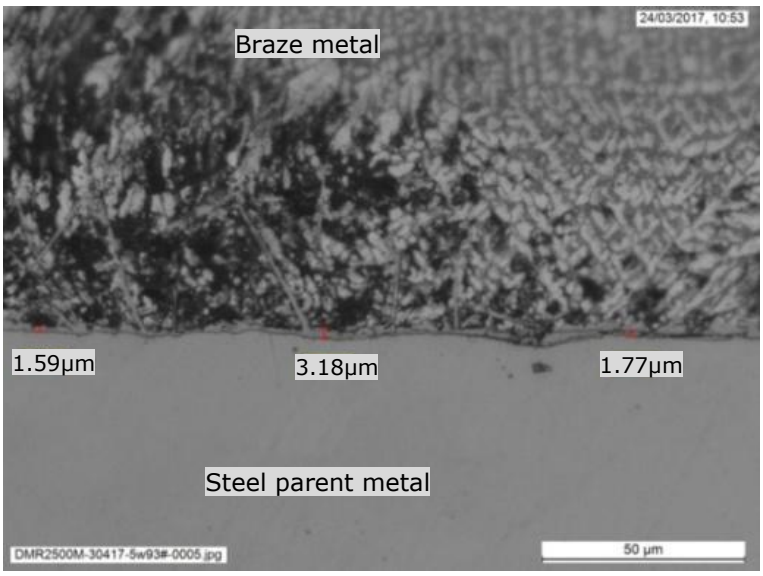

Figure 4.31) Optical microscopy image of the IMC layer from B1

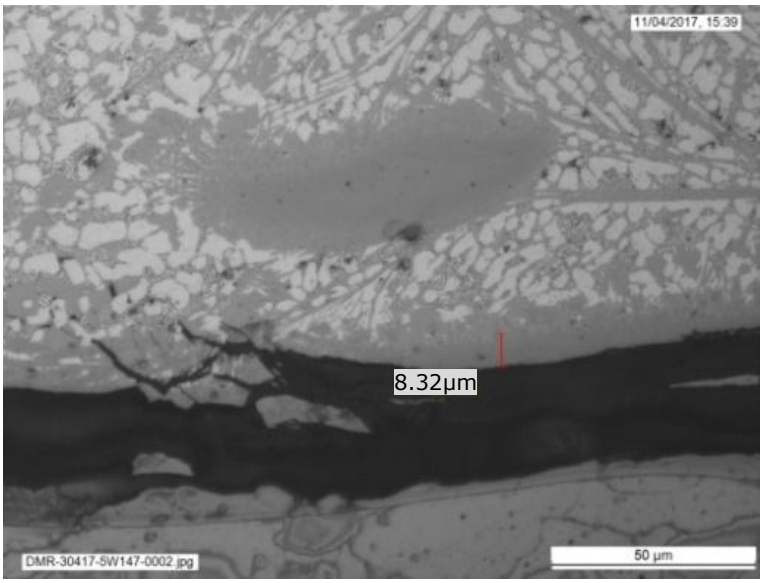

Figure 4.32) Optical microscopy image of the IMC layer from B2

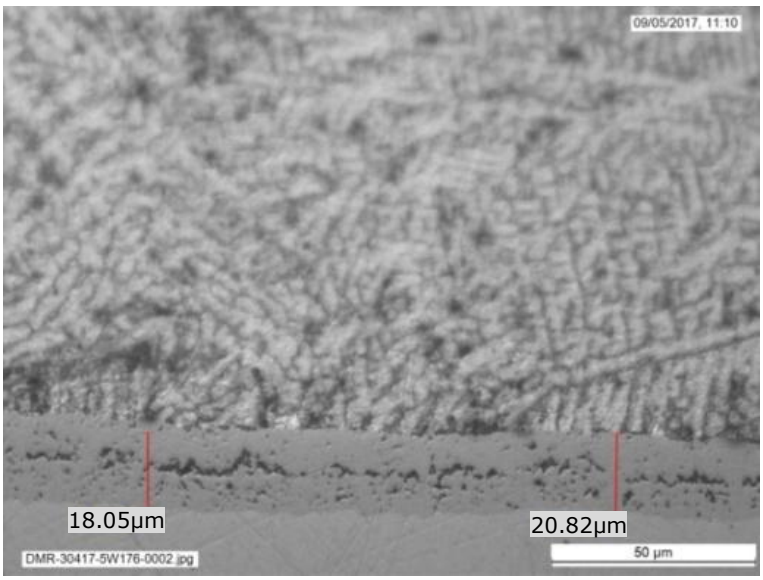

Figure 4.33) Optical microscopy image of the IMC layer from B3

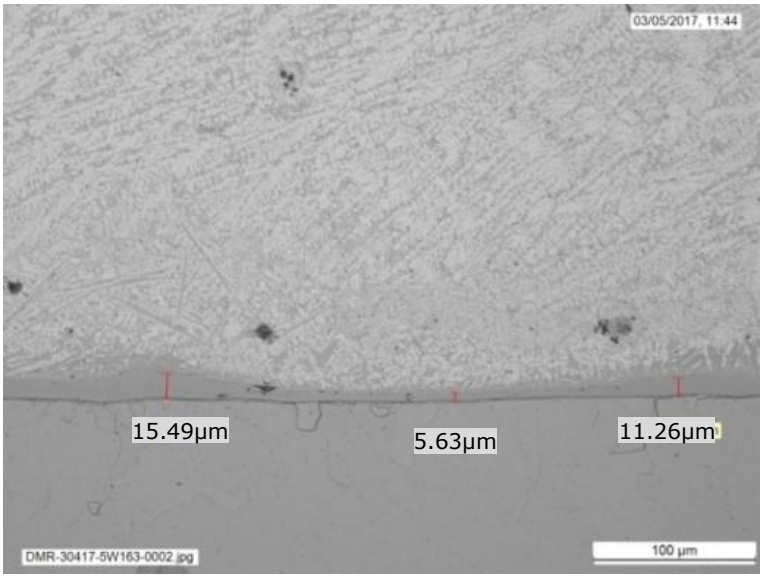

Figure 4.34) Optical microscopy image of the IMC layer from B4

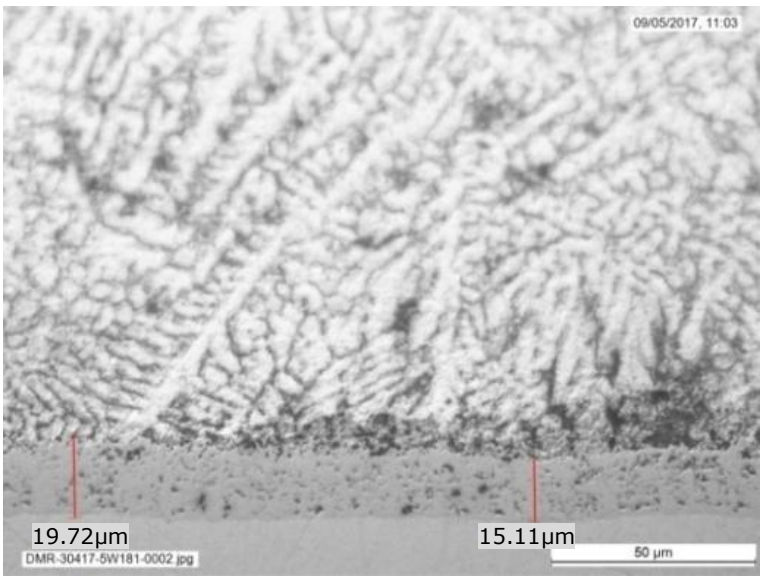

Figure 4.35) Optical microscopy image of the IMC layer from B5

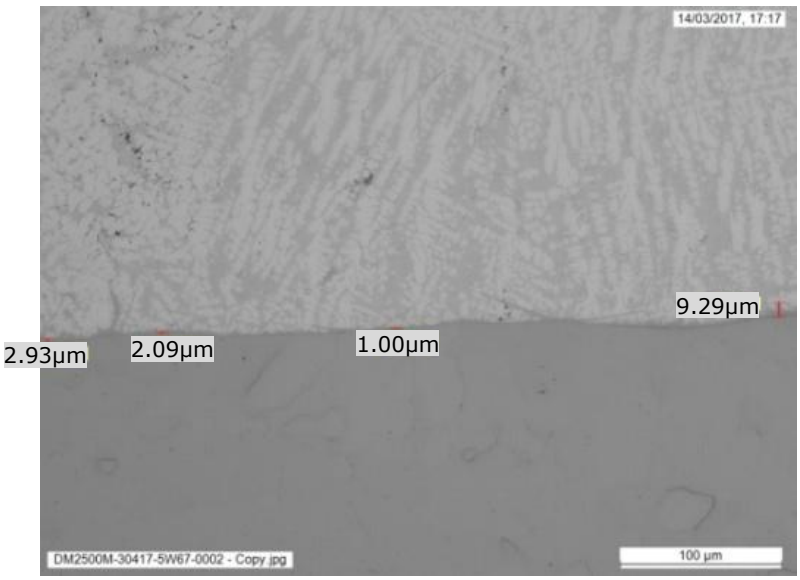

Figure 4.36) Optical microscopy image of the IMC layer from B6

4.3.5 Phase analysis via scanning electron microscopy and nano-hardness of the down-selected brazed joints

Cross-sections of brazed joints made with the various filler wire compositions were examined by SEM (scanning electron microscopy) to better view the IMC phases. An analysis of the elements in the IMC was performed by employing semi-quantitative EDX, using this technique the atomic % of elements within the various phases was quantified to help identify the IMC phases present. Specimens were also submitted for nano hardness measurements of the phases present. The nano hardness

data was converted to Vickers hardness equivalent in accordance with ISO 14577-2, the hardness data was employed to back up the EDX analysis to help identify the IMC phases present.

Figure 4.37 shows an SEM image of B1, produced in GA base steel with a 1.2mm AlSi12 filler wire. EDX1.1 was taken at the centre of the joint in a zone of continuous IMC, and at 27.9 at% Fe, there is strong likelihood that Fe_2Al_5 is present. EDX 1.2 has 14.2% at% Fe, which is likely to be $FeAl_3$. EDX2.1 was taken close to the braze toe, and has 31.3at% of Fe, suggesting Fe_2Al_5 is present also. Nano hardness of the continuous IMC layer (Loc 3) in contact with the steel substrate suggests that it is Fe_2Al_5, the presence of other elements does not appear to have reduced the hardness of the phase. Nano hardness of the outer area of the IMC layer in contact with the braze material (Loc 2) indicated the $FeAl_3$ phase, although this phase was softer than expected, possibly because of the presence of Si.

Figure 4.38 shows an SEM image of B2, produced in GA base steel with a 1.6mm AlSi12 filler wire. Cracks occurred in the IMC layer. EDX1.1 was taken in the continuous IMC layer close to the steel substrate. This area was Fe rich and likely to be FeAl or FeAl2, with Si in solution (42at%Al, 7.5at%Si in Fe). EDX1.2 was taken in the upper part of the continuous dense IMC layer, nearer to the Al parent material, this was thought to be Fe_2Al_5 with some ternary phase, or Si in solution (27.1at%Fe, 7.7at%Si in Al). EDX1.3 was taken in an island of IMC surrounded by the braze metal. It was thought to be $FeAl_3$ with some ternary phase or Si in solution (15.7at%Fe, 9at%Si in Al).

Figure 4.39 shows an SEM image of B3, produced in GA base steel with a 1.6mm ZnAl15 filler wire. EDX 1.1 was taken in the continuous IMC layer in contact with the steel substrate. This is likely to be $FeAl_3$ with some ternary phase of Zn in solution (19.9at%Fe, 14.3at%Zn in Al). The nano hardness results of this phase (Loc 1 and Loc 4) are too soft for $FeAl_3$, possibly confirming that the ternary phase was present to a significant proportion. EDX1.2 was taken in the braze metal, at 41.6at% Zn in Al, which was consistent with a solid solution mixture of the ZnAl15 filler wire.

Figure 4.40 shows an SEM image of B4, produced in GA base steel with a 1.6mm flux cored AlSi12 filler wire. EDX1.1 was taken in the continuous IMC layer in contact with the steel substrate. The phase present is likely to be Fe_2Al_5, with some ternary phase or Si in solution (25.5at%Fe, 6.8at%Si in Al). EDX1.3 was taken in the finger like IMC growing into the braze material. This was likely to be $FeAl_3$ with some ternary phase or Si in solution (17.2at%Fe, 8.3at%Si in Al).

Figure 4.41 shows an SEM image of B6, produced in GI base steel with a 1.2mm AlSi12 filler wire. SEM and EDX analysis were performed at two areas in the centre of the brazed joint. EDX1.1 shows the continuous IMC layer in contact with the steel substrate, which is likely to be $FeAl_3$

with some ternary phase (19.8at%Fe, 8.1at%Si in Al). EDX1.2 was taken in an island of IMC surrounded by braze metal, which is thought to be $FeAl_3$ or ternary phase, or Si in solution (13.1at%Fe, 9.5at%Si in Al). EDX2.1 was taken in the IMC layer at the interface with the steel, and is likely to be $FeAl_3$ or ternary phase (16.2st%Fe, 10.7at%Si in Al). EDX2.2 was taken in a long IMC needle that grew into the braze metal zone. The low Fe component suggests this was ternary phase (7.7at%Fe, 14.8at%Si in Al).

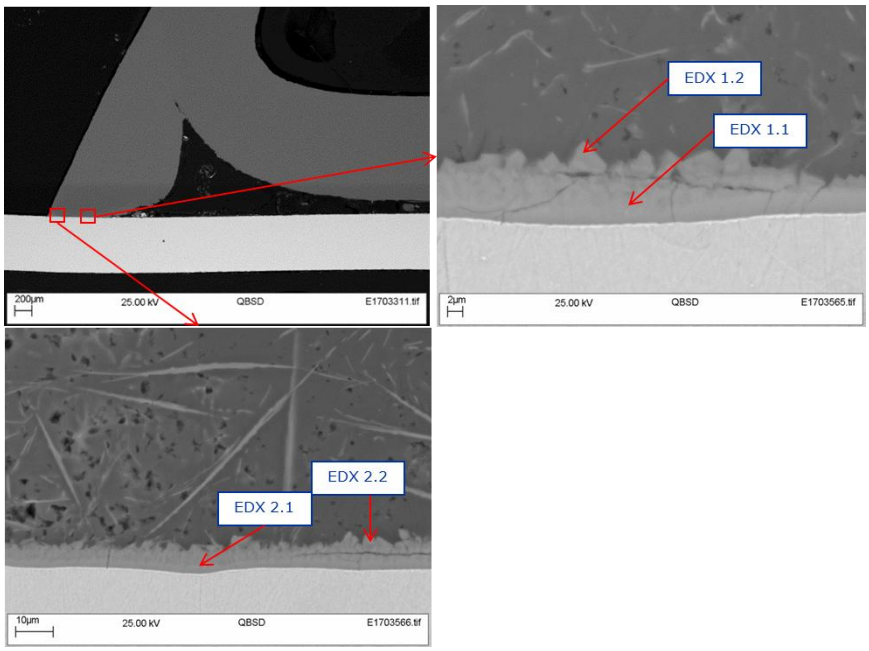

	Al	Si	Fe	Zn
EDX 1.1	Balance	27.9	2.5	6.3
EDX 1.2	Balance	14.2	0.3	7.8
EDX 2.1	Balance	31.3	2.4	6.2
EDX 2.2	Balance	17.9	0.8	6.9

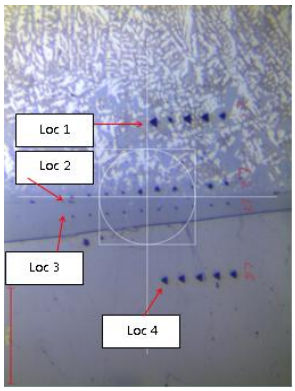

Location	Average Vickers Hardness (HV)
Loc 1	203
Loc 2	733
Loc 3	1178
Loc 4	193

Figure 4.37) SEM phase analysis of the IMCs for B1 and nano-hardness of a sample that has same base steel and filler wire

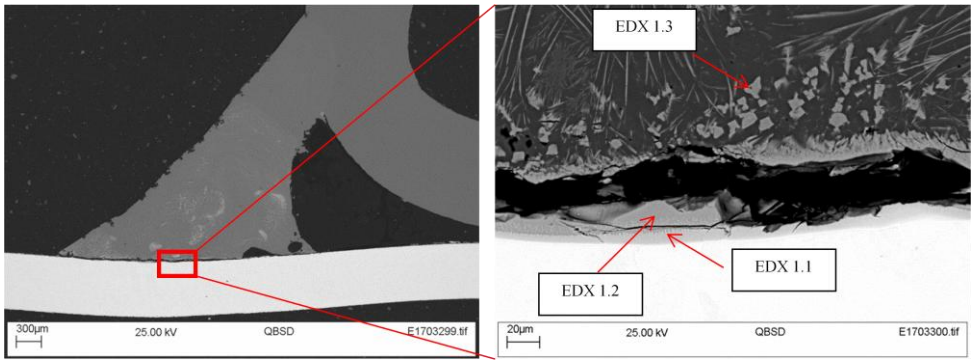

	Al	Fe	Zn	Si
EDX 1.1	42.0	Balance	0	7.5
EDX 1.2	Balance	27.1	0.3	7.7
EDX 1.3	Balance	15.7	0	9.0

Figure 4.38) SEM phase analysis of the IMCs for B2

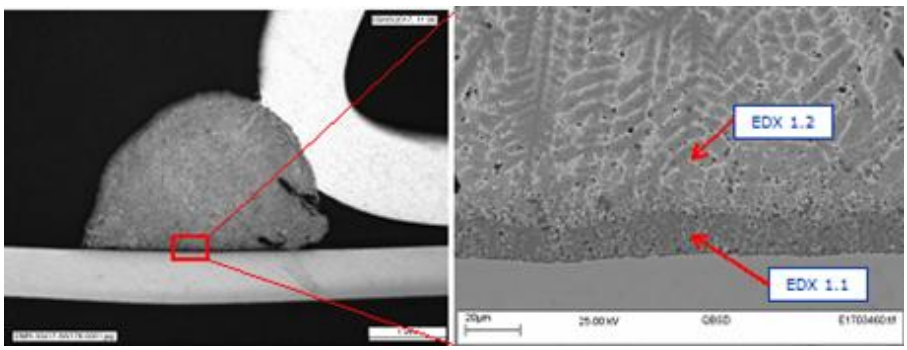

	Al	Fe	Zn	Si
EDX 1.1	Balance	19.9	14.3	0
EDX 1.2	Balance	0.3	41.6	0

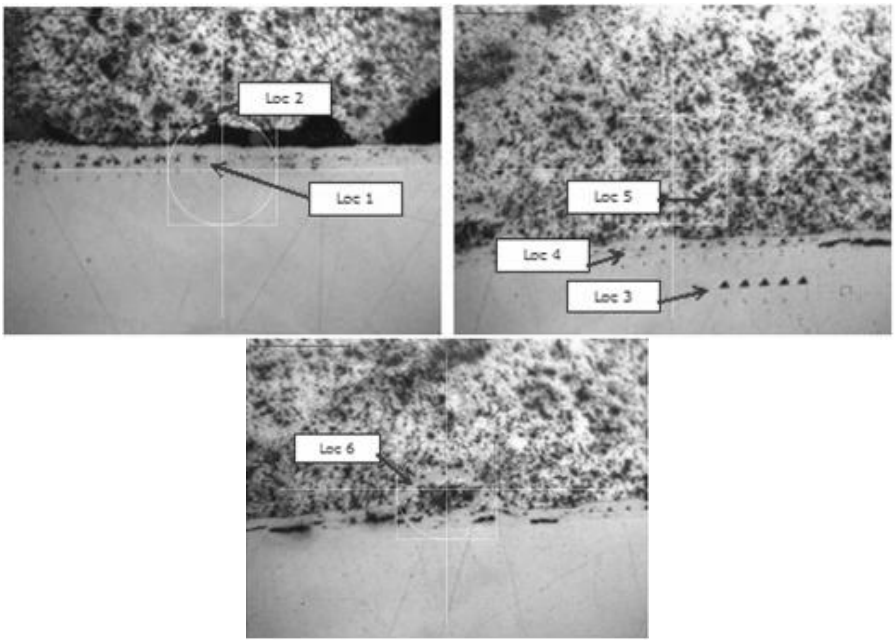

Location	Average Vickers Hardness (HV)
Loc 1	365
Loc 2	135
Loc 3	166
Loc 4	463
Loc 5	169
Loc 6	501

Figure 4.39) SEM phase analysis of the IMCs for B3 and nano-hardness of a sample that has same base steel and filler wire

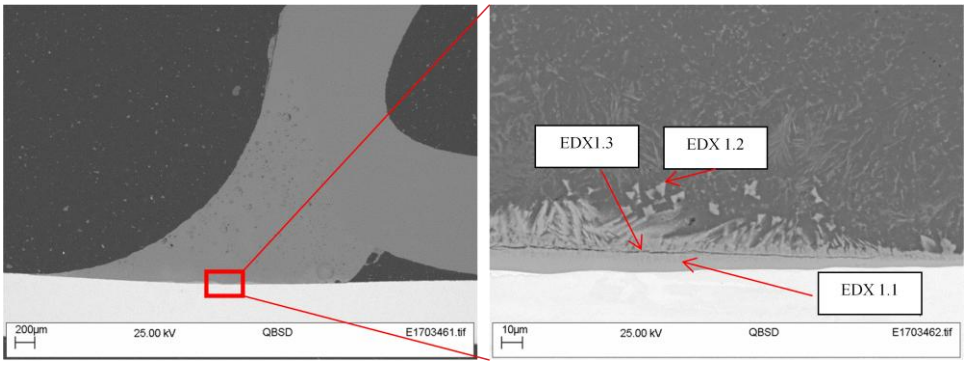

	Al	Fe	Zn	Si
EDX 1.1	Balance	25.5	0.6	6.8
EDX 1.2	Balance	10.4	0	8.3
EDX 1.3	Balance	17.2	0.5	8.3

Figure 4.40) SEM phase analysis of the IMCs for B4

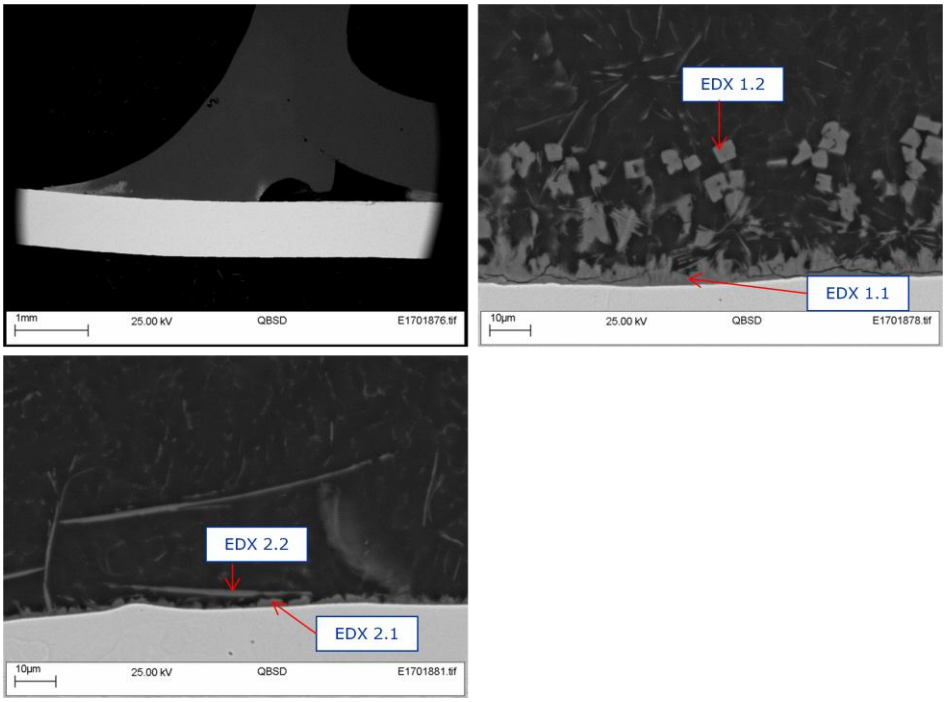

	Al	Si	Fe	Zn
EDX 1.1	Balance	8.1	19.8	0.4
EDX 1.2	Balance	9.5	13.1	0.4
EDX 2.1	Balance	10.7	16.2	0.4
EDX 2.2	Balance	14.8	7.7	0.7

Figure 4.41) SEM phase analysis of the IMCs for B6

4.3.6 Micro hardness surveys of down-selected brazed joints

Hardness tests were carried out using a diamond indenter with a load of 0.1kg to ISO 6507-1:2005. Figure 4.42 shows example locations of the hardness indents made.

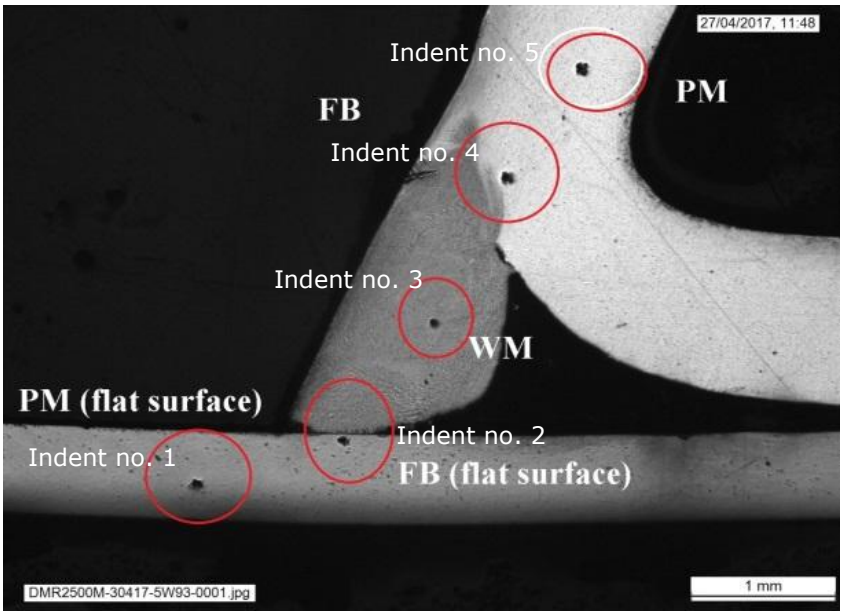

Figure 4.42) Image showing example locations of hardness indents

The results of these indents are shown in Table 4.11. The hardest fusion boundary between the base steel sheet and the braze metal occurs in sample B2 (GA base steel and 1.6mm AlSi12 wire). This had a hardness of 135 HV0.1, whereas the other samples had a fusion boundary hardness of 90 to 123 HV0.1. The hardest braze metal was also found in sample B2, which had a hardness of 134 HV0.1. The softest braze metal was in sample B4 (GA base steel with 1.6mm FCW) which had a hardness of 92 HV0.1.

Sample Number	Indent No.	Indent location (see Figure 4.42)	HV
B1	1	Parent Metal Steel	82
	2	Fusion Boundary - steel to braze deposit	90
	3	Braze deposit	100
	4	Fusion Boundary – aluminium to braze deposit	64
	5	Parent Metal Aluminium	67
B2	1	Parent Metal Steel	103
	2	Fusion Boundary - steel to braze deposit	135
	3	Braze deposit	134
	4	Fusion Boundary – aluminium to braze deposit	82
	5	Parent Metal Aluminium	74
B3	1	Parent Metal Steel	88
	2	Fusion Boundary - steel to braze deposit	95
	3	Braze deposit	119
	4	Fusion Boundary – aluminium to braze deposit	61
	5	Parent Metal Aluminium	59
B4	1	Parent Metal Steel	98
	2	Fusion Boundary - steel to braze deposit	123
	3	Braze deposit	90
	4	Fusion Boundary – aluminium to braze deposit	68
	5	Parent Metal Aluminium	74
B6	1	Parent Metal Steel	94
	2	Fusion Boundary - steel to braze deposit	101
	3	Braze deposit	92
	4	Fusion Boundary – aluminium to braze deposit	63
	5	Parent Metal Aluminium	69

Table 4.11) HV0.1 Hardness data from cross sections of selected brazed joints

4.3.7 Tensile shear testing of down-selected brazed joints

Table 4.12 shows the tensile data from the down-selected joints, along with the corresponding equivalent brazed joints which have had their widths and throat depths measured. Up to three specimens were extracted from a single brazed coupon. Figure 4.43 is the schematic of the specimens with its dimensions.

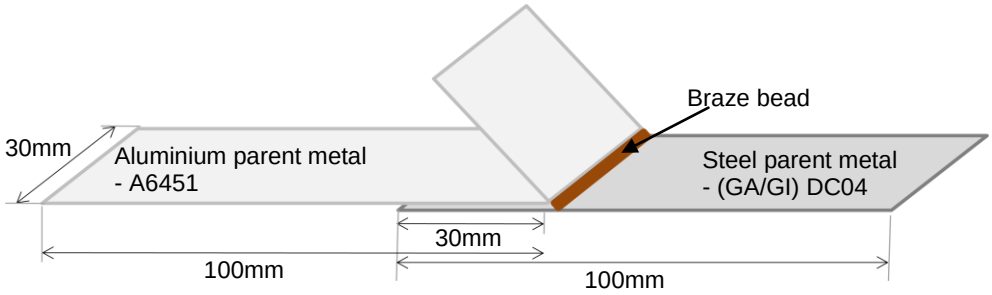

Figure 4.43 Schematic of the specimen for tensile tests

Some of the base steel and filler wire joint combinations were not suitable to produce tensile specimens, such sample B1 (GA base steel brazed using 1.2mm AlSi12 wire). This was due to distortion in the parent materials, causing the braze bead to align and solidify to one of the parent metals, rather than form a brazed joint onto the joint line.

The highest failure strength was seen in tensile sample B6 with the GI base material, when brazed using 1.2mm AlSi12 wire, with failure strengths ranging from 3.8kN to 4.5kN. This sample failed across the heat affected region within the aluminium parent material, and this can be seen in Figure 4.44.

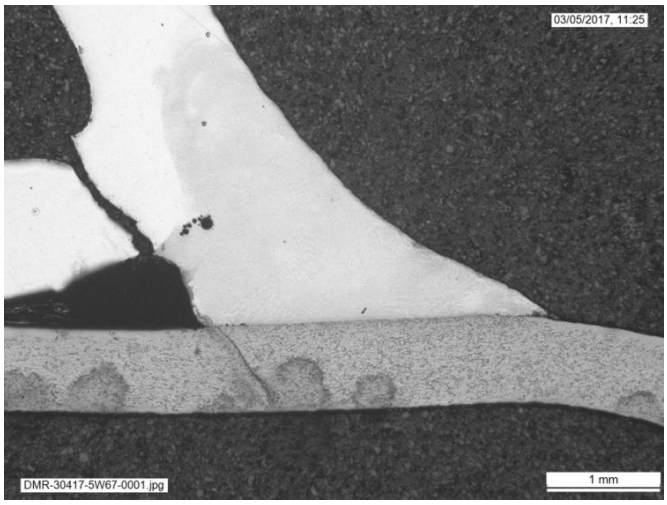

Figure 4.44) Image of tensile shear specimen after testing, B6

The second highest failure strength was tensile sample B5 (GA, 1.6mm ZnAl15 and painted flux) which had failure strengths of 2.7 to 2.9kN, which exhibited an interface failure.

Tensile samples B4 (GA base steel with 1.6mm FCW) and B3 (GA, 1.6mm ZnAl15) had very similar failure strengths. Tensile sample B4 had failure strengths of 2.3 to 2.8kN, and tensile sample B3 had failure strengths of 2.4 to 2.8kN. Both of these samples exhibited interface failures.

Sample B2 (GA, 1.6mm AlSi12 wire) had the lowest failure strength, of 1.4 to 1.6kN. This sample failed at the one interface between the steel and aluminium sheets.

Sample Number	Width mm	Throat mm	Fracture location	Failure strength kN	Displacement mm
B1	0.7	0.7	Interface	Short braze width resulting in low interface strength	
B2	3.0	1.7	Interface	1.4	0.31
				1.6	0.33
				1.4	0.27
B3	2.7	2.5	Interface	2.4	0.32
				2.6	0.37
				2.8	0.48
B4	2.9	1.6	Interface	2.8	0.86
				2.6	0.83
				2.3	0.58
B5	3.7	2.9	Interface	2.8	0.56
				2.7	0.51
				2.9	0.63
B6	3.1	1.6	HAZ	4.5	2.08
				4.1	1.52
				3.8	1.18

Table 4.12) Failure strengths and displacements to failure from tensile tests

4.3.8 Summary

All failures of the tensile samples with flare bevel groove joints made at the laser moving speed of 3m/min occurred at the interface through the IMC region except the sample with GI steel, B6.

The highest strength flare bevel groove joint overall was also sample B6 (GI base steel using 1.2mm AlSi12 wire). This had tensile strengths of 3.8 to 4.5kN. And the failures occurred at the HAZ of aluminium parent metals. None of other samples using GA steel could achieve the tensile strength over 3kN.

The highest strength flare bevel groove joints that used GA steel was sample B5 (GA, using 1.6mm ZnAl15 filler wire and painted flux) followed by B3 (GA using 1.6mm ZnAl15 filler wire) and B4 (GA using 1.6mm FCW). B5 had tensile strength of 2.7 to 2.9kN and B3 and B4 had that of 2.3 to 2.8kN.

The use of flux for GA steel such as B5 or B4, either by using the painted flux or cored flux in the filler wire, increases the wettability of the braze deposit onto the GA surface. B4 had the lowest bead contact angle, 18°. This was slightly better result than B6 using GI steel that had the bead contact angle of 20.1°. Through many literatures, GI steel has been proven that has good wettability with aluminium. B5 had relatively higher bead contact angle, 58.6° than B4 or B6. But, when compared with the other sample using the same ZnAl filler wire, B3 which had the bead contact angle of 73.1°, the wettability of B4 was apparently improved.

However, the use of flux also has disadvantages. The amount of soot on the joint surface and porosity in the braze deposit after the laser brazing process severely increases. Moreover, all failures in the GA samples occurred at the interface, through the IMC region, and the joint strength was lower that of the GI steel samples. Because, when higher heat input was applied for the purpose of the bigger braze deposit, the IMC thickness became thicker. On the other hands, when lower heat input was applied, the braze deposit size was smaller and sometimes, the zinc layer of the steel parent metal remained. All of these effects resulted in the interfacial fracture and lower joint strength.

4.4. Laser brazing of flare bevel groove joints at the lower laser moving speed of 1m/min

4.4.1 Processing parameters

To avoid the interfacial failure of GA steels and aluminium braze metals during the tensile shear testing, the laser moving speed was slower down from 3m/min to 1m/min. Lower laser speed was expected to grant the time to form larger braze deposit and remove the zinc layer of the

steel parent metal. And FCW wire with the diameter of 1.6mm showed the highest wettability and joint strength in the GA samples was selected for these trials.

Table 4.13 summarises the brazing conditions selected from the trials for further evaluation. As described in Section 3.5.3, these conditions were selected on the basis of producing the most visually acceptable results and indicating good bend test results.

Sample Number	Base steel	Wire type	Laser moving speed m/min	Beam Focal position (mm)	Laser power (kW)	Wire feed rate (m/min)	Wire stick out distance, mm	Wire feed angle (degrees)	Wire-to-joint-line angle (degrees)	Number of beams	Beam distribution trailing beam%/leading beam %	Beam bias off joint line (mm)
C1	GA	1.6mm FCW	1	36	3.5	4.0	12	50	0	Twin L+T	30/70	0.75 to Aluminium
C2	GA	1.6mm FCW	1	36	4	4.6	12	50	0	Twin L+T	30/70	0.75 to Aluminium
C3	GA	1.6mm FCW	1	36	4	5.5	12	50	0	Twin L+T	30/70	0.75 to Aluminium
C4	GA	1.6mm FCW	1	36	6	6.9	12	50	0	Twin L+T	30/70	0.75 to Aluminium
C5	GA	1.6mm FCW	1	36	6	8.5	12	50	0	Twin L+T	30/70	0.75 to Aluminium
C6	GA	1.6mm FCW	1	36	6	10.0	12	50	0	Twin L+T	30/70	0.75 to Aluminium

Key: L+T = leading and trailing twin spot configuration.

Table 4.13) Laser brazing conditions selected for further evaluation from visual inspection

4.4.2 Critical dimensions of down-selected brazed joints

Figures 4.46 to 4.51 show the cross-sections taken from each of the brazed joints selected. The widths of the braze deposits were measured from these sections, as were the throat depths and braze bead contact angle of each. These dimensions are summarised in Table 4.14.

Sample number	Braze width, mm	Throat depth, mm	Bead contact angle °
C1 (3.5kW, 4WFS)	4.3	2.0	20.5
C2 (4kW, 4.6WFS)	3.4	1.2	13.7
C3 (4kW, 5.5WFS)	5.6	2.6	16.6
C4 (6kW, 6.9WFS)	7.9	3.7	9.28
C5 (6kW, 8.5WFS)	6.3	3.4	18.6
C6 (6kW, 10WFS)	8.2	3.8	9.7

Table 4.14) Critical dimensions of selected braze joints – braze width, throat depth and wetting angle

The widths of the brazed deposits varied between 3.4mm (sample C2; 1m/min travel speed 4kW, 4.6m/min wire feed speed) to 8.2mm (sample C6; 1m/min travel speed 6kW, 10m/min wire feed speed)

The throat depths varied between 1.2mm (sample C2; 1m/min travel speed 4kW, 4.6m/min wire feed speed) to 3.8mm (sample C6; 1m/min travel speed 6kW, 10m/min wire feed speed)

The braze bead contact angles ranged from 9.28° (sample C4; 1m/min travel speed 6kW, 6.9m/min wire feed speed) to 20.5° (sample C1; 1m/min travel speed 3.5kW, 4.0 m/min wire feed speed).

Figure 4.45 shows a cross-section from C1 which was made at 1m/min travel speed, 3.5kW power and a wire feed speed of 4m/min. Some large pores can be seen in the cross-section, up to 0.5mm in diameter, however this braze produced a very smooth transition surface between the two parent metals.

Figure 4.46 shows the cross-section resulting from slightly hotter laser brazing conditions, 1m/min, 4kW power and a wire feed speed of 4.6 m/min. The increase in braze temperature has led to a reduction in braze contact angle from the previous sample, from 20.5° to 13.7° which is to be expected due to the increase in temperature causing reduced viscosity in the braze material. A greater volume of pores can be seen at the interface compared with C1.

Figure 4.47 shows a cross section of C3 (1m/min travel speed, 4kW power and 5.5m/min wire feed speed) which more wire was supplied with the same laser power comparing to C2. This braze shows a very consistent transition between the two parent materials, and minimal porosity can be seen.

Figure 4.48 shows a cross section from C4, which was produced using higher temperature laser brazing parameters (1m/min travel speed, 6kW power and 6.9m/min wire feed speed) in comparison to C2. Greater distortion can be seen on the steel sheet in this cross section than the previous cross-sections mentioned, however less porosity can be seen. As expected, the braze angle has further decreased to 9.3°. Due to the relative increase in wire feed speed, the braze width and throat depth have increased significantly in comparison to the previously discussed joints.

Figure 4.49 shows a cross section of C5 (1m/min, 6kWand 8.5m/min wire feed speed). This braze was made with a greater wire feed speed than C4, therefore lowering the brazing temperature in comparison. The effect on the braze is reduced distortion compared to C4, and reduced melting into the thickness of the aluminium which may be desirable.

Figure 4.50 shows a cross-section from C6 (1m/min travel speed, 6kW power, 10 m/min wire feed speed), which reduces the braze temperature even further by increasing the wire feed speed. It is due to this high wire feed rate that the braze width was the largest at 8176.9µm.

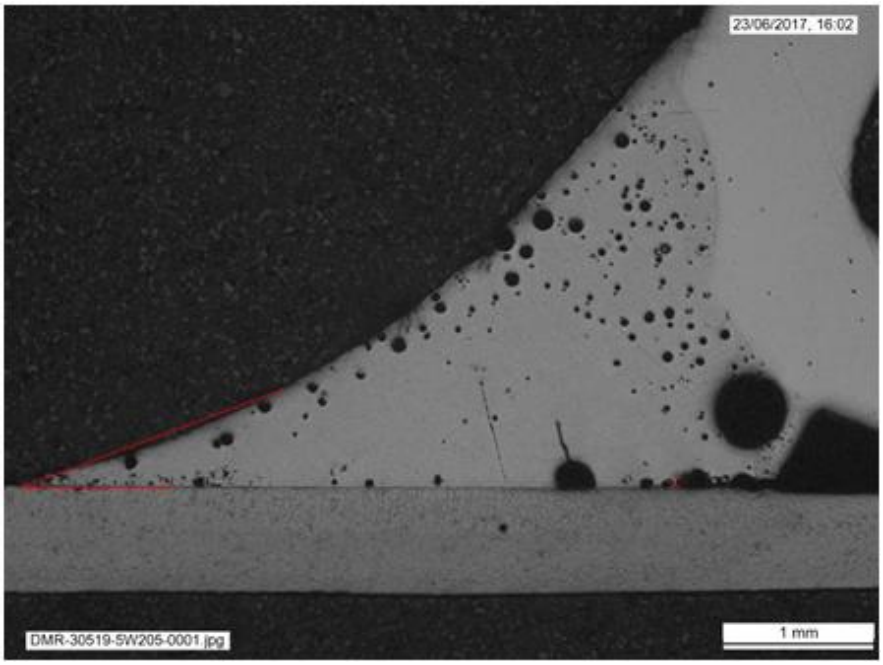

Figure 4.45) Cross-section of C1 (3.5kW power, 4m/min WFS)

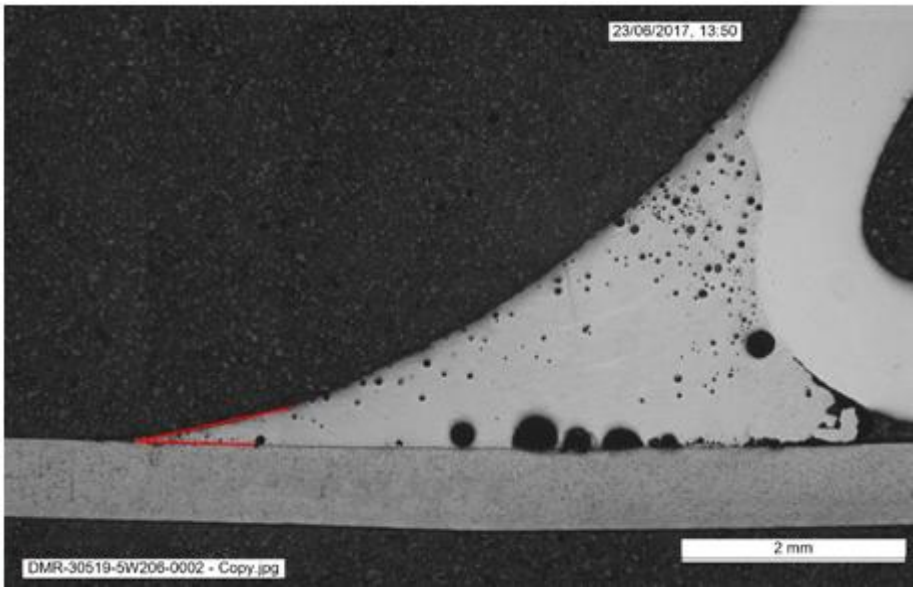

Figure 4.46) Cross-section of C2 (4kW power, 4.6 m/min WFS)

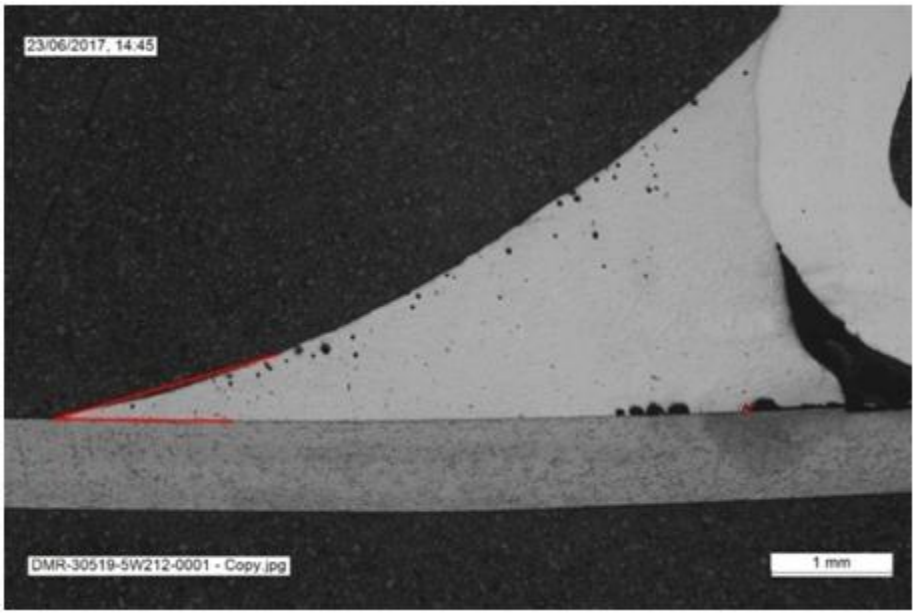

Figure 4.47) Cross-section of C3 (4kW power, 5.5 m/min WFS)

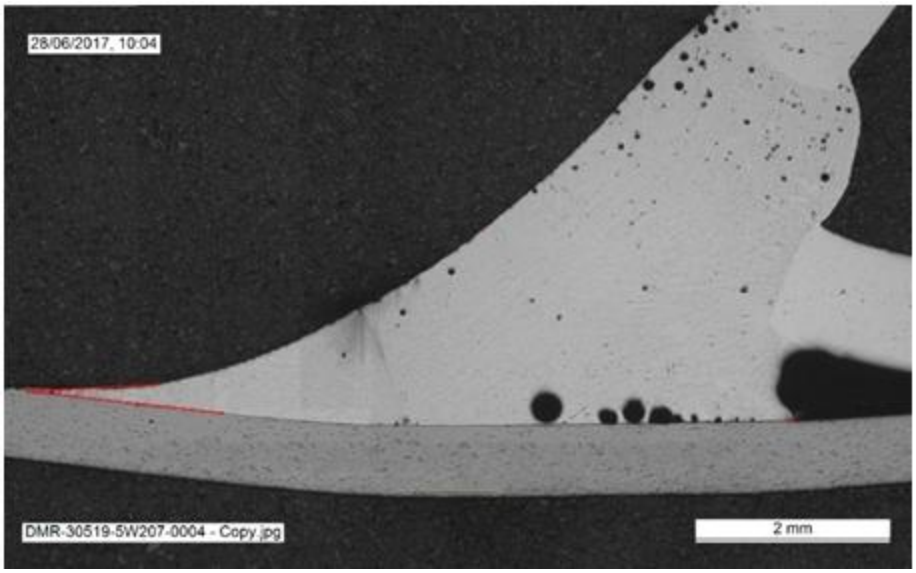

Figure 4.48) Cross-section of C4 (6kW power, 6.9 m/min WFS)

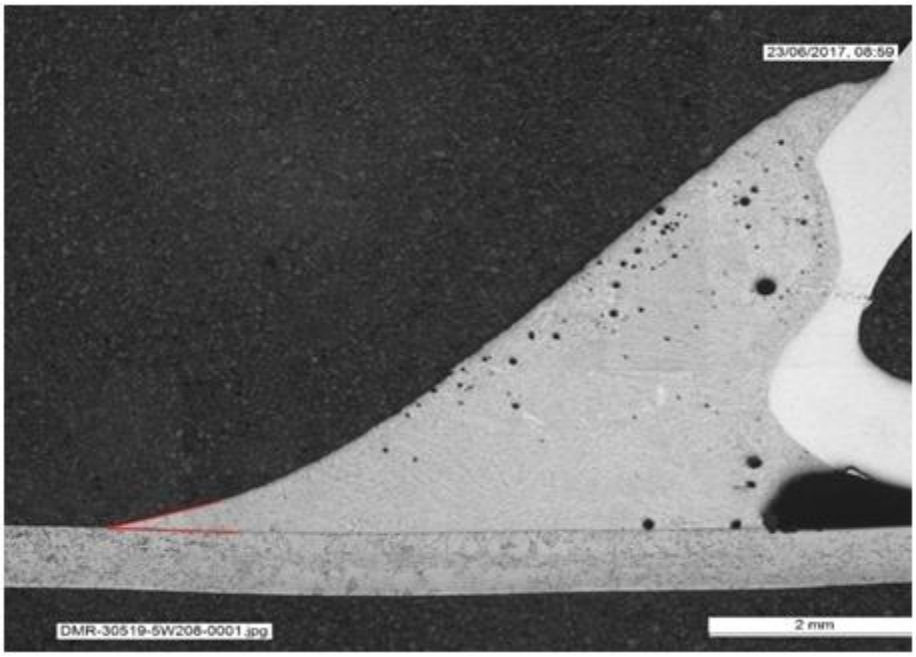

Figure 4.49) Cross-section of C5 (6kW power, 8.5 m/min WFS)

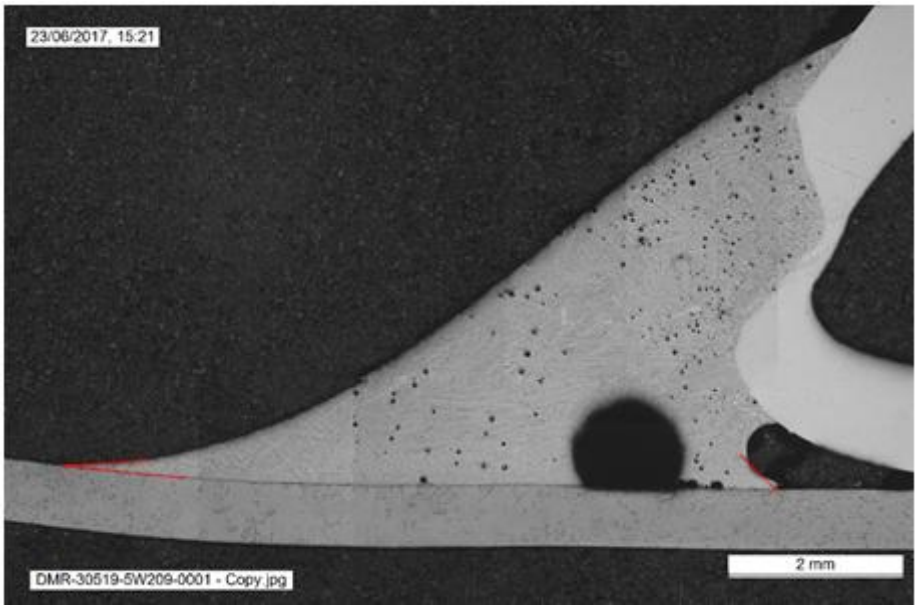

Figure 4.50) Cross-section of C6 (6kW power, 10 m/min WFS)

4.4.3 IMC thicknesses in down-selected brazed joints

Figure 4.51 to 4.56 show optical microscopy images of the IMC layers at the interface regions of the selected brazed joints. This section details the thickness of the IMC layers and the number of layers seen.

Figure 4.51 shows the IMC thickness formed in C1 at the interface between the base steel and the braze deposit. Only one type of IMC was seen which had a thickness range of 2-5µm, which was consistent along the width of the braze. No cracks can be at the interface in this figure.

Figure 4.52 shows the IMC thickness formed in C2 at the interface between the base steel and the braze deposit. Only one type of IMC was seen which had a thickness range of 1-5µm.

Figure 4.53 shows the IMC thickness formed in C3 at the interface between the base steel and the braze deposit. Only one type of IMC was seen which had a thickness range of 2-12µm.

Figure 4.54 shows the IMC thickness formed in C4 at the interface between the base steel and the braze deposit. Only one type of IMC was seen which had a thickness range of 5-8µm, and this range was consistent along the braze width.

Figure 4.55 shows the IMC thickness formed in C5 at the interface between the base steel and the braze deposit. Only one type of IMC was seen. Towards the centre of the braze, the IMC layer was at its thickest at 17µm. towards the toe of the braze, the thickness reduced to 2µm.

Figure 4.56 shows the IMC thickness formed in C6 at the interface between the base steel and the braze deposit. Only one type of IMC was seen which had a thickness range of 2-12μm.

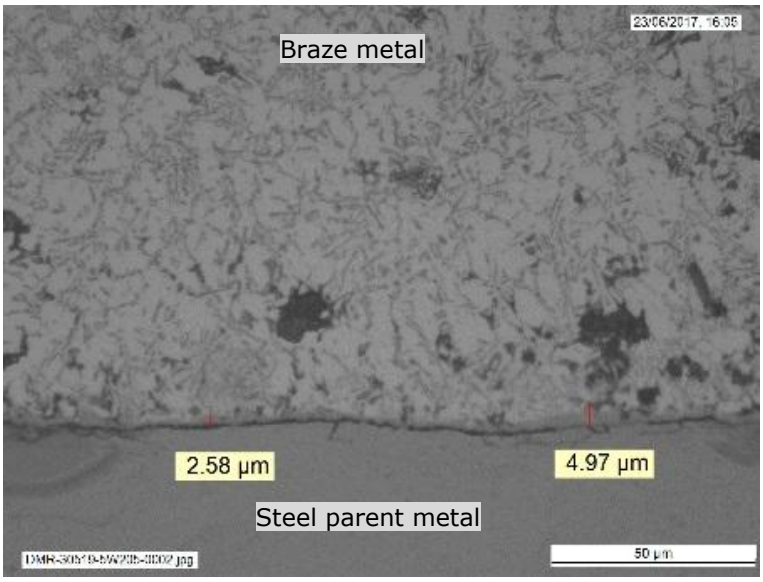

Figure 4.51) Optical microscopy images of the IMC layer from C1

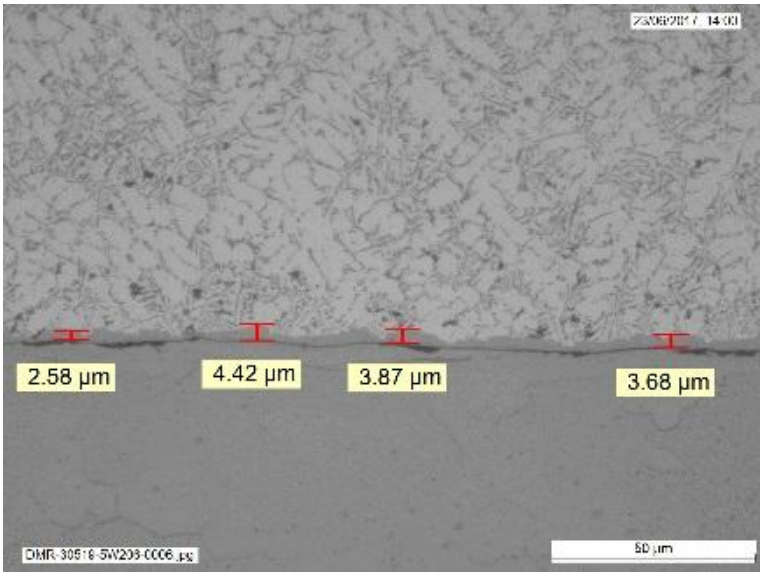

Figure 4.52) Optical microscopy images of the IMC layer from C2

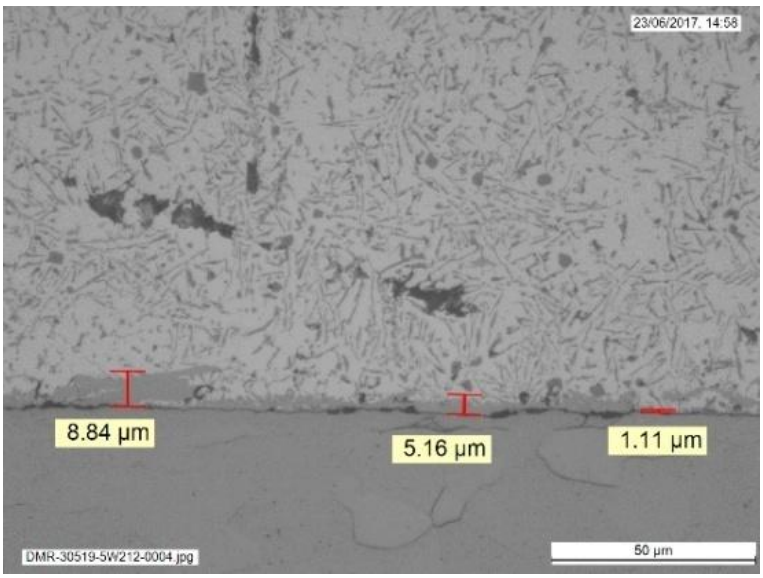

Figure 4.53) Optical microscopy images of the IMC layer from C3

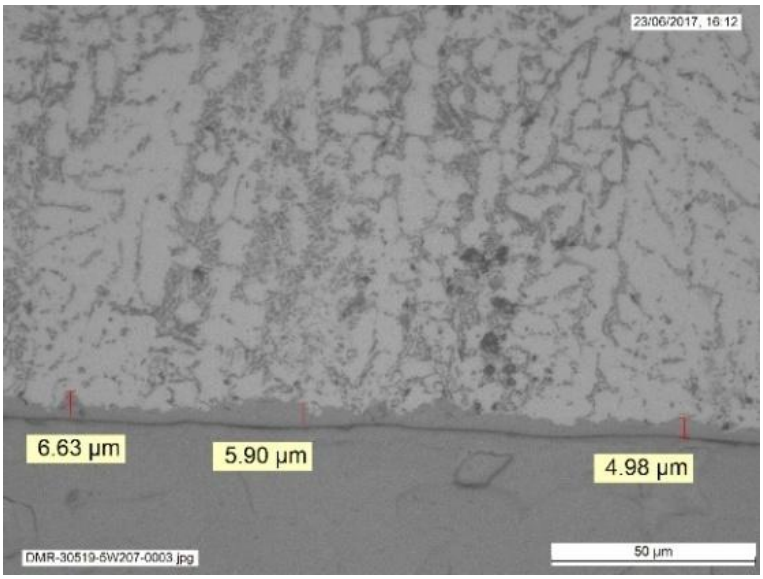

Figure 4.54) Optical microscopy images of the IMC layer from C4

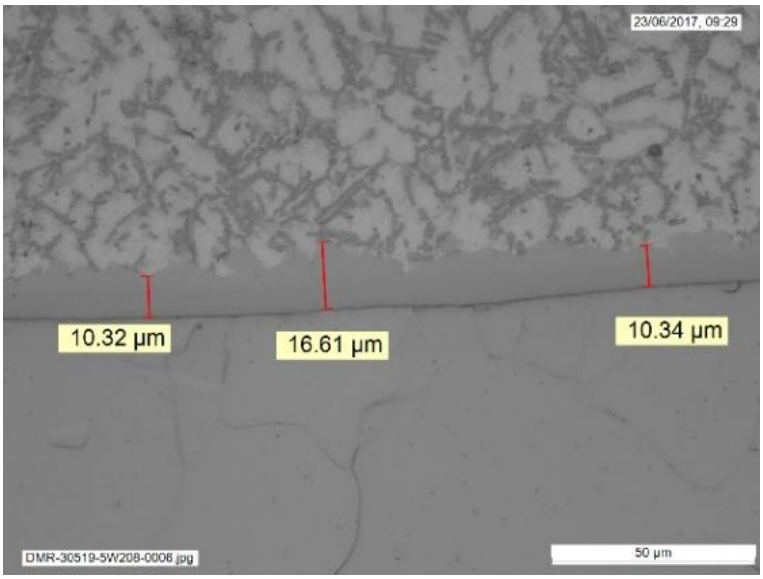

Figure 4.55) Optical microscopy images of the IMC layer from C5

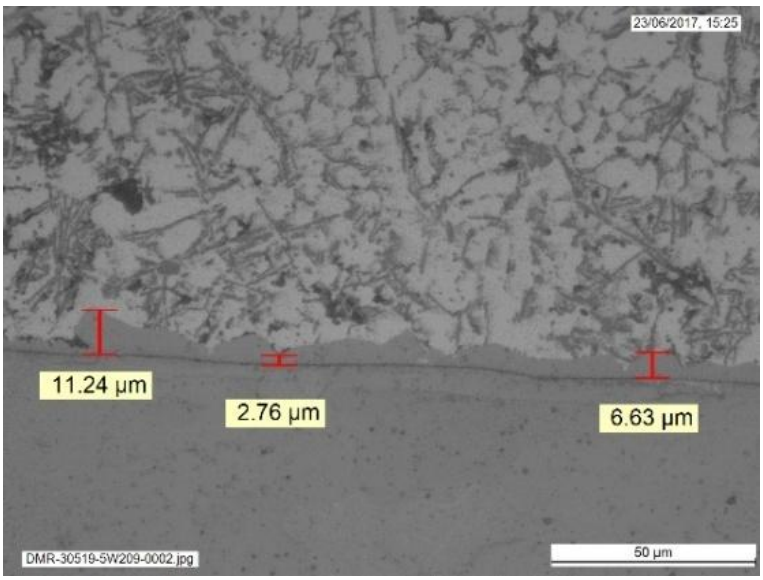

Figure 4.56) Optical microscopy images of the IMC layer from C6

4.4.4 Tensile shear testing of down-selected brazed joints

Table 4.15 shows the tensile data from selected brazed joints, along with the corresponding measured widths and throat depths. Up to three specimens were extracted from a single brazed coupon.

The highest failure strength was seen in tensile sample C1 (1m/min, 3.5kW, 1.6FCW, 4m/min wire feed speed) with failure strengths ranging from 3.4 to 5.1kN. These failures occurred mostly across the interface between the steel and aluminium sheets, however regions can be seen where the braze deposit had failed and the interface remains intact towards the toe of the braze.

Sample C5 (1m/min, 6kW, 1.6FCW, 8.5m/min wire feed speed) also had similar failure strengths of 3.7 to 5.0kN where the failure occurred in a combination of the braze throat and the interface between the parent materials within the same tensile specimen.

Sample C6 (1m/min, 6kW, 1.6FCW, 10m/min wire feed speed) had failure strengths within the smallest range therefore had the most consistent failure strength along the length of the braze sample. This was a failure range of 4.4 to 4.6kN. One of these tensile specimens failed entirely in the braze throat region and the other two tensile specimens failed in combination through the braze throat and the interface between the parent materials.

Sample C4 is also noteworthy to mention due to the failure modes seen in the three tensile specimens. The failure strengths ranged from 3.4 to 4.0kN however one sample failed in the aluminium parent material entirely and the braze region and thee interface between the parent metals remained fully intact. Other tensile samples with this sample set failed in combination through the braze throat and the interface.

Figure 4.57 shows the correlation between the failure load of each tensile specimen and the displacement required to reach that failure load. There is clearly a correlation between these as the more the tensile sample is displaced, the greater the failure load required. There is however scatter in the failure strengths of the three tensile specimens taken from each sample.

Figure 4.58 and Figure 4.59 show the relationship between failure strength to the braze width and failure strength to the throat depth respectively. No significant correlation can be seen between the failure strengths to the braze widths and throat depths, however the range of the failure strengths to vary significantly between the samples tested.

Sample Number	Fracture location	Failure Load, kN	Displacement, mm
C1	Interface, partially braze deposit	5.1	0.40
		3.4	0.60
		4.5	1.55
C2	Interface, partially braze deposit	4.6	2.08
		3.8	1.07
		4.2	1.09
C3	Interface, partially braze deposit	3.7	0.93
		4.2	1.46
		4.0	1.30
C4	Interface, partially braze deposit	3.8	0.81
		4.0	1.04
		3.4	0.74
C5	Interface, partially braze deposit	4.1	1.12
		3.7	1.11
		5.0	2.76
C6	Interface, partially braze deposit	4.6	1.74
		4.6	1.68
		4.4	1.60

Table 4.15) flare bevel groove joint configuration - Failure strengths and displacements to failure from tensile tests on selected flare bevel groove joint configurations

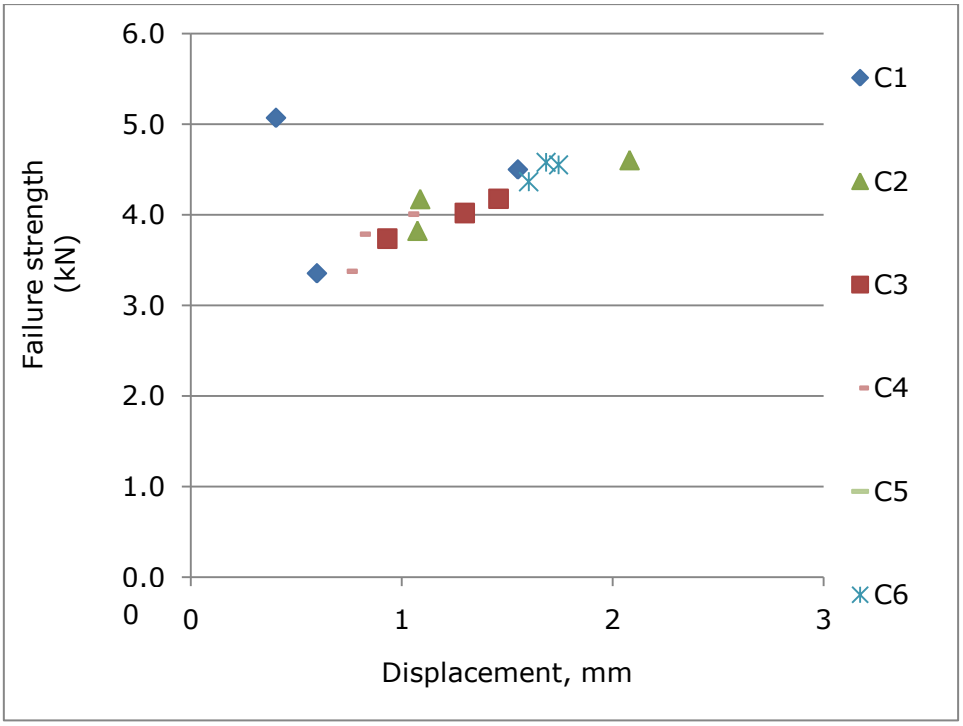

Figure 4.57) Relationship between failure strength and displacement for flare bevel groove brazed joints.

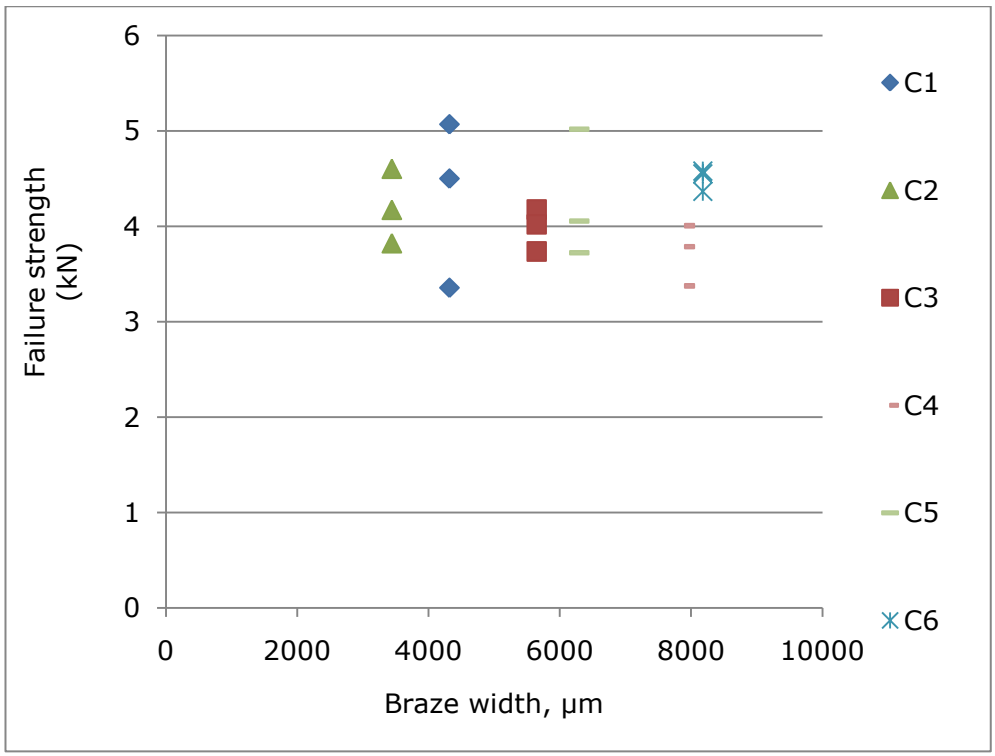

Figure 4.58) Relationship between failure strength and corresponding braze width, for flare bevel groove brazed joints.

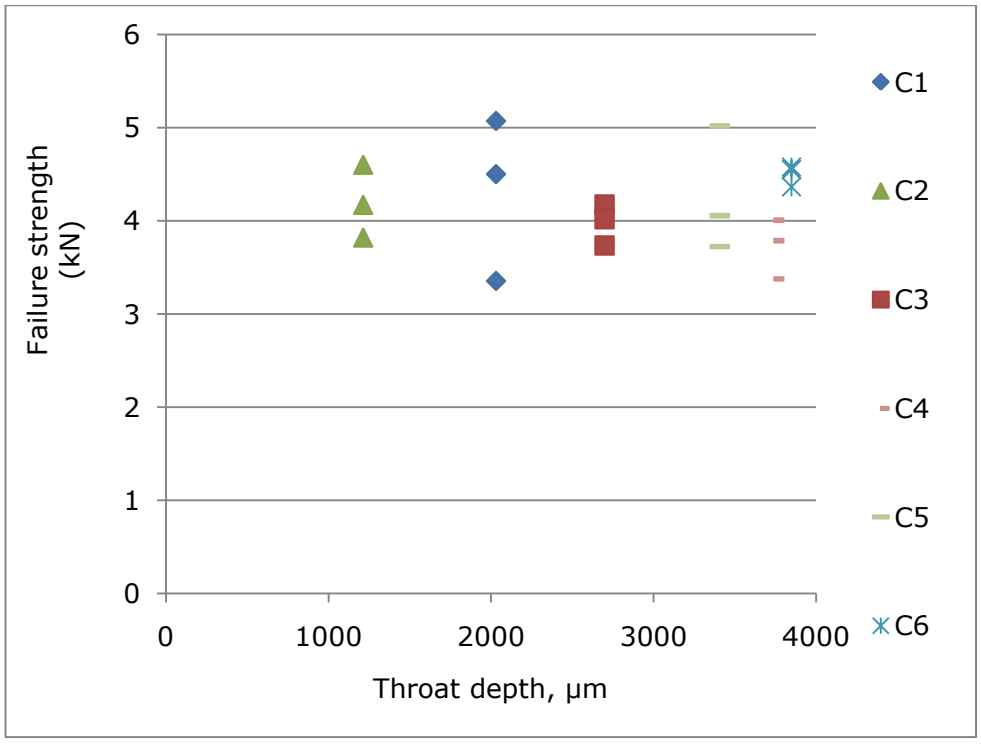

Figure 4.59) Relationship between failure strength and corresponding throat depth, for flare bevel groove brazed joints.

4.4.5 Comparison of samples C1~C6 with the GA steel sample using the FCW at the high laser moving speed of 3m/min

Table 4.16 shows the laser moving speed, the liner energy density, the volume of wire delivered and corresponding braze results. The liner energy density and the volume of wire delivered can be calculated as below: (The unit of laser moving speed and wire feed rate is changed from m/min to mm/sec for the calculation.)

- Liner energy density (E_l, kW·sec/mm):
  E_l = [Laser power, kW] / [Laser moving speed, mm/sec]

- Volume of filler wire delivered (V_w, mm^3/mm):
  $V_w = \pi$ x [Filler wire radius, mm]^2 * [Wire feed rate, mm/sec] / [Laser moving speed, mm/sec]

As the brazing speed down from 3m/min to 1m/min, E_l increased from 1.75 to 3 times and V_w increased 2 to 5 times. As a result, the braze width and failure strength of samples C1~C6 were significantly improved.

Sample number (Laser power, Wire feed rate)	Laser moving speed m/min	Liner energy density(E_l), kW·sec/mm	Volume of filler wire delivered (V_w), mm^3/mm	Braze width, mm	Failure Strength kN
B4 (6.0kW, 6m/min)	3	0.12	4.0	2.9	2.3~2.8
C1 (3.5kW, 4 m/min)	1	0.21	8.0	4.3	3.4~5.1
C2 (4kW, 4.6 m/min)	1	0.24	9.2	3.4	3.8~4.6
C3 (4kW, 5.5 m/min)	1	0.24	11.1	5.6	3.7~4.2
C4 (6kW, 6.9WFR)	1	0.36	13.9	7.9	3.4~4.0
C5 (6kW, 8.5 m/min)	1	0.36	17.1	6.3	3.7~5.0
C6 (6kW, 10 m/min)	1	0.36	20.1	8.2	4.4~4.6

Table 4.16) Laser moving speed, liner energy density, the volume of wire delivered and the braze results of the GA steel samples with FCW

4.4.6 Summary

To avoid interfacial fracture during shear tensile testing and increase the braze strength, the laser moving speed decreased to 1m/min. And the FCW with the diameter of 1.6mm was selected for this works, which showed the good wettability with the lowest wetting angle among the GA samples and the high fracture strengths in the section of 4.2 and 4.3. The laser power was increased from 3.5kW to 6.0kW while the wire feeding speed was increased from 4m/min to 10m/min. Tensile tests were performed three times for each condition.

All of the failure of the tensile specimens occurred in a combination of the braze throat and the interface between the parent materials, within the same specimen.

The highest failure strength, 5.1kN, was seen in the one of the tensile samples of C1 (1m/min, 3.5kW, 4m/min wire feed speed), however it also included the sample having the lowest failure strength of 3.4kN.

The braze width and throat depth were not proportional to the laser power or the wire feed speed, however the tensile samples of C6 which was applied the highest laser power and wire feed speed showed the longest throat depth and braze width along with the highest minimum strength, 4.4kN. Also, as mentioned before, it had the failure strengths within the smallest range of 0.2kN.

Only one type of IMC was seen in the samples tested. It is supposed to be Fe_2Al_5, which is formed at first during the brazing. When the laser powers of 3.5kW and 4kW were applied, the IMC thicknesses were less than 5μm except very small area of the C3. When the laser power was increased to 6kW, the IMC thickness was increased up to 17μm, but still most of the area of the interfaces had the IMC thickness less than 10μm.

4.5 Discussion

4.5.1 Overview

After broad ranging parameter development trials and a review of literature covering state of the art laser brazing aluminium to zinc coated steel, the brazing process was evolved to a point where controlled joint quality could be produced and process parameters could be modified to influence heat input for control of joint width and IMC growth.

An acceptable joint was deemed to be one with:

- A good visual appearance (i.e. smooth surface and transition between the materials.

- Acceptable mechanical properties of the joint. In shear testing the failure must occur not at the interface between the steel and the brazed deposit.

To achieve these aims trials were performed varying a range of major process factors, including laser energy and its distribution, location and angle of laser beam, filler wire chemical composition, location and feeding direction of filler wire, the use of fluxes.

These processing factors were varied with the aim of controlling the thermal and chemical balance within the joint to:

- Achieve a good wettability of the steel substrate and a large braze width
- Melt the filler wire and partially melt the aluminium parent to create a brazed joint.
- Minimise the thickness of the Fe-Al IMC layer.
- Minimise thermal distortion in the parent materials.

The discussion section will act to review and explain the approach taken and to detail the best practices that were able to produce the best brazed joints with the greatest repeatability.

4.5.2 Broad overview of the experimental trials

4.5.2.1 Parameters employed

The full range of parameters that were adjusted, in no particular order, are the laser beam power, the laser beam defocus position, the filler wire type, brazing speed, beam biasing either side of the joint line, use of single spot or twin spot and the orientation of the twin spots (see Figure 3.6), the wire feed rate, wire feed angle in the travel plane, wire to joint line angle in the work plane, the wire separation distance from the centre of the beams energy, the laser beam angle in the travel plane, and the laser beam angle in the work plane.

The main findings from the trials, on both flare bevel groove and overlap joints are that the leading and trailing spot orientation produced the most visually acceptable brazed joints. It was expected that side by side spots would produce a greater braze width due to the effective width of the two spots in this orientation, however this often lead to process instability, if too much heat was impinged on the steel sheet, leading to distortion problems. Whichever spot configuration is used, whether single spot or twin, the beam bias in relation to the joint line is critical for designing a braze joint. A very wide braze width was desired for joint strength, therefore biasing to the steel sheet as much as possible without causing distortion, and ensuring the braze deposit still fuses to

the aluminium sheet was important. Regarding laser beam defocus position, it would have been possible to braze with a range of defocused beam values, provided that overall beam intensity does not lead to a keyhole in the parent materials, and that other parameters are adjusted, such as laser beam power. Wire feed rate has a direct impact on the size and volume of the brazed joint, as does the speed of the brazing process. Clearly a slow braze speed with a higher wire feed rate would produce the biggest braze, however sufficient heat (via laser power and focus position, and consequently the wire separation distance to the heat source) to melt the wire are required.

4.5.2.2 Influence of the substrate GA vs. GI coated steel

A large brazed interface area is required to give strong joints. To generate this large brazed zone, good wetting of the steel substrate is necessary. In the case of pure zinc coatings like GI, the liquid zinc generated during brazing acts as a flux providing a highly wettable surface on the steel substrate.

As mentioned previously, the melting temperature of GA coating is much higher than that of the aluminium filler wire and the parent metal of aluminium, so low energy wetting onto the steel substrate is not possible. High temperatures are required to remove the GA layer and the resulting high steel temperature generates the formation of thick (>10μm) and brittle IMC.

Limited short trials were performed on GI coated steel with no study to optimise parameters. The very first joint created had a higher strength and better wettability than any of the joints made in the extensive study of GA coated steels. The only joints to produce a parent material failure in shear testing were made in the GI coated steel. This means wide range of LWB parameter windows can apply between GI steel and 6000 aluminium to achieve acceptable joint strength.

4.5.3 Requirements for the production of high quality joints

4.5.3.1 Laser energy distribution: Spot size and twin spot approach

One of the main requirements to produce a high strength joint is to achieve a large brazed area [5, 10]. To achieve this, a large area of the steel surface must be made wettable which means a large area must be heated by the laser beam. It is possible to generate a large hot area with a relatively small focus spot size of laser, provided that time is allowed for thermal conductivity to spread the heat into a greater area. However, this approach is not suitable for the process desired by the automotive industry; a small intense beam would locally overheat the

steel at the focal point generating local thick deleterious IMC layer. In order for heat to spread by conductivity the process must run slowly and 3m/minute brazing speed could never be achieved.

So to heat a large area of the GA steel surface in an attempt to create a wettable zone able to accommodate a large brazed joint the optical parameters of the laser system were selected to give a large spot size. Focal spot sizes 2.3 to 3.7mm were trialled. These were achieved with the following optical setup:

- 150µm fibre diameter, 160mm collimator, 300mm focal lens, +26mm defocus = 2.3mm spot size.
- 200µm fibre diameter, 160mm collimator, 300mm focal lens, +46mm defocus = 3.7mm spot size.

The experimental trials revealed that the best focal spot size was 3.7mm, this was used to produce all of the best joints in flare bevel grooves and overlap joints.

Although initial trials looked at a single laser beam focus spot, early in the project a twin spot optic giving two focal spots was employed.

This was influenced by several factors:

- Work performed by Laukant [10] and Sascha Frank [9] employed twin spots, each performing different tasks. An initial spot that was either pre-heating the steel substrate or ablating the zinc coating and a secondary spot with higher power that was responsible for melting the aluminium filler wire to create the brazed joint. In particular Sascha Frankwas also able achieve a high strength braze onto GI coated steel at a speed of 3.6m/minute.
- In order to create a high strength joint a large joint width (brazed area) [5, 10]. The use of a twin spot enabled a larger area to be heated, giving a greater potential for the creation of a wide joint interface.

The twin spot optics approach proved to be very useful, as by altering the relative position of the spots a wider or narrower heated area could be created. Trials were performed using two spots side by side, to create a very broad brazed zone, this resulted in moderately good results, but not the very best brazed joints. Spots diagonal to one another were also trialled, with the lead spot positioned onto the steel substrate and the trail spot on the aluminium parent, with the filler wire being fed into either the lead or trail spot (in a manner similar to Laukant [10]). This approach also produced joints of promising quality, but not the best of the trials.

The best approach that was determined from the experimental trials was to use two spots with a spot separation of 0.6mm 'in series' (leading and trailing):

- For overlap joints made with 1.2mm wires, such as AlSi12, and AlMg5, the best joints were made with a power distribution of 30% in the leading spot and 70% in the trailing spot, with the filler wire fed into the trailing spot at a 45° angle (Wire-to-joint-line angle). In this way the raw beam of the first spot could act to remove the GA coating and pre-heat the steel, before the braze metal was deposited by the trailing spot which melted the filler wire and partially melted the parent aluminium. For 1.6mm wires, such as 1.6mm ZnAl15 and FCW, the best joints were made with a power distribution of 70% in the leading spot and 30% in the trailing spot, with the filler wire being fed at 0° wire-to-joint-line angle.

- For flare bevel groove joints the 'in series' (leading and trailing spot) approach was also the best. However, due to the difficulty of depositing a large volume of wire to fill the relatively wide flare bevel groove joint, it was found that the best results were achieved with the filler wire fed in directly to the front spot. In this way, very high wire feed rates could be achieved and both the leading and trailing spots contributed to the melting of the filler wire and deposition of the braze material. This approach was found to be the most stable when an energy distribution of 70% in the leading spot and 30% in the trailing spot was employed.

4.5.3.2 Gas shielding and plume control

The shielding gas arrangement was set up to provide an inter shield that prevents oxidation of the hot metal. It is important to balance the flow rate, angle and direction of the gas shield to fully envelope the braze while it is in the liquid state, but not to create a high pressure flow that introduces turbulence into the melt zone. In order to generate a sufficient flow volume and direction, without excessive turbulence a multiple pipe arrangement was used. The flow of 30l/minute argon was equally distributed among the four pipes (17mm outer diameter), which were angled at 45° and trailed the brazing process.

4.5.3.3 Positioning of laser focal spots: Bias and offset

The position of the laser spots is critical, for accurate positioning of the braze deposit, and thermal management of both parent materials. By beam biasing to the joint line, or to one of the parent materials,

increasing the braze width and minimising the effects of distortion can be achieved. In the overlap configuration, earlier trials used beam biasing onto the aluminium sheet, in attempt to reduce distortion of the steel sheet, however these brazes resulted in very small braze widths that were less than the thickness of the aluminium sheet, 1.2mm. From the best of the overlap joint made with different wires, the beam was biased onto the steel sheet, increasing the braze widths to greater than 2.2mm in all cases. In the flare bevel groove joint configuration, the best joints were made by very small changes in the beam bias, ranging from 0.5mm onto the aluminium, to 0.25mm onto the steel. This was determined experimentally, when over-melting of the steel or aluminium was seen, and to distribute the thermal energy of the brazing process onto both parent metals.

The wire separation distance, wire feed angle and wire-to-joint-line angle are parameters that can be adjusted for finer control of the laser brazing process. Small adjustments in wire separation distance can increase or decrease the temperature inflicted on the wire, whilst under the defocused beam, due to the Gaussian nature of the beam energy distribution. The wire feed angle and wire-to-joint line angle also change the volume of wire that is exposed to the beam.

4.5.3.4 Filler wire

In the project several different filler wire compositions were employed:

- AlSi12 (AA4047) aluminium alloy wire, 1.2mm in diameter.
- AlSi12 aluminium alloy wire, 1.6mm in diameter.
- AlMg5 (AlMg5) aluminium alloy wire, 1.2mm in diameter.
- ZnAl15 alloy wire, 1.6mm in diameter.
- AlSi12 1.6mm flux cored wire.

In general, for laser welding/brazing applications of aluminium to aluminium it is accepted that AlSi12 filler wires are beneficial for achieving a smooth visually appealing joint with a highly repeatable process, but the resulting joint may have poor ductility. The AlMg family of filler wires do not generally produce such appealing joints and result in more surface oxidation of joints, but the mechanical properties of joints made with AlMg5 wires are better than those made with AlSi12 wires, specifically the AlMg5 wires give a more ductile joint. ZnAl15 wires are not commonly used for structural aluminium joining in any automotive applications.

The literature review revealed that in laser brazing of aluminium onto GI coated steel, there was a relationship between filler wire composition

and the strength of the resulting brazed joint. In general, the literature showed that Zn-Al fillers give the highest strength joints, followed by Al-Si wires, with Al-Mg giving the lowest joint strengths [5, 6, 9, 10, 16].

Hardness testing of the braze zone (Tables 4.4 and 4.10) showed how the composition of the filler wire influenced the general mechanical properties of the brazed metal deposit. The hardness of the brazed zones followed the expected relationship in mechanical properties of the filler wires, namely:

- AlSi12 wire: 79HV.
- AlMg5 wire: 85–100HV.
- ZnAl15 wire: 136–184HV.

<AlMg5 (AA5556) wire>

A set of trials were performed with the AlMg5 wire in overlap configuration. Very few brazed joints were created that had any significant strength. Figures 4.5 shows that joint made with the AlMg5 wire were among the lowest in strength of those produced, with failures occurring at the IMC layer at the steel to aluminium interface. Several reasons can be attributed to this, firstly there was a difficulty encountered in achieving good wetting onto the GA substrate, Figure 4.5 shows the joints with AlMg5 wire had the smallest braze width of all. Also, the IMC layer created when brazing with the AlMg5 wire was thick, in the region of 9-14μm. The IMC layer appeared to be mostly constituted of highly brittle Fe_2Al_5 and cracks were often observed in the layer. Due to the relatively poor performance of overlap joints with AlMg5 wire, no flare bevel groove trials were performed

<AlSi12 (AA4047) wire>

The AlSi wire was reported in literature to be capable of producing high strength joints in combination with GI steel and in a fluxed process some high strength joints in GA coated steel were reported. Also, the presence of silicon in the iron – aluminium system has been reported to inhibit the formation of brittle Fe-Al IMC [5,9,10,16]. Results of the trials showed that brazed joints made with AlSi12 wire still contained IMCs, mainly with Fe_2Al_5 present in the dense layer on the surface of the steel substrate and some distributed $FeAl_3$ above this layer in contact with the braze material. The presence of silicon to relatively high percentage in the IMC layer suggested that either a ternary phase was also present or a high level of Si was in solution within the Fe-Al phases. With the correct thermal balance, the thickness of IMC layer could be controlled to between 5 and 10μm across the various specimens

produced. On GA coated steels a thinner IMC layer should be achieved to maximise brazed joint strength. Unfortunately, this did not appear to be possible within the scope of the experiments performed. Joints with the AlSi12 wire exhibited better strength than the AlMg5 wire, but the failure modes were at the IMC layer on the steel to aluminium interface.

<ZnAl15 wire>

The ZnAl wire was also reported to have the ability to inhibit the formation of brittle Fe-Al IMCs [6,7,8]. This is because liquid aluminium has a greater affinity for zinc than for iron. In addition, the lower melting temperature of the Zn based system compared to the Al rich wires, means lower braze temperatures can be applied and there is less thermal energy available for the diffusion of iron into the braze.

The trials performed made several key findings:

- The process of brazing with ZnAl15 wires was less stable than with AlSi12 wires, mainly because the liquid created did not flow or wet to the substrate as well.
- The laser process was observed to cause significant zinc evaporation, this evaporation created a plume that may have dissipated the laser energy and made the process more sensitive. In addition, the evaporating zinc oxidised and left a film of soot on the joints.

However, despite the difficulties, when stable joints were produced, the highest strength of any joints was achieved, although joints failed at the IMC layer on the steel–aluminium interface. At the interface an IMC layer thickness of between 7-21μm was the measured in the centre of the best joints. The IMCs consisted of a base layer of Fe_2Al_5 directly onto the steel substrate, with $FeAl_3$ above it in contact with the braze zone. The presence of a significant proportion of Zn in this IMC layer suggested that either a ternary phase was present, or that a significant amount of zinc was in solution within the Fe-Al phase. Also, very interestingly, in areas outside the joint centre, where less heat was generated a zone existed where only a ZnAl15 phase was present with no Fe-Al at all. Unfortunately, it was not possible to replicate this across the entire joint interface.

<AlSi12 (AA4047) flux cored wire (FCW)>

To reduce the heat energy on the steel substrate, trials with the flux cored wire were performed. The effect of the flux in increasing the wettability of the GA substrate was immediately obvious. Figure 4.7 and Figure 4.28 show that the FCW produced by far the widest

brazed joints at the laser moving speed of 3m/min and the joint strengths achieved were among the best achieved, although less than those achieved with the GI coated steel. Analysis of the joint interface showed that formation of IMCs was not prevented by the use of the FCW, but a thinner IMC layer was generated at 4μm in the joint centre. The IMC layer in the joint centre appeared to be Fe_2Al_5 with some ternary phase or Si in solution within the Fe-Al IMC. Outside the joint centre in the cooler areas of the joint low Fe contents were measured in the IMC layer thickness, which strongly suggest the presence of a ternary phase with little or no Fe-Al IMC. Although, at the high brazing speed of 3m/min, the joint strength achieved with the FCW was better than that achieved in the AlSi12 wire without flux, the joints were still not as strong as those made in GI coated steel and failure still occurred at the IMC layer on the interface between the steel and the aluminium.

The lower brazing speed of 1m/min was obviously useful to acquire larger braze widths by granting more time to feed and melt the filler wire and remove the zinc coating of the steel parent material. The samples at the brazing speed of 1m/min shows significantly higher failure strengths of 3.4kN to 5.1kN, then that of tensile samples produced at the brazing speed of 3m/min, reached a maximum failure load of 2.8kN. And the failure occurred in a combination of the braze throat and the interface between the parent materials.

<ZnAl15 wire with painted on flux>

Towards the end of the project, a limited number of trials with ZnAl15 wire with painted flux were performed. Although this is a two-step process of painting the flux followed by brazing, if the laser brazing results were superior in comparison to the other filler wires, this could become a one step process by implementing a flux cored ZnAl15 wire. The effect of the flux in increasing the wettability onto the GA substrate was apparent, as seen in Figure 4.29, where the ZnAl15 wire with painted on flux had the largest braze width and throat depth of all the flare bevel groove samples.

The trials performed made several key findings:

- The painted flux did improve the stability of the brazing process as the liquid created flowed and wetted to the substrate better than when not using the painted flux.
- No difference was observed to the amount of zinc evaporation seen by the laser process. More soot was seen from the brazing process due to the presence of the flux, in addition to the evaporating zinc oxidising.

- Other than creating a greater braze width and throat depth, the IMC layer resulted in no change from the compounds seen or its thickness.

4.5.3.5 Process energy

Another major factor was the process energy employed. The energy was input into the process simply by laser power, although a balance of many factors determined how that energy was distributed within the dynamic brazing process:

- Distribution of energy between the dual focus spots.
- Energy reflected from; the filler wire, the aluminium substrate, the GA coated steel substrate.
- Energy absorbed into; the filler wire, the aluminium substrate, the GA coated steel substrate.
- Energy dissipated by the plume produced by the process.
- Thermal energy conducted away by; the aluminium and GA coated steel substrates, the clamping fixtures, the shielding gas.

A balance of the energy introduced into the process along with the factors that distribute and dissipate that energy are critical to obtain the best possible brazed joints. After experimental trials had helped to find the best laser spot positions, wire feed angles, shielding gas and clamping arrangements, minor adjustments to the process could be employed to begin to optimise the joints. Optimisation took place by balancing the laser power with the wire feed speed to:

- Create a large wettable area to produce brazed joints with a wide joint interface.
- Ensure that the thermal balance was in the correct range. Too low heat and a lack of fusion/wettability of the braze material resulted, too much heat and excessive Fe diffusion lead to the production of thick IMC layers. IMC layers more than 10μm were well known to give poor mechanical performance and the target IMC layer thickness was 3-10μm.

With the other factors under control, the process parameters adjusted to produce the best brazed joints were mostly a balance of laser power with wire feed speed.

The energy balance against the volume of molten material created to generate the best brazed joints can be seen by comparing the relationship between the liner energy density ($E_{l,}$ [Laser power] / [laser moving speed]) against the volume of filler wire delivered (V_w, π x [wire

radius]^2 x [wire feed rate] / [braze speed]), this is shown in Figure 4.60. It can be seen that the energy required to melt and deposit a good quality braze in AlSi12 and AlMg5 wire follows one relationship and the energy needed for ZnAl15 wire is significantly lower compared to the volume of material melted. This relationship is quite logical as ZnAl15 has a significantly lower melting point than AlSi12 and AlMg5 (382°C compared to 582°C and 620°C each). The close correlation of the points to also indicates the tight process window by which a balanced joint can be created; if the heat input is slightly too high, a thick IMC layer is generated, if the heat input is too low, poor wetting occurs and there is insufficient fusion.

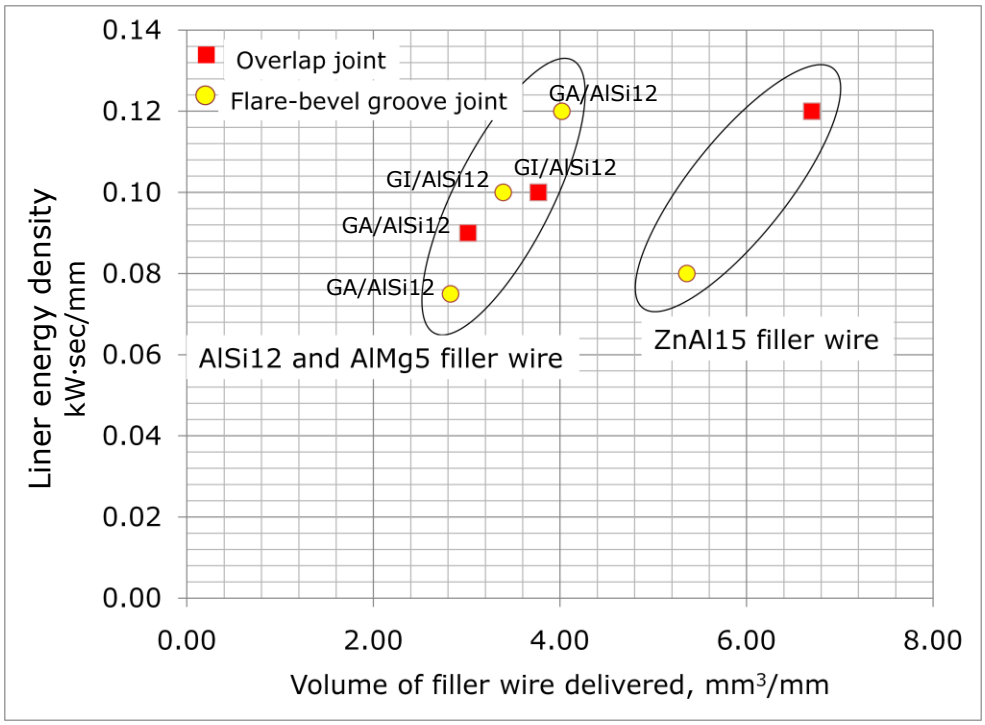

Figure 4.60) The relationship between liner energy density vs. volume of filler wire delivered for the best brazed joints at the laser moving speed of 3m/min

5. Conclusion and recommendation for further work

LWB trials has conducted between 6000 aluminium and GA steel with the flare bevel groove joint in the efforts to join aluminium roofs to galvannealed steel side frames of car bodies. Additional trials for overlap joints performed for the wide use of LWB in the automotive industry. Also, brazing between 6000 aluminium and GI steel were tested to compare the joining strength with that of GA steel. The most of trials performed at the laser moving speed of 3m/min which is supposed to be the least brazing speed for the use in the serial assembly lines of car bodies.

The key findings for LWB between aluminium and GA steel were:

- Parent material cleanliness has significant effects on the quality of laser brazed joints between aluminium and GA steel. Upstream (pre-brazing) facilities are necessary, to satisfy material cleaning requirements.

- Soot adhered to the surface of the joint region, irrespective of which filler type was used during the laser brazing process. This is more significant however when using flux, either as a wire core or as a painted on surface treatment. Consequently, the work carried out in this project has indicated that a post braze cleaning step would be necessary prior to other production based operations (e.g. painting).

<For overlap joints with GA steel>

- At the laser moving speed of 3m/min, the highest failure tensile strength was achieved using 1.6mm ZnAl15 filler wire, achieving up to 3.8kN. These failures however, occurred at the interface between the steel and braze deposit.

- For the 1.2mm diameter AlSi12 (AA4047) and AlMg5 (AA5556) filler wire, the most promising laser brazing results were achieved with a power distribution of 30% in the leading spot and 70% in the trailing spot, with the filler wire fed into the trailing spot at a 45^{o} angle (wire-to-joint-line angle). In this way the raw beam of the first spot could act to remove the GA coating and pre-heat the steel, before the braze metal was deposited by the trailing spot which melted the filler wire and partially melted the parent aluminium.

- For the 1.6mm diameter ZnAl15 and flux cored wire, the most promising laser brazing conditions were achieved with a power distribution of 70% in the leading spot and 30% in the trailing spot, with the filler wire being fed at 0° wire-to-joint-line angle.

<For flare bevel groove joints with GA steel>

- At the laser moving speed of 3m/min, the highest failure tensile strength was achieved using 1.6mm ZnAl15 filler wire with painted flux, achieving up to 2.9kN. These failures however, occurred at the interface between the steel and braze deposit.

- The 'leading and trailing' spot configuration produced laser brazed joints that best met the visual and mechanical requirements. However, due to the difficulty of depositing a large volume of wire to fill the relatively wide flare bevel groove joint, it was found that the best results were achieved with the filler wire fed in directly to the front spot. In this way, very high wire feed rates could be achieved and both the leading and trailing spots contributed to the melting of the filler wire and deposition of the braze material. This approach was found to be the most stable when an energy distribution of 70% in the leading spot and 30% in the trailing spot was employed.

- Based on the experimental results, that the reason for the better brazing results when the leading spot has 70% and the trailing spot has 30% of the energy distribution is likely to be due to the effectiveness and ability of the initial beam to melt the wire at a faster rate than if the lower energy spot was leading. Due to the relevantly high speed of the process, this results in the most stable brazing conditions in flare bevel groove joints.

- To avoid the failure at the interface between the GA steel and braze deposit during tensile shear testing, additional trials at the slow brazing speed of 1m/min performed. Although this brazing speed does not meet the requirement for the automotive serial production line, the samples made at this brazing speed shows significantly higher failure strengths of 3.4kN to 5.1kN, whereas tensile samples produced at the brazing speed of 3m/min, reached a maximum failure load of 2.8kN. And all of the failure of the tensile specimens occurred in a combination of the braze throat and the interface between the parent materials. This is likely to be due to the larger braze widths but thin IMC layers by granting the more time to feed and melt the filler wire and remove the zinc coating of the steel parent material with lower heat energy conditions.

These research findings suggest the best laser conditions and filler wire to braze aluminium to steel for mixed-material car bodies. The limitation of LWB for GA steel is also presented.

To achieve the acceptable joining strength between GA steel and 6000 aluminium at the high brazing speed, generally 3m/min or above, further works recommended:

- Finding filler wires or flux materials which can chemically react with the GA coating to evaporate the zinc coating under low heat energy conditions. This effort has been made from the beginning of this research, but major filler wire and flux manufacturers could not suggest better one than the FCW used in this research.

- A zinc coating removal process before the laser brazing might be the most realistic solution in the automotive industry. It can save the heat energy and time to remove the zinc coating during the laser brazing process. Through recent brazing tests performed between 6000 aluminium and uncoated steel, the possibility of the wide processing window for sound joining strength was shown. Also, for the zinc coating removal process, several mechanical and thermal solutions are under consideration for a next research project.

References

[1] FKA. Determination of Weight Elasticity of Fuel Economy for Conventional ICE Vehicles, Hybrid Vehicles and Fuel Cell Vehicles; Report 55510; Forschungsgesellschaft Kraftfahrwesen (FKA): Aachen, Germany, 2006

[2] T. Watanabe, H. Takayama, and A. Yanagisawa, "Joining of aluminum alloy to steel by friction stir welding," J. Mater. Process. Technol., vol. 178, no. 1–3, pp. 342–349, 2006.

[3] Livsey, D. W., Ridley, N.: Diffusion Bonding of Superplastic Aluminium Alloys Using a Transient Liquid Phase Interlayer (Zinc). In: Diffusion Bonding 2. Ed. Stephenson, D. J., Elsevier Science Publishers London and New York (1991) p. 83 – 100

[4] F. Wagner, I. Zerner, M. Kreimeyer, T. Seefeld, and G. Sepold, "Characterization and properties of dissimilar metal combinations of Fe/Al and Ti/Al-sheet materials," 208 th Int. Congr. Appl. Lasers Electro-Optics, pp. 2001–2365, 2001.

[5] C. H. J. Gerritsen and C. M. Allen, "ND : YAG laser joining of aluminium sheet to galvanised steel sheet : initial studies," Granta, vol. 44, no. 0, 2004.

[6] J. Fan, C. Thomy, and F. Vollertsen, "Effect of thermal cycle on the formation of intermetallic compounds in laser welding of aluminum-steel overlap joints," Phys. Procedia, vol. 12, no. PART 1, pp. 134–141, 2011.

[7] S. Yan, Z. Hong, T. Watanabe, and T. Jingguo, "CW/PW dual-beam YAG laser welding of steel/aluminum alloy sheets," Opt. Lasers Eng., vol. 48, no. 7–8, pp. 732–736, 2010.

[8] A. R. Marder, "Metallurgy of zinc-coated steel," Prog. Mater. Sci., vol. 45, no. 3, pp. 191–271, 2000.

[9] D. Pradhan, A. K. Guin, P. Raju, M. Manna, M. Dutta, and T. Venugopalan, "Fe-Zn alloy coating on galvannealed (GA) steel sheet to improve product qualities," J. Mater. Eng. Perform., vol. 23, no. 9, pp. 3336–3346, 2014

[10] S. Kobayashi and T. Yakou, "Control of intermetallic compound layers at interface between steel and aluminum by diffusion-treatment," Mater. Sci. Eng. A, vol. 338, no. 1–2, pp. 44–53, 2002.

[11] Kreimeyer M, Wagner F, Sepold G. Development of a combined joining- forming process for aluminum-steel joints. In: ICALEO 2004 – 23rd international congress on applications of laser and electro-optics, San Francisco,

[12] T. Sakayama et al.,
"自動車ボディにおける鋼板とアルミニウム合金板との異種金属接合技術
Dissimilar metal joining technologies for steel sheet and aluminum alloy sheet in auto body," 新日鉄技報, vol. 393, no. 103, pp. 91–98, 2012.

[13]P. Peyre, G. Sierra, F. Deschaux-Beaume, D. Stuart, and G. Fras, "Generation of aluminium-steel joints with laser-induced reactive wetting," Mater. Sci. Eng. A, vol. 444, no. 1–2, pp. 327–338, 2007.

[14]G. Sierra, P. Peyre, F. Deschaux Beaume, D. Stuart, and G. Fras, "Galvanised steel to aluminium joining by laser and GTAW processes," Mater. Charact., vol. 59, no. 12, pp. 1705–1715, 2008.

[15]J. Sun, Q. Yan, Z. Li, and J. Huang, "Effect of bevel angle on microstructure and mechanical property of Al/steel butt joint using laser welding-brazing method," Mater. Des., vol. 90, pp. 468–477, 2016.

[16]S. Frank, "Flux-free laser joining of aluminum and galvanized steel," J. Mater. Process. Technol., vol. 222, pp. 365–372, 2015.

[17]A. Mathieu, S. Pontevicci, J. claude Viala, E. Cicala, S. Matteï, and D. Grevey, "Laser brazing of a steel/aluminium assembly with hot filler wire (88% Al, 12% Si)," Mater. Sci. Eng. A, vol. 435–436, pp. 19–28, 2006.

[18]J. Sun, Q. Yan, W. Gao, and J. Huang, "Investigation of laser welding on butt joints of Al/steel dissimilar materials," Mater. Des., vol. 83, pp. 120–128, 2015.

[19]Thomy, C.; Wirth, A.; Kreimeyer, M.; Wagner, F.; Vollertsen, F.: Joining of dissimilar materials - new perspectives for lightweight design in the transportation industries. Proc. IIW International Conference Welding & Materials, Dubrovnik & Cavtat, July 01-08, 2007, 311-326

[20]C. Dharmendra, K. P. Rao, J. Wilden, and S. Reich, "Study on laser welding-brazing of zinc coated steel to aluminum alloy with a zinc based filler," Mater. Sci. Eng. A, vol. 528, no. 3, pp. 1497–1503, 2011.

[21]G. Filliard, M. El Mansori, L. Tirado, S. Mezghani, C. Bremont, and M. De Metz-Noblat, "Industrial fluxless laser weld-brazing process of steel to aluminium at high brazing speed," J. Manuf. Process., vol. 25, pp. 104–115, 2017.

[22]G. QIN, Y. SU, and S. WANG, "Microstructures and properties of welded joint of aluminum alloy to galvanized steel by Nd:YAG laser + MIG arc hybrid brazing-fusion welding," Trans. Nonferrous Met. Soc. China, vol. 24, no. 4, pp. 989–995, 2014.

[23]H. Laukant, C. Wallmann, M. Korte, and U. Glatzel, "Flux-Less Joining Technique of Aluminium with Zinc-Coated Steel Sheets by a Dual-Spot-Laser Beam," Adv. Mater. Res., vol. 6–8, pp. 163–170, 2005.

[24]W. Reimann, S. Pfriem, T. Hammer, D. Päthe, M. Ungers, and K. Dilger, "Influence of different zinc coatings on laser brazing of galvanized steel," J. Mater. Process. Technol., vol. 239, pp. 75–82, 2017.

[25] Kazutoshi Saida, Haruki Ohnishi and Kazutoshi Nishimoto, 'Fluxless Laser Brazing of Aluminum Alloy to Galvanized Steel', Proceedings of the 8th International Welding Symposium organized by Japan Welding Society, 2008, pp231.

[26]Tsuyoshi M and Seji S et al, 2013: 'Dissimilar metal joining technology using newly developed aluminium flux cored wire (FCW) to join aluminium alloy and steel', Kobelco technology review No. 31 Jan.

[27]Tsuyoshi M and Seji S: 'Joining of aluminium alloy to galvannealed steel sheet by laser-brazing'. **https://www.jstage.jst.go.jp/article/jwstaikai/2006f/0/2006f_0_148/_pdf** April 10, 2017

[28]Nishimoto K, Okumoto Y, Harano T et al: 'laser pressure welding of aluminium and galvannealed steel' Welding International, 23:10, 734-743.

[29]Nishimoto K, Harano T, Okumoto Y, Atagi K, Hiroo, Fujii Hand Katayama S, 2009: Mechanical properties of laser-pressure-welded joint between dissimilar galvannealed steel and pure aluminium, Welding International, 23:11, 817-823.

[30]Nishimoto K, Okumoto Y, Harano T, Atagi K, Fujii H and Katayama S, 2009: HR-TEM observation of laser pressure weld of galvannealed steel and pure aluminium, Welding International, 23:11, 824-829.

[31]Wakisaka T and Suzuki T: 2012: 'Laser brazing aluminium alloy and galvannealed steel with Zn-Si filler metal' Japan welding journal? p274-279.

[32]Achar D R G, Ruge J and Sundaresan S, 1980: Aluminium 56 291–293.

[33]Wakisaka T, Okumura T, Suzuki T, 'Laser welding Al and Fe members with Zn filler', US patent number 8492675 B2.

[34]**https://www.rit.edu/affiliate/nysp2i/sites/rit.edu.affiliate.nysp2i/files/pdfs/e-coating_process_final.pdf** (March 10 2017)

[35]B.C. De Cooman, 2003: 'Coating Technologies' **https://www.slideshare.net/BrunoCharlesDeCooman/introduction-to-steel-coating-technologiesbcdecooman2016** (March 10 2017)

Appendix A

Summary of brazing trials performed for the overlap joint configuration and the aim of each trial and summary of findings

▪ Materials: GA steel-A6451 ▪ Filler wire: AA4047, 1.2mm in diameter ▪ Single or twin spot laser beam was positioned at 25° from the vertical axis in the work plane.	
Aim and condition of trial	Summary of findings
Aim: to get starting conditions for laser brazing overlap joints. • Single spot laser beam with: • Laser moving speed: 2.8m/min • Laser power: 4kW • defocused at +36mm • bias of joint line: 0~0.5mm to A6451 • Wire feed rate: 4m/min	The brazed joint cracked and the interface region was very brittle. Some regions appeared very hot and distorted, which could have been due to the low wire feed rate.
Aim: conduct a Design set of experiments (DOE) using single spot conditions. A wide range of parameters were selected to define process space for stable conductions. • Single spot laser beam with: • moving speed: 1~5m/min • power: 2.5~5kW • defocused at +36mm • bias of joint line: 0~1.0mm to Al • Wire feed rate: 2~9.5m/min	The parameter set used was too coarse, therefore stable brazing conditions were not found within the experimental set.

Aim: to see if there were benefits with using a trailing wire configuration. A trailing wire position allowed the front of the beam to ablate zinc coating without the wire shadowing the material surface. • Single spot laser beam • moving speed: 0.8~1.4m/min • power: 1~3kW • defocused at +36mm • targeted on the joint line • Wire feed rate: 1.2~2.0m/min	Some visually appealing brazed joints were made but with very low strength. These brazed joints were made at very slow to ensure zinc removal, however low joint strength occurred due to large IMC thicknesses. The trailing wire feed must be placed closer to the laser beam to ensure sufficient melting, but the gas pipes were too far back from the melt pool leading to shielding issues.
Aim: Trials were made with the wire leading in front of the brazing process again and twin beams were trialled for the first time in leading and trailing, side by side and diagonal orientations, in an attempt for the front beam to ablate zinc coating on steel surface, and the second beam to melt the wire and form a braze deposit. • Twin spot laser beam • moving speed: 1.0~1.4m/min • power: 3.8~5.0kW • defocused at +36mm / bias of joint line: 0~1.3mm to Al • Wire feed rate: 2.0~4.0m/min	Good visual appearance made in both diagonal beam positions, and also leading and trailing positions. Some cracking was apparent when samples were bend tested by hand. IMC layer thickness of 50 to 100μm was seen.
Aim: to introduce a wire-to-joint-line angle of 25°, to avoid the wire shadowing the beam onto the steel surface. The wire was leading from the front of the brazing process as previously. The twin beams are aligned in a 45 degree configuration where the leading beam is positioned on the steel. • Twin spot laser beam: • moving speed: 1.2~1.5m/min • power: 3.8~5.0kW • defocused at +36mm • bias of joint line: 0~0.7mm to Al • Wire feed rate: 2.7 ~3.5m/min	Some visually appealing brazed joints were made and cross sections were made from a selected few. Large IMCs were seen, approximately 50-100μm in length.

Aim: The trials continued with the previous condition. In some trials, a 0.2mm gap was introduced. Some slightly higher wire feed rates were trialled. • Twin spot laser beam: • moving speed: 1.0~1.4m/min • power: 2.0~5.0kW • defocused at +36mm • bias of joint line: 0~1.0mm to Al side • Wire feed rate: 2.0 ~3.5m/min	Increasing the wire feed rates at the low speeds lead to the wire sticking as the process has insufficient heat. A 0.2mm gap between the two plates reduced zinc porosity, as observed in radiographs.
Aim: Laser moving speed was increased to 3m/min to meet the industrial requirement. These brazed joints were conducted as part of a DOE study. The parameter range is described below. • Twin spot laser beam • moving speed: 3.0m/min • power: 3.0~4.5kW • set at 45° with the front beam on the steel surface • defocused at +26 to 36mm • bias of joint line: 0.3~0.7mm to Al side • Wire feed rate: 1.0~2.0m/min	2 brazed joints showed encouraging joint strength during a bend test; 4W108 and 4W125. Cross-sections highlighted that these brazed joints had insufficient width, of approximately 1mm. Much smaller IMCs, at 5-25µm, were observed. The small joint width could have been due to beam biasing onto the aluminium sheet rather than the steel.
Aim: Twin spot with leading and trailing beam configuration was tested, in a power ratio of 70:30, were the colder spot was leading. • Twin spot laser beam • moving speed: 3.0m/min • power: 3~4.5kW • defocused at +36mm • bias of joint line: 1.0mm to steel side • Wire feed rate: 8.0~10.0m/min	A noticeable reduction in porosity was seen when using a leading and trailing beam configuration in a 70:30 split when the lower power spot was leading.

▪ Materials: GA steel-A6451 ▪ Filler wire: AA5556, 1.2mm in diameter ▪ The twin spot beams were defocused at +36mm, and the beam was positioned at 25° from the vertical axis, in the work plane. ▪ All brazed joints were made at 3m/min.	
Aim and condition of trial	Summary of findings
Aim: To find starting conditions using AA5556 wire in overlap configuration. • The laser power was 3.5-4.5kW. • The beam bias range was 2mm onto the steel, to 1mm onto the aluminium. • The beam position was either set at 45 ^{O} with the front beam on the steel surface, or leading and trailing. • Wire feed speed was 1-10m/min • The wire separation distance was adjusted to either be fed into the leading beam or into the rear beam, up to 2mm either side of the centre of the beam energy. • Wire-to-joint-line angle was adjusted between 0 to 45 degrees.	In these trials, a leading and trailing spot orientation resulted in the most stable brazing conditions with the wire feeding into the front beam, with the wire wire-to-joint-line angle at 45 degrees. Tensile samples were made but strengths were generally lower than AA4047 wire trials and are less visually appealing.
Aim: These trials looked to vary the wire separation in an effort to maintain stable brazing conditions as reported in the previous trials, but to reduce heat input to minimise IMC thickness. During trials with leading and trailing beams, adjusting the power densities of the front and rear beams were experimented, up to a 70:30 power split. • The laser power was 4-4.5kW. • The beam bias was 1mm onto the steel sheet in all trials. • - Wire feed speed was 7-8m/min	The IMC thickness range was between 5-15μm and tensile strengths were not increased compared with previous trials.

▪ Materials: GA steel-A6451 ▪ Filler wire: ZnAl15, 1.6mm in diameter ▪ The twin spot beams were defocused at +46mm, and the beam was positioned at 25° from the vertical axis, in the work plane. Due to repair of the previously used collimating a lens, a new collimating lens was used that uses a 200μm fibre, rather than 150μm fibre. Therefore, the defocus of the beam was increased by 10mm to ensure the same spot size impinges at the material surface. All further trials were used with this lens.	
Aim and condition of trial	Summary of findings
Aim: First trials of the second GA material with 1.6mm Zn Al wire. A leading and trailing beam configuration was used, in a power ratio of 70:30. In some trials, the lower power spot was leading, and in others it was trailing. • The laser power was 3-5kW. • The processing speed was 3 to 4m/min. • The beam bias was 1mm onto the steel sheet. • Wire feed speed was 8-10m/min	With this wire, it was found that leading and trailing beams with the higher power spot in front had better visual appearance.

▪ Materials: GA steel-A6451 ▪ Filler wire: FCW, 1.6mm in diameter ▪ The twin spot beams were defocused at +46mm, and the beam was positioned at 25° from the vertical axis, in the work plane.	
Aim and condition of trial	Summary of findings
Aim: to find suitable laser brazing conditions using FCW. All trials used a leading and trailing beam configuration in a power ratio of 30:70, where the higher power density spot was leading. • The laser power was 4.5-6kW • The processing speed was 3m/min. • The beam bias was 0 to 1mm onto the steel sheet.	With this wire, it was found that leading and trailing beams with the higher power spot in front had better visual appearance.

• - Wire feed speed was 5.5-10m/min	

▪ Materials: GI steel-A6451 ▪ Filler wire: AA4047, 1.2mm in diameter ▪ The beams were defocused at +46mm, and the beam was positioned at 25° from the vertical axis, in the work plane.	
Aim and condition of trial	Summary of findings
Aim: Using the conditions that were selected for A1, a sample was made on GI material, for a comparison. • Twin spot laser beam • A leading and trailing beam configuration was used, in a power ratio of 70:30, where the lower power spot was leading. • The laser power was 5kW. • The processing speed was 3.8m/min. • The beam bias was 1mm onto the steel sheet. • Wire feed speed was 10m/min.	Greater tensile strength resulted from the GI material.

Appendix B

- Summary of brazing trials performed for flare bevel groove joints and the aim of each trial and summary of findings.

▪ Materials: GA steel-A6451 ▪ Filler wire: AA4047, 1.2mm and 1.6mm in diameter ▪ The twin spot beams were defocused at +36 mm or +46mm depending on the collimating lens used.	
Aim and condition of trial	Summary of findings
Aim: To determine starting conditions with 1.2mm filler wire • Laser beam positioned at 45 degrees to the joint line, with the front spot leading on the steel. • The Beam was positioned vertically. • These brazed joints were made at 1m/min. • The power ranged from 1.8 to 3.75kW. • The wire feed rates ranged from 2.7 to 4m/min. • The beam bias of the joint line ranged from 0 to 1mm to the aluminium sheet.	Some of these brazed joints were much distorted due to excessive heat input. The process appeared unstable as there are discontinuities in the braze bead.
Aim: To try leading and trailing beam orientation to see if this had an effect on zinc ablation from the steel surface and whether IMC thickness was reduced. • The beam was positioned vertically. • These brazed joints were also made at 1m/min. • The power ranged from 2-4.5kW. This was increased in comparison to previous trials due to the increase in wire feed rate. • The wire feed rate was kept constant at 4m/min in an effort to increase the braze width in comparison with previous brazes. • The beam bias of the joint line ranged from 1-1.2mm to the aluminium sheet.	Some of the brazing conditions resulted in cracks seen in the braze, and distortion in the parent materials. It is likely that the laser brazing parameters were causing too much heat input into the brazing process zone. By beam biasing onto the aluminium, the beam energy interacting with the steel sheet was reduced; however, distortion was still a problem in some samples. Cross-sections were taken which indicated the IMC layer thicknesses ranged from 50 to 100μm

Aim: To reduce the heat input in comparison with the previous set of trials, therefore these trials were made using a power range of 2-2.3kW. • These trials also had leading and trailing beam orientation. • The beam was inclined at 22° in the work plane. • These brazes were all made at 1m/min. • The wire feed rate was kept constant at 4m/min. • The beam bias of the joint line was kept constant at 1mm to the aluminium sheet.	Some of these brazes were visually appealing on the surface, and had very good braze widths and throat depths. These samples were sent for tensile testing but resulted in interface failures.
Aim: To reduce the IMC thickness, increased the braze speed up to 3m/min, so these trials aimed to determine the process window at this speed. • The power range was 4.5-5kW. • A defocused beam of +36mm was used, and the beam was inclined at 22° in the work plane. • The wire feed rate ranged from 2-10m/min. • These trials also had leading and trailing beam orientation in a 30:70 power ratio, with the higher power spot leading. • Beam bias was up to 1mm, either side of the joint line.	Some of these brazes were visually appealing and cross-section were taken, to determine braze width, throat depth and IMC layer thickness. Under optical microscopy, cracks were observed at the interface between the steel and the IMC layers.
Aim: Similar parameters were used in this set of trials as the previous set; however the beams were orientated at 45 degrees in a 30:70 power ratio, with the leading higher power spot placed on the steel surface. • The power was 5kW on all samples. • Brazing speed was kept constant at 3m/min. • The wire feed rates ranged from 7-10m/min. Beam bias was 0 to 0.5mm onto the aluminium.	These brazes resulted in a lot of distortion. A beam orientation of 45 degrees was deemed unsuitable for the other brazing conditions. No cross sections were taken.

Aim: To see if improved braze beads could be achieved with the beam in a leading and trailing orientation, with a 30:70 power ratio, with the higher power spot leading. • The power was constant at 5kW. • Brazing speed ranged from 3-4.1m/min. • The wire feed rate ranged from 4-10m/min. • There was a beam bias range of 0-1mm onto the aluminium.	Some visually appealing brazed joints were made with small IMC layers (less than 10µm). *However, at these speeds, the wire was not able to fill the void between the two sheets, but formed a narrow bridge between the two sheets.* The braze widths in these samples were less than the aluminium sheet thickness, 1.2mm. *A thicker 1.6mm AA4047 wire applied for the next trials.*
Aim: These trials used 1.6mm AA4047 filler wire for the first time, in an effort to increase the braze width at speed of 3m/min or greater. • The beams were in a leading and trailing orientation, with a 30:70 power ratio, with the higher power spot leading. • The power ranged from 5-8.5kW. • Brazing speed ranged from 3-4m/min. • A defocused beam of +46mm was used, and positioned at 22° in the work plane • The wire feed rate ranged from 2-10m/min. • There was a beam bias range of 0.5mm, wither side of the joint line.	The larger diameter wire was trialled in attempt to fill in the void region between the aluminium and steel sheets, however at these high speeds of 3 to 4m/min, the larger wire diameter of 1.6mm was still not capable of bridging the gap. Cross sections were made but interface failures occurred during the preparation process.
Aim: To further the investigation from the last set of trials, with the same base steel and wire configuration, but to try different beam orientations. The beams were orientated at 45 degrees in a 30:70 power ratio, with the leading higher power spot placed on the steel surface. The second trial was a side by side beam configuration with the higher power spot positioned onto the steel. The third trial was with the beams orientated at 45 degrees in a 70:30 power ratio, with the lower power spot positioned on the aluminium. • The power was 6kW in all trials • Brazing speed was 3m/min. • A defocused beam of +46mm was used, and positioned at 22° in the work plane • The wire feed rate was 6m/min. • There was on the joint line in all trials.	Lower power spot leading and placed onto the aluminium resulted in the *most visually appealing* sample, and tensile specimens were made. The *failure strengths of these brazed joints were between 1.4 to 1.5kN*.

▪ Materials: GA steel-A6451 ▪ Filler wire: ZnAl15, 1.6mm in diameter ▪ The twin spot beams were defocused at +36 mm or +46mm depending on the collimating lens used, and positioned at 22° in the work plane	
Aim and condition of trial	Summary of findings
Aim: This was the first trial of GA material using 1.6mm ZnAl15 filler wire. • A leading and trailing beam orientation was used in a 30:70 power ratio, with the higher power spot leading. • The power was 3 kW. • Brazing speed was constant at 3m/min. • The wire feed rate was constant at 4m/min. • There was beam bias of 0.5mm onto the aluminium.	A brazed joint was made with discontinuities seen in the braze bead. At this high speed of 4m/min and a low power of 3kW, the braze region is likely to have been too cold.
Aim: Due to the lower melting point of this wire, the heat input per unit length of sample was reduced. • A leading and trailing beam orientation was used in a 30:70 power ratio, with the higher power spot leading. • The power ranged from 2-4kW. • Brazing speed was constant at 3m/min. • The wire feed rate was constant at 4-10m/min. • There was a beam bias range of 0 to 1mm onto the aluminium.	A consistent braze bead was not possible, this could be due to the lower melting temperature of the filler wire and subsequent vaporisation of the wire. The conditions resulted in a very hot brazing condition, often cutting through the steel sheets. No cross sections were taken from these samples.
Aim: this was the second set of trials using GA base steel and 1.6mm ZnAl15 filler wire, and the aim of the trials was to reduce the heat input, and therefore reduce IMC thickness, which was achieved by increasing brazing speed up to 4m/min. • The beams were in a leading and trailing orientation, with a 30:70 power ratio, with the higher power spot leading. • The power ranged from 1-5kW. • Brazing speed ranged from 3-4m/min. • The wire feed rate ranged from 2-10m/min. • There was a beam bias range of 0-0.5mm onto the aluminium.	Visually appealing brazes were made, with samples subsequently being cross-sectioned. Some of the profiles had steep laser brazed angles. IMC layer thicknesses of 6 to 20µm were seen. It was not possible to make a tensile sample of these brazes due to the distortion seen in the tensile geometry.

Aim: to repeat for the 4th time, GA base steel trials with 1.6mm ZnAl15 filler wire to produce tensile data. • Using a twin spot, positioned in leading and trailing configuration, in a 30:70 power ratio, with the higher power spot leading. • These brazed joints were made at 3m/min. • The power ranged from 4-6kW. • The wire feed rates ranged from 7-10m/min. • The beam bias of the joint line ranged from 0-0.5mm to the steel sheet.	These samples were made on a smaller tensile geometry to avoid distortion, resulting in *failure strengths of2.3 to 2.8kN* for a sample width of 30mm.

▪ Materials: GA steel-A6451 ▪ Filler wire: FCW, 1.6mm in diameter ▪ The twin spot beams were defocused at +46mm, and positioned at 22° in the work plane	
Aim and condition of trial	Summary of findings
Aim: To achieve high quality brazed joints with 1.6mm FCW. • Using a twin spot, positioned in leading and trailing configuration, in a 30:70 power ratio, with the higher power spot leading. • These brazed joints were made at 3m/min. • The power was at 6.0kW. • The wire feed rates ranged from 6-10m/min. • The beam was targeted on the joint line.	Cross sections were taken and tensile data also collected. This resulted in *tensile data of 2.3 to 2.8kN* for a specimen of width 30mm.

▪ Materials: GI steel-A6451 ▪ Filler wire: AA4047, 1.2mm in diameter ▪ The twin spot beams were defocused at +36, and positioned at 22° in the work plane	
Aim and condition of trial	Summary of findings
Aim: A single GI sample was made for comparison. • A leading and trailing orientation was used in a 30:70 power ratio, with the higher power spot leading. • The power was 5kW. • Brazing speed was 3m/min. • The wire feed rate was 9m/min. There was no beam bias as the beam was targeted on the joint line.	Wetting of the 1.2mm AA4047 filler wire onto the GI material was superior to that seen on GA materials that have previously been tested. This sample was tensile tested and produced failure strengths of 3.8 to 4.5kN across a 30mm sample width.

▪ Materials: GI steel-A6451 ▪ Filler wire: ZnAl15, 1.6mm in diameter ▪ The twin spot beams were defocused at +36, and positioned at 22° in the work plane	
Aim and condition of trial	Summary of findings
Aim: To see if the braze geometry on the GI base steel was improved by using 1.6mm ZnAl15 filler wire. • A leading and trailing beam orientation was used in a 30:70 power ratio, with the higher power spot leading. • The power ranged from 3-5kW. • Brazing speed was constant at 3m/min. • The wire feed rate was constant at 4m/min. There was no beam bias as the beam was targeted on the joint line.	From the small amount of trials conducted on the GI base steel and 1.6mm ZnAl15 filler wire, the wetting of the filler wire was not as consistent onto the GI surface as the previous set of trials with AA4047 wire.